June 2018

Framework Integrating Climate Model, Hydrology, and Water Footprint to Measure the Impact of Climate Change on Water Scarcity in Lesotho, Africa

John W. Pryor
University of South Florida, pryor.john.1991@gmail.com

Framework Integrating Climate Model, Hydrology, and Water Footprint to Measure the Impact of Climate Change on Water Scarcity in Lesotho, Africa

by

John W. Pryor

A thesis submitted in partial fulfillment
of the requirements for the degree of
Master of Science in Environmental Engineering
Department of Civil and Environmental Engineering
College of Engineering
University of South Florida

Major Professor: Qiong Zhang, Ph.D.
Mauricio E. Arias, Ph.D.
James R. Mihelcic, Ph.D.

Date of Approval:
May 3, 2018

Keywords: SWAT, Bluewater, Climate Scenario, Streamflow, Water Stress

ACKNOWLEDGMENTS

I would like to take this opportunity to thank those who were instrumental in helping me complete this research.

First are my parents, Gary and Cathy Pryor. Without their love and support I would have sold out to industry long ago. Next, I would like to thank my advisor and committee members. Dr. Qiong Zhang, for her patience and guidance throughout this long experience as well as her ability to push me to find answers to questions I though hopeless, Dr. James Mihelcic, for creating the MI program and bringing me to USF, and Dr. Mauricio Arias, for advising me and helping me complete the model. I would like to thank Billy Makakole, who provided me critical streamflow data for this study. I can't thank enough the people in my village, who allowed me to live among them and treated me like one of their own. I would also like to thank Melissa Lopresti, for helping me stay sane during my Peace Corps service and allowing me to use her electricity. Finally, I would like to thank Mimi, who taught me I could find a friend in the most unlikely of places.

This material is based upon work supported by the National Science Foundation under Grant No. 0965743. Any opinions, findings, and conclusions or recommendations expressed in this material are those of the author(s) and do not necessarily reflect the views of the National Science Foundation

TABLE OF CONTENTS

LIST OF TABLES iii

LIST OF FIGURES iv

ABSTRACT vii

CHAPTER 1: INTRODUCTION 1
1.1 Climate Change and Water Scarcity 1
1.2 Water Scarcity in Lesotho 5
1.3 Motivation and Objectives 10

CHAPTER 2: LITERATURE REVIEW 11
2.1 History of Measuring Water Scarcity 11
2.2 Water Footprint Analysis 12
2.3 Soil and Water Assessment Tool 17
2.4 General Circulation Models 21
2.5 Bias Correcting Climate Models 22

CHAPTER 3: METHODOLOGY 26
3.1 Study Site and Overview of Methodology 26
3.2 The ArcSWAT Model 29
3.2.1 Digital Elevation Model 29
3.2.2 Soils Map 29
3.2.3 Land Use Map 30
3.2.4 Weather Data 30
3.2.5 Future Climate Data 31
3.2.6 Limitations of Data 34
3.2.6.1 Limitations of SWAT Input Data 35
3.2.6.2 Limitations of Global Climate Model Data 36
3.2.7 Calibration and Validation 37
3.3 Indicators of Hydrologic Alteration Analysis 40
3.4 Water Scarcity 40

CHAPTER 4: RESULTS AND DISCUSSION 45
4.1 Results 45
4.1.1 Bias Correction 45

4.1.2 Indicators of Hydrologic Alteration Results 50
4.1.3 Calibration and Validation Results 53
4.1.4 Climate Change Impact on Precipitation 57
4.1.5 Projected Blue Water Yield (Streamflow) 61
4.1.6 Water Scarcity Analysis 64
4.1.6.1 Historic Water Scarcity 64
4.1.6.2 Future Water Scarcity 65
4.2 Discussion 76

CHAPTER 5: CONCLUSION AND RECOMMENDATIONS 81

REFERENCES 83

LIST OF TABLES

Table 1: Summary of common water scarcity indices 15

Table 2: Soil and Water Assessment Tool database search of articles containing water scarcity, water footprint, and climate change studies 17

Table 3: Common bias correction methodologies 25

Table 4: Limitations of Soil and Water Assessment Tool (SWAT) input data 36

Table 5: General performance ratings for recommended statistics for a monthly time step 39

Table 6: Calibration and validation periods for streamflow gauging stations 40

Table 7: Global sensitivity key parameters with the final minimum and maximum ranges for calibration 53

Table 8: Calibration and validation statistics for the three streamflow gauges 54

Table 9: Relative changes in average precipitation for each Representative Concentration Pathway (RCP) during the wet season (Oct-Apr) and dry season (May-Sept) 57

Table 10: Relative change in streamflow for wet season (Oct-Apr) and dry season (May-Sept) for each Representative Concentration Pathway 61

LIST OF FIGURES

Figure 1: Model framework used by Rodrigues et al (2014) to calculate blue and green water scarcity 4

Figure 2: Map of Lesotho with the Senqu River Basin in red 6

Figure 3: Water withdrawal percentage between agriculture, industry, and urban and household use within Lesotho 7

Figure 4: Estimated amount of water used daily in a typical rural household in Lesotho based upon research by (Thompson et al, 2001) and the author's own experience 8

Figure 5: Review of articles within the SWAT database 19

Figure 6: Map of Senqu River Basin study site 27

Figure 7: Modeling framework for evaluating blue water scarcity using the Soil and Water Assessment Tool (SWAT) 28

Figure 8: The Probability Density Function (PDF) (a) and Cumulative Distribution Function (CDF) (b) of a synthetic data set 33

Figure 9: Projected population increase in Lesotho from 2020 to 2100 43

Figure 10: ICHEC precipitation Cumulative Distribution Function mapping results for station 1 45

Figure 11: ICHEC minimum temperature Cumulative Distribution Function mapping results for station 1 46

Figure 12: ICHEC maximum temperature Cumulative Distribution Function mapping results for station 1 46

Figure 13: Monthly mean precipitation results for ICHEC bias correction 47

Figure 14: Monthly standard deviation precipitation results for ICHEC bias correction 47

Figure 15: Monthly mean maximum temperature results for ICHEC bias correction 48

Figure 16: Monthly mean minimum temperature results for ICHEC bias correction 48

Figure 17: Monthly standard deviation of maximum temperature results for ICHEC bias correction 49

Figure 18: Monthly standard deviation of minimum temperature results for ICHEC bias correction 50

Figure 19: Flow Duration Curve displaying impact of the Katse dam on streamflow at the SG-5 gauging station as well as the Kruskal-Wallace p-statistic 51

Figure 20: Flow Duration Curve displaying impact of the Mohale dam on streamflow at the SG-17 gauging station as well as the Kruskal-Wallace p-statistic 51

Figure 21: Flow Duration Curve displaying impact of the Katse and Mohale dam on streamflow at the SG-3 gauging station as well as the Kruskal-Wallace p-statistic 52

Figure 22: Calibration results for the SG5 streamflow gauge station 55

Figure 23: Calibration results for the SG17 streamflow gauge station 55

Figure 24: Calibration and validation results for the SG3 streamflow gauge station 56

Figure 25: Average Monthly Percent Change in Precipitation for Representative Concentration Pathway 4.5 for both mid-century (2020-2060) and late-century (2061-2100) 59

Figure 26: Average Monthly Precipitation Percent Change for Representative Concentration Pathway 8.5 for both mid-century (2020-2060) and late-century (2061-2100) 60

Figure 27: Average Monthly Percent Change in Streamflow Representative Concentration Pathway 4.5 for both mid-century (2020-2060) and late-century (2061-2100) 62

Figure 28: Average Monthly Streamflow Percent Change for Representative Concentration Pathway 8.5 for both mid-century (2020-2060) and late-century (2061-2100) 63

Figure 29: Historic water scarcity from 1979-2005 64

Figure 30: Water Scarcity Scenario 1 mid-century (2020-2060) for Representative Concentration Pathway 4.5 66

Figure 31: Water Scarcity Scenario 1 late century (2061-2100) for Representative Concentration Pathway 4.5 66

Figure 32: Water Scarcity Scenario 1 mid-century (2020-2060) for Representative Concentration Pathway 8.5 67

Figure 33: Water Scarcity Scenario 1 late-century (2061-2100) for Representative Concentration Pathway 8.5 68

Figure 34: Water Scarcity Scenario 2 mid-century (2020-2060) for Representative Concentration Pathway 4.5 69

Figure 35: Water Scarcity Scenario 2 late-century (2061-2100) Representative Concentration Pathway 4.5 69

Figure 36: Water Scarcity Scenario 2 mid-century (2020-2060) Representative Concentration Pathway 8.5 70

Figure 37: Water Scarcity Scenario 2 late-century (2061-2100) Representative Concentration Pathway 8.5 70

Figure 38: Water Scarcity Scenario 3 mid-century (2020-2060) Representative Concentration Pathway 4.5 71

Figure 39: Water Scarcity Scenario 3 late-century (2061-2100) Representative Concentration Pathway 4.5 72

Figure 40: Water Scarcity Scenario 3 mid-century (2020-2060) Representative Concentration Pathway 8.5 72

Figure 41: Water Scarcity Scenario 3 mid-century (2020-2060) Representative Concentration Pathway 8.5 73

Figure 42: A comparison of the frequency of water scarcity events between each Regional Climate Model for scenario 3 from 2020-2100 74

Figure 43: Comparison between each scenario of the frequency a Regional Climate Model (RCM) produced a water scarcity value greater than 100% with respect to the other RCMs 75

ABSTRACT

Water scarcity is a problem that will be exacerbated by climate change. Being able to model the effect of climate change on water scarcity is important to effectively plan the use of future water resources. This research integrated the Soil and Water Assessment Tool (SWAT), climate model, and water footprint analysis to measure the impact of climate change on future water scarcity. This was achieved through two objectives. The first objective was to create a modeling framework that links the output from climate model to SWAT and combined streamflow outputs from SWAT with water footprint analysis to measure how climate change will impact water scarcity of a river basin. This was accomplished through creating a SWAT model within ArcMap and inputting a topographic, soil, land use, and weather data. Climate Forecast System Reanalysis (CFSR) data were used in lieu of observed weather data due to a lack of available data. SWAT-CUP (Calibration and Uncertainty Program) was used to calibrate two upstream streamflow gauges, then calibrate and validate a third streamflow gauge at the outlet of the Senqu basin in Lesotho. The two upstream streamflow gauges were calibrated from 1986 to 2002. The downstream streamflow gauge was calibrated from 1985 to 2002 and validated from 2003 to 2013. Three Regional Climate Models (RCM), ICHEC-EC-EARTH, MIROC-MIROC5, and CCCma-CanESM2 were downloaded from the Coordinated Regional Downscaling Experiment (CORDEX) dataset. Each RCM was downloaded with two different Coupled Model Intercomparison Project (CMIP5) Representative Concentration Pathways (RCP), RCP 4.5 and RCP 8.5. The RCMs were bias corrected using a cumulative distribution function mapping technique.

These RCMs as well as an average of the RCMs were used as input for the SWAT model to generate future streamflow outputs. The streamflow outputs provide the future blue water availability of the Senqu River. The results showed an overall decrease in streamflow in both RCPs. The second objective was to apply the framework to Lesotho and use the information from the ArcSWAT model and data from the Blue Water Footprint analysis to measure the future potential Blue Water Scarcity of Lesotho. This was accomplished through the Blue Water Footprint of Lesotho generated from the 5th National Blue Footprint analysis. The annual blue water scarcity was calculated as the ratio of the Blue Water Available to Blue Water Footprint. Three approaches were adopted to analyze the water scarcity of Lesotho. The first approach used the national Blue Water Footprint in the water scarcity calculation to investigate the worst-case scenario. The second approach used the modified blue water footprint based on the population living within the Senqu river basin. The third approach used a modified blue water footprint that accounted for the projected population growth of Lesotho. The results of scenario 1 showed there was moderate water scarcity in a period of four years in climate scenario of RCP8.5. The results of scenario 3 showed there were multiple cases of water scarcity in both RCP 4.5 and RCP 8.5 with two years of severe water scarcity. This research is limited by data availability and the results for Lesotho could be improved by accurate dam data and the fine scale water footprint analysis. The modeling framework integrating climate model, hydrology, and water footprint analysis, however, can be applied to other remote places where limited data are available.

CHAPTER 1: INTRODUCTION

1.1 Climate Change and Water Scarcity

The climate of the world has been changing. Over the past 50 years there has been an observed decrease in the frequency of cold days, cold nights, and frost and an observed increase in hot days and hot nights (Pachauri et al., 2014). Anthropogenic climate change is the change in climate due to emission of greenhouse gases associated with human activity. Since the industrial revolution human contribution to the amount of Carbon Dioxide (CO_2) in the atmosphere has grown with an increase of 70% between 1970 and 2004 (Pachauri et al., 2014). Previous studies have shown that climate change affects hydrological cycles and the amount of streamflow (Arnell, 2003, Arnell, 2004, Vorosmarty, 2000, Fry et al., 2012). Mountainous regions are especially susceptible to the effects of climate change (Parish and Funnell, 1999). Any change in the climate in a mountain range can have cascading effects on the lowlands. Many mountains throughout the world are the source for lowland river networks as well as function as long term water storage in the form of snow. Small amount of changes around the freezing temperature threshold will vary the amount of streamflow and peak discharge (Diaz et al., 2003).

As climate change affects various ecosystems, the amount of freshwater available for the world will be impacted and more people are likely to be vulnerable to water scarcity and its consecutive effects. Climate change is predicted to exacerbate water scarcity (Schewe et al., 2014). One recent example is the city of Cape Town, South Africa. Cape Town has been suffering through a two year drought that started in 2015 and was expected to run out of water in April 2018 (Onishi and Sengupta, 2018). Nearly 80% of the world's population is exposed to a

high risk of water scarcity (Vorosmarty et al., 2010). And the global water demand is expected to increase by approximately 55% by 2050 (Oecd, 2012). Access to adequate water supply and proper sanitation methods are essential to mitigating disease throughout the world (Prüss-Ustün et al., 2014). It is estimated that by 2025 about 1.8 billion people will face absolute water scarcity (Wwdr, 2016).

The ability and tools used to measure water scarcity have evolved over the years. There are five main approaches developed to measure water scarcity. These are:

1) The Water Stress Index (Falkenmark et al., 1989, Gleick, 1996, Ohlsson, 2000) which evaluates water scarcity on a per capita availability.
2) The Criticality Ratio (Alcamo et al., 2000, Chaves and Alipaz, 2007, Mcnulty et al., 2010, Raskin et al., 1997) which measures water scarcity as a ratio of the Annual Withdrawal to the Available Water Resources.
3) The Water Poverty Index (Asheesh, 2003, Smakhtin et al., 2005, Sullivan, 2002) which uses environmental and social metrics, such as ecosystem productivity, community, human health, and economic welfare, to measure whether individuals are water secure at the household and community level.
4) The International Water Management Institute (IWMI) indicator (Seckler et al., 1999) evaluates water scarcity by taking the ratio of the freshwater available for human requirements to the main water supply.
5) The Water Footprint Analysis (Hoekstra et al., 2011) which evaluates water scarcity using the water footprint of a country rather than the water withdrawal. The water footprint of a country is the amount of water appropriated for consumption, industry, and agriculture.

Blue water is defined as freshwater either in streams or groundwater. It is used to grow food, manufacture goods in industries, and sustain population in urban and rural settings. As population increases the demands for food, water, and material goods will increase (Postal, 2000). Along with population growth, climate change is a factor that may affect blue water availability. Using the water footprint instead of water withdrawal allows for a more accurate measurement as a significant portion of the water that is withdrawn is returned to the environment. The use of blue water for agriculture, industry, and domestic is accounted for in a blue water footprint analysis. A total of five global water footprint analyses have been conducted (Fader et al., 2011, Hoekstra and Chapagain, 2007, Hoekstra and Hung, 2005, Hoekstra and Mekonnen, 2012, Wang and Zimmerman, 2016). The most recent global water footprint analysis was conducted by Wang and Zimmerman (Wang and Zimmerman, 2016).

The Water Footprint accounting methodology has been incorporated with SWAT to assess water scarcity (Rodrigues et al., 2014). SWAT (Soil and Water Assessment Tool) is a semi-distributed hydrological model developed by the United States Department of Agriculture used for long term simulations of a variety of hydrological and related physical-chemical processes (Arnold et al., 1998). The framework introduced by Rodrigues et al. (2014) uses the SWAT output of soil moisture, evapotranspiration, and streamflow to calculate green and blue water scarcity, while blue water is freshwater, green water is water from precipitation that is absorbed by soil and used by plants (Figure 1).

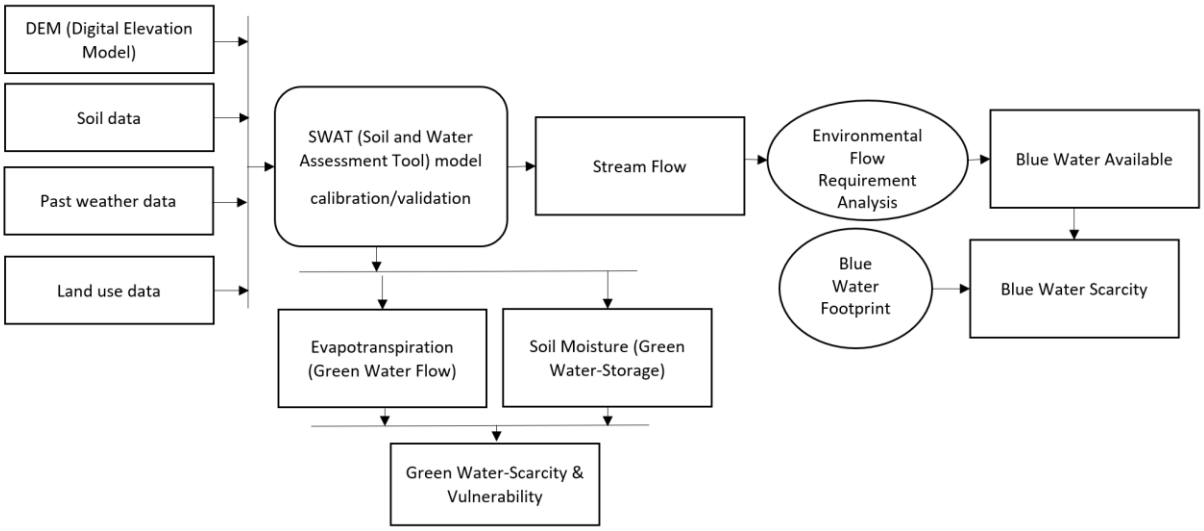

Figure 1: Model framework used by Rodrigues et al. (2014) to calculate blue and green water scarcity.

This study expanded the framework developed by Rodrigues et al. (2014) to include climate change scenarios. Specifically, a model framework was created that integrates climate change with water availability analysis using ArcSWAT and combines with water footprint analysis to measure blue water scarcity. SWAT has been used to evaluate the impact of climate change on blue and green water resources (blue water streamflow, seasonal average change in green water storage and green water flow) of the Athabasca River Basin in Canada (Shrestha et al., 2017). Shrestha et al. (2017), however, did not include the water footprint analysis to assess water scarcity.

1.2 Water Scarcity in Lesotho

The framework created in this study was applied to the Senqu River Basin within Lesotho as a case study. SWAT has been used in many hydrological studies with respect to climate change (Cousino et al., 2015, Kang et al., 2015, Le and Sharif, 2015, Li et al., 2016, Mittal et al., 2015, Parajuli et al., 2016); however, limited studies have been conducted in the continent of Africa.

A search in the SWAT database (https://www.card.iastate.edu/swat_articles/) for SWAT models related to Africa resulted in 81 articles. One of the articles, Maliehe and Mulungu (2017), conducted a SWAT study of the water demands of the South Phuthiatsana catchment within Lesotho. Of the 81 articles, only 9 included climate change studies, however none of the climate change studies related specifically to South Africa. One of the nine studies did conduct a climate change study for the entire Africa including Lesotho but did not specifically focus on it. Of the 81 articles, only 15 related to South Africa, and none was conducted specifically for Lesotho or the Senqu River Basin with consideration of climate change. The study that included Lesotho in a climate change study evaluating the blue water availability for the entire continent of Africa was conducted by Faramarzi et. al (2013). While the blue water availability is calculated, water scarcity is not evaluated in the study.

Lesotho is a land locked country inside of South Africa with a surface area of 30,355 square kilometers. It ranges from 1400 to 3400 meters in altitude above sea level. Lesotho has the highest low point of any country in the world at 1400 meters above sea level and is the only country in the world that lies entirely above 1000 meters. Water is one of the main exports of Lesotho (London, 2017), mostly from the Senqu river.

The Senqu river originates in the Lesotho highlands and flows westward 2200 km to the west coast where it is discharges into the Atlantic Ocean. The Senqu River basin as shown in Figure 2, has a total catchment area of approximately 1 million square kilometers (Heath and Brown, 2007).

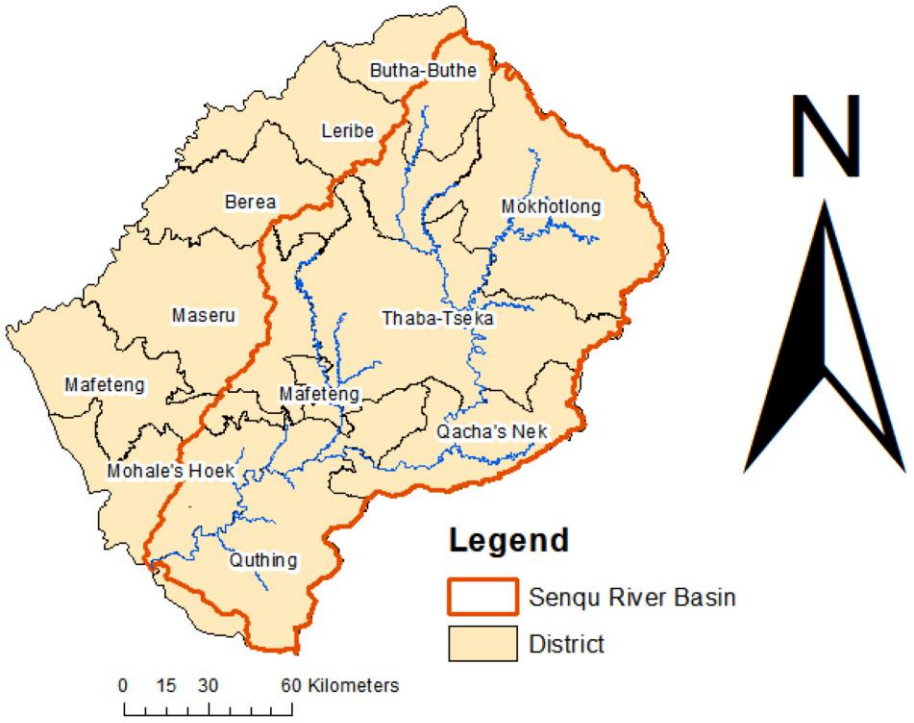

Figure 2: Map of Lesotho with the Senqu River Basin in red.

Water withdrawal within Lesotho is broken up into three main sectors: agriculture, industry, and urban and household use (Cridf, 2017). Industry, urban and household use each make up 46% of water withdrawal individually, while agriculture makes up 8%. This is represented graphically in Figure 3.

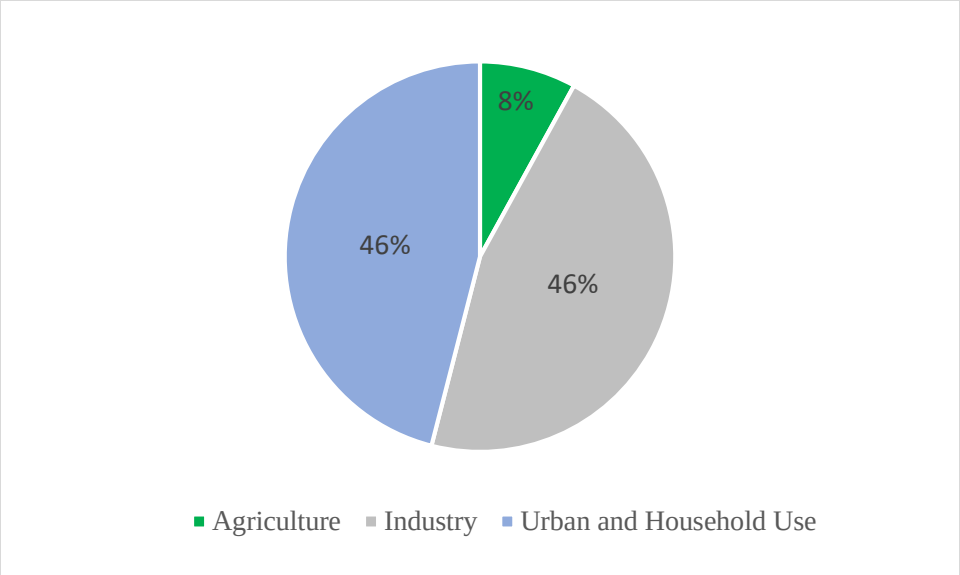

Figure 3: Water withdrawal percentage between agriculture, industry, and urban and household use within Lesotho.

The average household within Lesotho uses between 1000 and 2500 liters/month (Bello et al., 2010) and has an average of 5 members (Ministry of Health [Lesotho], 2014). Within the sector of urban households, 97% of them have access to an improved source of drinking water while only 49% have access to improved sanitation (Ministry of Health [Lesotho], 2014). In rural households, 77% of households have access to an improved source of drinking water and 52% have access to improved sanitation (Ministry of Health [Lesotho], 2014). Research containing information on specific household water allocation could not be found. However, the household water allocation observed as a Peace Corps Volunteer within Lesotho for 2 years is similar to a study conducted by Thompson et al. (2001), which evaluated the change in household water use in the three east African countries of Kenya, Tanzania, and Uganda. Figure 4 presents a graphical representation of typical household use in Lesotho using the research of Thompson et al. (2001) as a guideline.

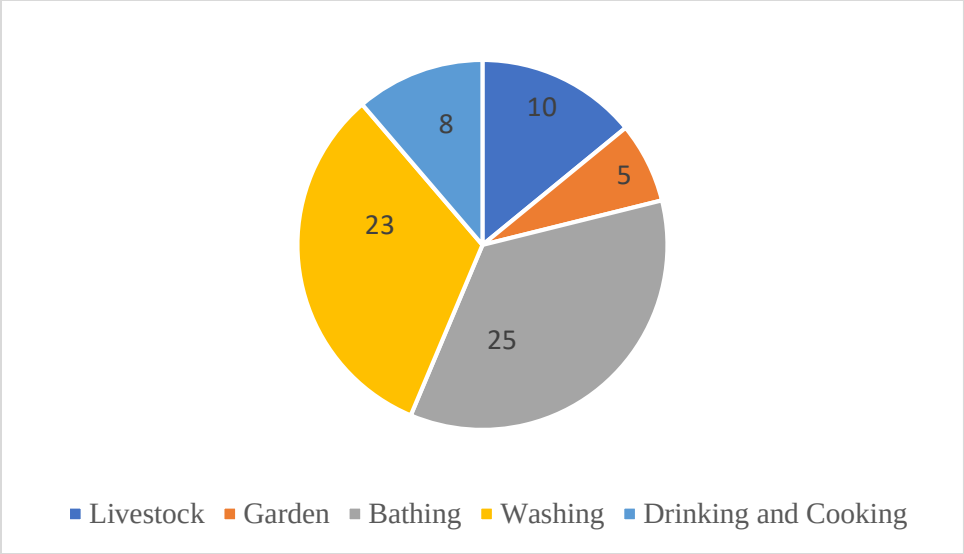

Figure 4: Estimated amount of water used daily in a typical rural household in Lesotho based upon research by (Thompson et al., 2001) and the author's own experience. Washing includes washing dishes, clothes, and cleaning the house.

It was estimated that a majority of daily household water use is allocated to bathing and washing; 25 liters and 23 liters respectively. Washing refers to washing dishes, clothes, and cleaning the house. Basotho (the people of Lesotho) typically have gardens where vegetables are grown, and as such have 5 liters allocated daily. Eight liters are allocated to drinking and cooking and 10 liters for livestock care.

In Lesotho the Senqu River is used by Basotho for grazing animals, growing crops, catching fish and harvesting reeds, thatching grass, growing grass for handicrafts, wild vegetables, trees, medicinal plants and sand (Heath and Brown, 2007). Changes to water available from this river has the potential to impact the livelihood of many Basotho who reside along it. A major stressor on water availability from the Senqu River Basin is the Lesotho Highlands Water Project (LHWP).

Two dams, the Katse and Mohale, divert water from the Senqu River basin and send it to the Vaal River basin in the Gauteng Province in South Africa (Lhwp, 2008). This lowers the amount of water available to the Basotho downstream. The LHWP plans to implement three more dams along the Senqu river.

Lesotho's high elevation mountainous areas are projected to be more sensitive to climate change (IPCC, 2007). Lesotho is also vulnerable to climate change due to its reliance on rain-fed subsistence agriculture, on water resource exports and on hydroelectricity (Mdg, 2013). The 2013 Lesotho Millennium Development Goals status report predicted shorter growing seasons and an increase in extreme weather events (Mdg, 2013). Lesotho has experienced extreme weather events in current history, for example, a drought in 2015 and 2016 which crippled many parts of the country.

Between 75% and 80% of Lesotho's rural population relies on agriculture for their livelihood (Mdg, 2013). Any significant change in the amount of blue water available for agriculture could greatly affect the livelihood of many Basotho as well as have negative impacts on their hygiene and sanitation (Fry et al., 2008).

1.3 Motivation and Objectives

While many SWAT studies exist that evaluate climate change or evaluate water scarcity, there are no studies that could be found that utilize the streamflow outputs of SWAT to measure water scarcity with respect to climate change. There are also no studies found that evaluate the effects of climate change on the Senqu River basin within Lesotho. Therefore, the objectives of this study were: 1) To create a modeling framework that uses ArcSWAT streamflow outputs combined with water footprint analysis to measure how climate change will impact water scarcity of a river basin. 2) To apply the framework on the Senqu River basin within Lesotho to provide the insights of water scarcity in the region.

CHAPTER 2: LITERATURE REVIEW

2.1 History of Measuring Water Scarcity

Measuring water scarcity has evolved over the past few decades. Water Scarcity was first measured on a per capita basis. Falkenmark, Gleik developed a Water Scarcity Index that assumes everyone uses 1000 m^3 per day (Falkenmark et al., 1989, Gleick, 1996). This became a benchmark water scarcity indicator that has been accepted by the World Bank (Brown, 2011). Ohlsson created the Social Water Stress Index by taking the Water Scarcity Index and dividing it by the United Nations Development Program Human Development Index providing an insight into how economic, technological, or other means affect overall fresh water availability in a region (Ohlsson, 2000). The focus then changed from looking at water scarcity per capita to a national scale. The Water Resource Vulnerability Index (Chaves and Alipaz, 2007, Mcnulty et al., 2010, Raskin et al., 1997, Vorosmarty et al., 2005) calculated water scarcity by looking at water consumption at a national scale. The criticality ratio is commonly used in water resource analysis and is defined as the ratio of water withdrawals for human use to total renewable water resources (Alcamo et al., 2000). As population continued to increase a link between water availability and projected population growth was created (Asheesh, 2003). The need to continue to link social and economic variable to water scarcity led to the creation of the Water Poverty Index.

The Water Poverty Index is a comprehensive tool that incorporated social metrics including ecosystem productivity, community, human health, and economic welfare into

measuring water scarcity (Sullivan, 2002). Unfortunately, it is complex and lacks a standardization on how each metric is weighted.

(Pfister et al., 2009) combined the Water Scarcity Index with Life Cycle Impact Assessment to evaluate water stress of an area based on energy used in backup technology, the fraction of freshwater consumption that contributes to depletion, as well at the total water withdrawal from the watershed. Hoekstra (2003) established a method to measure water stress using water footprints. This method is explained more in the following sections. Rijsberman (2006) and Brown (2011) have discussed in length the different water scarcity indices that have been developed. Table 1 provides an overview of the different Water Scarcity Indices that have been developed.

2.2 Water Footprint Analysis

Hoekstra et al. (2011)argues that using the water footprint helps to correct common errors made in other indices. Other indices (Chaves and Alipaz, 2007, Raskin et al., 1997, Vorosmarty et al., 2005) use water withdrawal as an indicator of water use. The Water Footprint differs from Water Withdrawal in that: 1) It does not include blue water use insofar as this water is returned to where it came from, 2) It is not restricted to blue water use, but also includes green and grey water, and 3) It is not restricted to direct water use, but also includes indirect water use(Hoekstra et al., 2011). Blue water is defined as water that is sourced from surface or groundwater and is used in domestic, industry, or agricultural. Green water is water from precipitation stored in soil and is evaporated, transpired, or used by plants. Gray water is water used to create pollutants.

The three most common errors among other indices are:

1) Water withdrawal does not include the water that is returned from the catchment after use. Thus, using this as an indicator at the scale of the catchment is not a good method. A better indicator of blue water consumption is the blue water footprint.
2) Total available water is not a good metric to use to define water availability as it ignores the portion needed to maintain the environment. Thus, the demand required by the environment should be subtracted from the total water available.
3) Evaluation of water scarcity on an annual usage and availability does not paint an accurate picture of variations during the year. Monthly values would be more accurate. (Hoekstra et al., 2011)

A total of five global water footprint studies have been published to date (Fader et al., 2011, Hoekstra and Chapagain, 2007, Hoekstra and Hung, 2005, Hoekstra and Mekonnen, 2012, Wang and Zimmerman, 2016). The most recent water footprint study conducted by Wang and Zimmerman improves on previous water footprint studies by using a hybrid water footprint accounting model with better spatial and sectoral resolution (Wang and Zimmerman, 2016). Wang and Zimmerman report Water Footprints on a national scale.

The Water Footprint of a nation can be calculated through two approaches known as the top-down (input-output) approach and the bottom-up (process-based) approach. In the top-down approach the water footprint of national consumption is shown in equation 1.

$$WF_{cons,nat} = WF_{area,nat} + V_i - V_e \quad (1)$$

In equation 1, $WF_{cons,nat}$ is the water footprint of national consumption measured in m^3/year, $WF_{area,nat}$ is the water footprint within the nation (m^3/year), $V_i$is the virtual-water import (m^3/year), and V_e (m^3/year) is the virtual-water export. Virtual water is defined as the embedded water within a product.

The bottom-up approach is based on calculating the water footprint of a group of consumers where the consumers consist of the inhabitants of a nation and is defined within equation 2.

$$WF_{cons,nat} = WF_{cons,nat,dir} + WF_{cons,nat,indir} \qquad (2)$$

In equation 2, $WF_{cons,nat,dir}$ is the direct water footprint used by the consumer measured in m^3/year. $WF_{cons,nat,indir}$ is the indirect water footprint (m^3/year) and refers to the water consumption and pollution of water that can be associated with the production of the goods and services used by the consumer.

More detail on the calculation of the Water Footprint using both of these methods can be found in the Water Footprint Assessment Manual (Hoekstra et al., 2011). The main difference between the two methods is the different use of input data. The bottom up approach depends on the quality of national consumption data while the top down approach relies on the quality of trade data (Hoekstra et al., 2011).

Table 1: Summary of common water scarcity indices.

Author	Index Name	Equation	Indicators
Falkenmark et al. (1989)	Water Stress Index/Water Scarcity Index	WSI=WA/P WSI=Water Stress Index (m^3/capita/year); WA=Water Availability; P=Population	No Stress: WSI>1700; Water Stress: WSI=1000-1700;
Gleick (1996); Falkenmark and Widstrand (1992)	Basic Human Water Requirements	WSI=WA/P WSI=Water Stress Index (m^3/capita/year); WA=Water Availability; P=Population	
Ohlsson (2000)	Social Water Stress Index	SWSI=WSI/HDI; SWSI (Social Resource Water Stress Index); WSI=Water Stress Index; HDI=Human Development Index	Relative Sufficiency: SWSI=0-5; Stress: SWSI=6-10; Scarcity: SWSI=11-20; Beyond the Barrier: SWSI>20
Raskin et al. (1997)	Water Rescource Vulnerability Index (WTA Ratio)	WTA=W/WA; WTA=Water Resource Vulnerability Index; W=Annual Withdrawal; WA=Available Water Resources	No Water Stress: WTA=0-10%; Low Water Stress: WTA=10%-20%; Mid Water Stress: WTA=20%-40%; High Water Stress: WTA=40%-80%;
Vorosmarty (2000)	Local Relative Water Use and Reuse Index	(D+I+A)/Qc ; D=Domestic Water Withdrawal; I=Industrial Water Withdrawal; A=Agricultural Water Withdrawal; Qc=Sum of all local discharges	

Table 1: Continued.

Author	Index Name	Equation	Indicators
Sullivan (2002)	Water Poverty Index	WPI=sum(w_i *x_i)/sum(w_i) WPI: water poverty index value x_i: component i of the WPI structure (assessment as %) w_i: weight applied to the component i.	The lowest possible level of water poverty: WPI = 100 Level of water poverty: 0 < WPI < 100 the highest possible level of water poverty: WPI = 0
Smakhtin et al. (2005)	Water Stress Indicator (WSI)	WSI=Withdrawals/(MAR-EWR); MAR=Mean Annual Runoff; EWR=Environmental Water Requirements	WSI>1 Overexploited (Current water use tapping into EWR); .6<=WSI<1 Heavily exploited.
Seckler et al. (1999)	IWMI (International Water Management Institute)	WS = PWS/UWS UWS: utilizable water supply PWS: primary water supply	Physical water scarcity: WS ≥ 60% (the region will not be able to meet water demand in future) to people)
Hoekstra (2003)	Blue Water Footprint Analysis	BWS=BWF/(BWA-EWN); BWS=Blue Water Scarcity; BWF=Blue Water Footprint; BWA=Blue Water Available; EWN=Environmental Water Needs;	low blue water scarcity (<100%): moderate blue water scarcity (100–150%): significant blue water scarcity (150–200%): severe water scarcity (>200%).

2.3 Soil and Water Assessment Tool

SWAT is a semi-distributed hydrological model developed by the United States Department of Agriculture used for long term simulations of a variety of processes (Arnold et al., 1998). SWAT operates on a daily time step and is composed of eight major model components including: weather, hydrology, soil temperature and properties, plant growth, nutrients, pesticides, bacteria and pathogens, and land management (Arnold et al., 2012). ArcSWAT is a geographic information system (GIS) interface for SWAT.

SWAT has been used for a myriad of watershed , land use management, water quality, and climate change studies (Cousino et al., 2015, Hayhoe, July 2007, Li et al., 2016, Parajuli et al., 2016, Park et al., 2011, Pierce et al., 2009, Prasad et al., Elhassan et al., 2015, Geza and Mccray, 2008, Lam et al., 2010, Ullrich and Volk, 2009, Arias et al., 2014, Arias et al., 2012).

There are many SWAT studies that focus on climate change, water scarcity, and water footprints, but there are not any that could be found that use SWAT outputs to measure the effects of climate change on water scarcity using the water footprint analysis. A search through the SWAT database (https://www.card.iastate.edu/swat_articles/) for relevant literature was conducted and the results are provided in Table 2.

Table 2: Soil and Water Assessment Tool database search of articles containing water scarcity, water footprint, and climate change studies.

Number of Articles	Search Term	Application Category
13	water footprint	
53	water scarcity	
7	water scarcity	climate change
0	water footprint	climate change

Table 2 demonstrates that while there are a number of articles that focus on water scarcity, there are only 7 that evaluate both water scarcity and climate change. Notable articles that appeared in the search result that relate to just water scarcity include Rodrigues et al. (2014) which created a modeling framework for measuring water scarcity using the water footprint concepts, but did not include a climate change analysis. Schuol et al. (2008) modeled the blue and green water availability of Africa and measured water scarcity using the Water Stress Index. From the 7 articles measuring both water scarcity and climate change impact only Abu-Allaban et al. (2015) and Shrestha et al. (2017) measure the water scarcity impact of climate change on a river basin. However, they do not evaluate water scarcity using the water footprint, but evaluate the relative change in streamflow. Faramarzi et al. (2013) modeled the impact of climate change of blue and green water availability of Africa and evaluated the relative change in total water yield of the continent.

The search of the SWAT database relating to the Senqu basin within Lesotho returns even less studies. Only one SWAT study has been conducted within Lesotho. Maliehe and Mulungu (2017) evaluate the water demand of the South Phuthiatsana river basin. There have been no SWAT studies relating to climate change conducted within Lesotho. Faramarzi et al. (2013) included Lesotho in the assessment of climate change impacts on the blue and green water availability in Africa but did not measure water scarcity of Lesotho. Figure 5 shows the total number of articles within the SWAT database of a particular topic. The 'X' denoted in Figure 5 is the gap in knowledge this paper fills, by combining SWAT with the water footprint analysis to measure the impact of climate change on water scarcity in Lesotho.

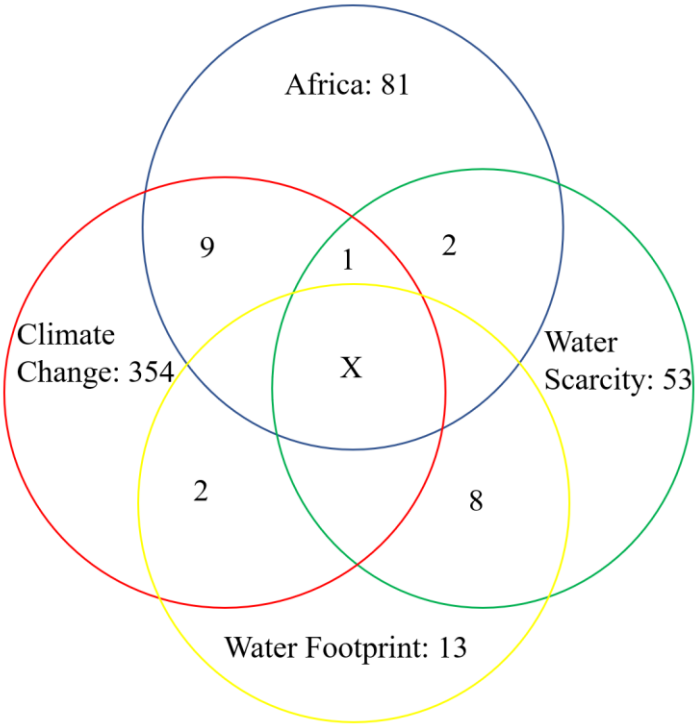

Figure 5: Review of articles within the SWAT database. The total number of articles for a topic is listed. 'X' is the gap in knowledge this paper fills, by combining SWAT with the water footprint analysis to measure the impact of climate change on water scarcity in Lesotho.

SWAT divides a watershed into sub-basins or sub-watersheds and then further divides these sub-basins into hydrologic response units (HRUs). A sub-basin possesses a geographic position in the watershed and is spatially related to other sub-basins. HRUs are portions of a sub-basin that possess unique land use/management/soil attributes. Input data including topography, weather, land use, and soil properties, are used to calculate the runoff, sediment and nutrient loadings from each HRU and then summed together to determine the total loadings from the sub-basin (Arnold et al., 2012, Arnold et al., 2002).

The main inputs needed to perform a SWAT hydrological analysis are a digital elevation model (DEM), daily weather data, soil map, and land use map. Input weather data includes min/max temperatures, precipitation, solar radiation, wind speed, and relative humidity on a daily time step (Arnold et al., 2002).

SWAT outputs variables on three levels titled the HRU output file, the sub-basin output file, and the main channel or reach output file. A summary output file is also created. These files contain a number of outputs including: flow in cubic meters per second (cms) and flow out (cms) of sub-basins, evapotranspiration (cms), sediment concentration in and out (mg/kg) of sub-basins, organic Nitrogen and Phosphorus loads (kg). For a full list of outputs see the SWAT input output manual (Arnold et al., 2002). The SWAT output used in this study will be the FLOW_OUT variable measured in cms.

Water balance is the driving force behind all of the processes in SWAT. The hydrologic cycle simulated by SWAT is based on the water balance equation:

$$SW_t = SW_0 + \sum_{i=1}^{t} \left(R_{day} - Q_{surf} - E_a - w_{seep} - Q_{gw}\right) \quad (3)$$

In equation 3, SW_t is the final water content (mm H_2O), SW_0 is the initial soil water content on day i (mm H_2O), t is the time (days), R_{day} is the amount of precipitation on day i (mm H_2O), Q_{surf} is the amount of surface runoff on day i (mm H_2O), E_a is the amount of evapotranspiration on day i (mm H_2O), w_{seep} is the amount of water entering the vadose zone from the soil profile on day i (mm H_2O), and Q_{gw} is the amount of ground water return flow on day i (mm H_2O). Detailed information regarding the calculation of each of the variables can be found in (Neitsch et al., 2011).

A SWAT model can be calibrated in a number of ways. However, the first step in calibration for any model includes a determination of the most sensitive parameters in the SWAT model through the use of a sensitivity analysis. A sensitivity analysis is the process of determining rate of change in model output with respect to changes in model input (parameters) (Arnold et al., 2012).

There are generally two types of sensitivity analysis that are performed, local and global. A local sensitivity analysis consists of changing one variable at a time while a global consists of allowing all the variables to change. The disadvantage of using a local sensitivity analysis is the value of one parameter depends on the value of related parameters. The disadvantage of global sensitivity analysis is that it requires a large amount of simulations.

2.4 General Circulation Models

When modeling the impact of climate change within SWAT, global coupled ocean-atmosphere general circulation models (GCM) are used to simulate future meteorological variables. GCMs are mathematical models developed to study the climate of the Earth. Many GCMs have been developed by various institutions to study the future impact of climate change on Earth.

In order to compare the projections from many models, a standard set of climate scenarios was developed in 1995 by the Working Group on Coupled Modeling (WGCM) under the World Climate Research Programme (WCRP) called the Coupled Model Intercomparison Project (CMIP) (Pcmdi, 2017). The goal of the CMIP was to provide climate scientists with a database of coupled GCM simulations that follow standardized boundary conditions (https://cmip.llnl.gov/history.html). Climate scenarios were developed by CMIP to better understand the uncertainty between the human contributions to climate change, the response of the Earth system to human activities, the impacts of a range of future climates, the implications of different approaches to mitigation and adaption (Moss et al., 2010). Emission scenarios are descriptions of future potential emissions that affect the Earth's radiation balance and are used to provide input to climate models.

Currently the United Nations Intergovernmental Panel on Climate Change (IPCC) fifth assessment report (AR5) (Ipcc, 2013) analyzes the impact of climate change using the 4th phase of CMIP known as CMIP5. The emission scenarios used within CMIP5 are defined as Representative Concentration Pathways (RCP). There are four RCPs named RCP2.6, RCP4.5, RCP6.0, and RCP 8.5. Each of these numbers represents the estimated targeted radiative forcing at the year 2100. For example, RCP4.5 represents a concentration pathway that approximately results in a radiative forcing of 4.5 W m^{-2} at the year 2100 relative to pre-industrial conditions (Taylor et al., 2011).

One limitation of using GCMs for regional hydrological studies is the coarseness of the resolution. To overcome this limitation the WCRP established the Coordinated Regional Downscaling Experiment (CORDEX) dataset (Lennard et al., 2015). CORDEX created a framework in which scientists around the world created high-resolution Regional Climate Model (RCM) projections using the CMIP5 RCPs. Where various GCMs resolution ranged from 88 km to 785 km the CORDEX RCM resolution is 69 km (Enes, 2017). RCMs were created for Africa and were selected for use in this study due to their finer resolution over GCMs.

2.5 Bias Correcting Climate Models

If the output from a GCM or RCM is not corrected for biases, the model will produce simulations that are not realistic (Hansen et al., 2006, Sharma et al., 2007). Bias correction methods use a transformation algorithm to adjust RCM and GCM outputs. The purpose of bias correction is to identify possible biases between observed and simulated climate variables.

It is assumed that the correction algorithms and its parameterization for current climate conditions are also valid for future conditions. Multiple bias correction methodologies have been developed and those that have been used in research include: change factor and downscaling methods (Park et al., 2011), stochastic weather generators (Le and Sharif, 2015), cumulative distribution functions (Pisinaras, 2016), change factor for temperature and quantile mapping for precipitation (Basheer et al., 2016), artificial neural networks (Kang et al., 2015), or through the use of a fitted histogram equalization function (Yan et al., 2015) and daily bias corrected and constructed analogs (Ficklin et al., 2015). A complete review of downscaling methods can be found in (Maraun et al., 2010). Table 3 provides the main bias correction methodologies used.

The six main methods of bias correcting summarized in Table 3 are linear scaling, local intensity scaling (LOCI), power transformation, variance scaling, delta change, and distribution mapping. Linear scaling corrects the RCM data by adjusting the mean monthly values with a correction factor. While the bias correction is fairly simple to perform, it adjusts all events, including extreme weather events, with the same correction factor. It also cannot correct for the frequency of which precipitation events occur. LOCI attempts to make up for the disadvantages of linear scaling by adjusting the RCM data to have the same mean, wet-day frequencies, and intensity as the observed data (Schmidli et al., 2006). However, LOCI cannot reproduce the effect of regional processes and does not allow for precipitation variances to be corrected. Power transformation and variance scaling adjust both the variance and mean of precipitation and temperature respectively. However, the power transformation of precipitation is unable to accurately correct the probability of dry days and precipitation intensity. The delta-change approach does not account for potential future changes in climate. In other words, the delta-change approach does not allow the number of dry vs wet days to change (Graham et al., 2007).

Distribution mapping matches the cumulative distribution function (CDF) of the simulated data to the observed data. The simulated data now matches the statistics of the observed data e.g. the mean and standard deviation as well as the probability of a precipitation event of the simulated data now match the observed data. The distribution method, however, cannot accurately correct the interannual variability of the simulated data. Teutschbein and Seibert (2012) conducted a review of these bias correction methodologies and compared each of them against each other to see which method provided more accurate monthly streamflow. The distribution mapping method was found to be the best correction method in the study.

Table 3: Common bias correction methodologies.

Name	Literature	Summary	Advantages	Disadvantages
Linear Scaling	Lenderink et al. (2007)	Adjusts monthly mean values and offers corrected data with a variability more consistent with the original RCM data (Graham et al 2007a). Corrected RCM simulations will perfectly agree in their monthly mean values with the observations	Accounts for bias in mean	1) All events are adjusted with the same correction factor. 2) Unable to correct for bias in wet-day frequency and intensity.
Local Intensity Scaling	Schmidli et al. (2006)	Adjusts both mean and wet-day frequencies and wet day intensities in three steps. The adjusted control and scenario precipitation both have the same mean, wet-day frequency and intensity as the observed time series.	Adjusts mean and wet day frequencies and intensities.	1) Does not reproduce the effect of regional process. 2) Does not allow for difference in variance to be corrected.
Power Transformation of Precipitation	Leander and Buishand (2007)	Uses an exponential form, $a \cdot P^b$ to adjust variance of precipitation time series. Find parameter b by matching coefficient of variation (CV) of RCM with CV of observed daily precipitation. Then long term monthly mean of observed precip is matched with historical RCM using linear scaling.	Accounts and corrects for both mean and variance in precipitation time series	1) Limited to precipitation 2) Does not provide corrected RCM data with accurate probability of dry days and precipitation intensity. (Teutschbein and Seibert, 2012)
Variance Scaling of Temperature	Chen et al. (2011)	RCM-simulated time series is adjusted by linear scaling then are shifted on a monthly basis to a zero mean. (Teutschbein and Seibert, 2012)	Corrects for mean and variance	Limited to temperature
Distribution mapping	Sennikovs and Bethers (2009)	Corrects the distribution function of RCM-simulated climate values to agree with the observed distribution function. Create a transfer function to shift the occurrence distributions of precipitation and temperature (Teutschbein and Seibert, 2012)	Simulated data statistically matches observed data	Does not correct interannual variability and temperature/precipitation correlation properties of simulated data

CHAPTER 3: METHODOLOGY

3.1 Study Site and Overview of Methodology

The Senqu river basin within Lesotho was evaluated in this research. Figure 6 denotes a detailed map of the Senqu basin with the locations of the dams, streamflow gauge stations, Climate Forecast System Reanalysis (CFSR) stations, and RCM stations. The Senqu river basin contains three different streamflow gauges, SG5, SG17, and SG3. SG5 and SG17 are upstream from the basin outlet streamflow gauge, SG3. SG17 lies directly downstream of the Mohale dam, and SG5 lies downstream of the Katse dam. Mean annual temperature range from 15.2 °C (59.36 °F) in the lowlands to 7 °C (44.6 °F) in the highlands. Precipitation varies from year to year and most of it occurs during the seven-month wet summer season from October to April. The peak rainfall period is from December to February and most parts of the country record over 100 mm per month (Lms, 2013). The Senqu river basin has a basin area of approximately 20000 km^2 and ranges in elevation from 1400 m to 3470 m. Figure 7 shows an overview of the methodology as well as the data sets presented in this study and how they are used to ultimately calculate water scarcity.

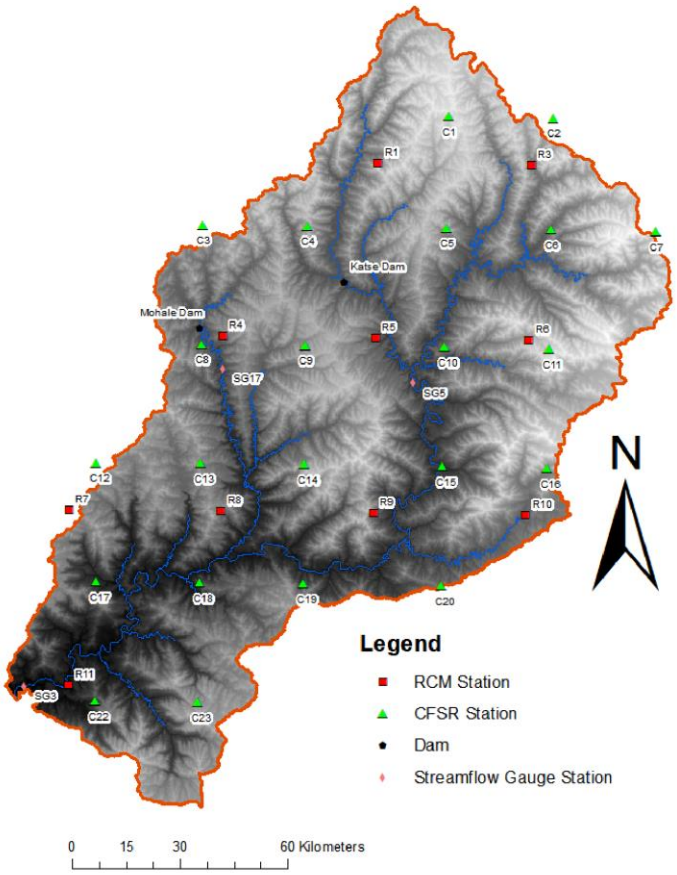

Figure 6: Map of Senqu River Basin study site. Locations of dams, gauging stations, Regional Climate Model (RCM) stations, and Climate Forecast System Reanalysis (CFSR) stations are displayed.

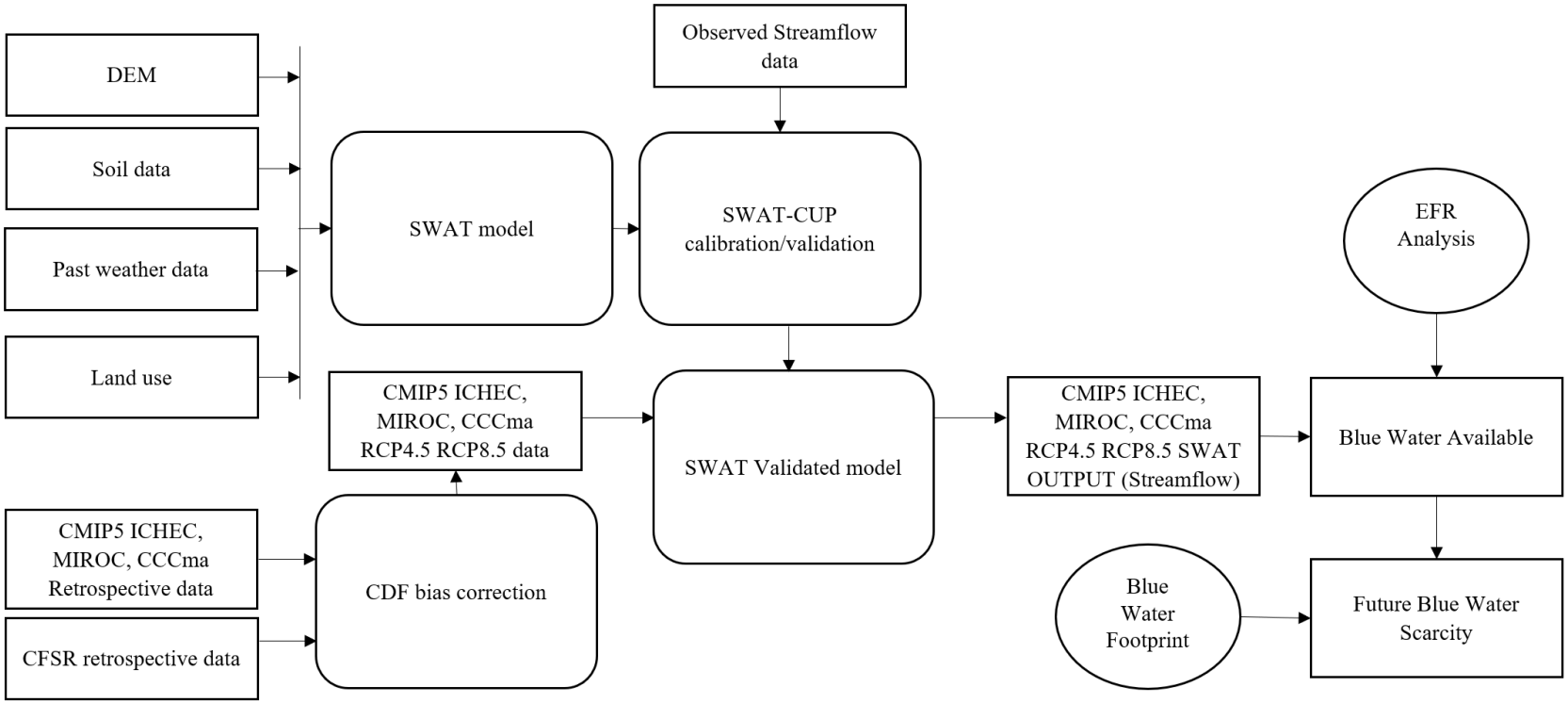

Figure 7: Modeling framework for evaluating blue water scarcity using the Soil and Water Assessment Tool (SWAT). The abbreviations in the figure are: DEM (Digital Elevation Model), CFSR (Climate Forecast System Reanalysis), CMIP5 (Coupled Model Intercomparison Project), SWAT-CUP (SWAT Calibration and Uncertainty Program), EFR (Environmental Flow Requirement), RCP (Representative Concentration Pathway), CDF (Cumulative Distribution Function)

3.2 The ArcSWAT Model

SWAT is used in this study to evaluate the blue water available in the Senqu river basin by using streamflow (FLOW_OUT) at the river basin exit, SG3. The FLOW_OUT SWAT output variable is measured in cubic meters per second (cms) and is used as a measure of the total water available of the Senqu river.

The inputs that are required for SWAT to perform a hydrologic analysis are a digital elevation model, soils map, land use map, and weather data. To also perform a climate change study, future climate data will be inputted into the ArcSWAT model. Detailed information on the inputs are below.

3.2.1 Digital Elevation Model

A 90 m digital elevation model (DEM) of Lesotho was obtained from CGIAR Consortium for Spatial Information based on the global Shuttle Radar Terrain Mission (http://srtm.csi.cgiar.org). This information was used to delineate rivers and watersheds within the ArcSWAT interface.

3.2.2 Soils Map

A soils map of the world was downloaded from the Food and Agriculture Organization (Team, 2007). The area covering Lesotho was extracted using ArcMap and was projected into UTM35S. Lesotho is largely composed of Rhodic Ferralsols, Lithosols, Solodic Planosols, Eutric Planosols, and Chromic Cambisols.

3.2.3 Land Use Map

A land use map was downloaded from the Regional Centre for Mapping of Resources for Development (RCMRD) GeoPortal (http://geoportal.rcmrd.org). The map has data from 2014 and contains the land use classifications of Natural Forest, Plantation Forest, Grassland, Shrubland, Orchard, Annual Cropland, Vegetated Wetland, Water Body, Settlement, Mine and Quarry, and Otherland.

3.2.4 Weather Data

Past weather data from 1970-2010 including daily precipitation, and temperature recordings were procured from the Lesotho Meteorological Services (LMS). SWAT also requires the location of local weather stations. After these data were acquired, it was determined to be unfit for use in the SWAT model. Continuous data are needed for the SWAT model, and the data from LMS is missing several months and some years of data. Because of this, modeled data from the Climate Forecast System Reanalysis (CFSR) were used. CFSR model simulations provide climate data in areas where regional climate data may not be available due to lack of resources. The CFSR is a global, high resolution, coupled atmosphere-ocean-land surface-sea ice system designed to provide the best estimate of the state of these coupled domains (Ncar, 2017). The CFSR simulations use data from the National Centers for Environmental Prediction (NCEP). CFSR daily precipitation and temperature data are available globally for time periods from 1979 to March 2011. The data are given at a 38-km resolution. A study by Fuka et. al (2014) demonstrated that using CFSR precipitation and temperature data to force a watershed model provides stream charge simulations that are as good or better than models forced using traditional weather gauging stations data (Fuka et al., 2014). This data has been obtained for

Lesotho and the locations of the CFSR station are shown in Figure 6 located at the beginning of this section. Each CFSR station is denoted with a 'C' followed by a number.

3.2.5 Future Climate Data

Future climate projections were obtained from the Coordinated Regional Downscaling Experiment (CORDEX) dataset. This data includes precipitation, min/max temperature, relative humidity, solar radiation, and wind speed on a daily timescale. CORDEX are regionally downscaled climate models established by the World Climate Research Program (WCRP) (Lennard et al., 2015). The RCPs chosen for study were 4.5 and 8.5. The RCPs are described in further detail in (Moss et al., 2010). The models in this study were also chosen based on their location in the family tree, which indicates the similarity among models (Knutti et al., 2013). The models chosen are relatively independent based on their location in the tree. (Pierce et al., 2009) showed that regardless of the GCMs selected based on the quality of their simulation in the region of interest, the results do not provide systematically different results then choosing models randomly. They found that using a multi model ensemble is superior to using any one model. After approximately five models, the model skill asymptotes meaning adding more models does not significantly change the accuracy of the results.

GCMs are used to generate large scale climate scenarios. When performing an impact assessment on a smaller region, it is necessary to downscale the outputs from the GCMs. This is due to scale related sensitivities. GCMs that are not downscaled do not accurately capture weather events on a regional scale. CORDEX data provides downscaled GCM data that was used in this study. The GCMs chosen from the CORDEX database were ICEHC-EC-EARTH, MIROC-MICROC5, and CCCma-CanESM2. Each of the GCMs were downscaled using the

RCA4 model developed by the Swedish Mereological and Hydrological Institute (Kjellstrom et al.)

The bias correction chosen for this study is the distribution mapping method. This method is found throughout literature and has been given many names including 'probability mapping' (Block Paul et al., 2009, Ines and Hansen, 2006), 'quantile-quantile mapping' (Boé et al., 2007, Johnson and Sharma, 2011, Piani et al., 2010), and 'histogram equalization' (Rojas et al., 2011, Sennikovs and Bethers, 2009). Distribution mapping is done by creating a transfer function to shift the occurrence distributions of precipitation and temperature (Sennikovs and Bethers, 2009). For precipitation events the Gamma distribution (Thom, 1958) with shape parameter α and scale parameter β is assumed to be suitable. x is the normalized daily precipitation and the *pdf* is the probability density function.

$$pdf(x) = \frac{e^{\frac{-x}{\beta}} \cdot x^{\alpha-1}}{\beta^{\alpha} \cdot \Gamma(\alpha)}; x \geq 0;\ \alpha, \beta > 0 \qquad (4)$$

This methodology has been used in multiple studies to analyze precipitation data (Block Paul et al., 2009, Boé et al., 2007, Ines and Hansen, 2006, Johnson and Sharma, 2011, Piani et al., 2009, Piani et al., 2010). The shape parameter, α, controls the profile of the distribution. If $\alpha<1$ this indicates an exponentially shaped Gamma distribution which is asymptotic at both axes. If $\alpha=1$ this is a special case and characterizes an exponential distribution. If $\alpha>1$ the shape is a skewed unimodal distribution curve. The scale parameter, β, determines the dispersion of the Gamma distribution (Teutschbein and Seibert, 2012). If β is small it leads to a more compressed distribution which has lower probabilities of extreme events. Whereas if β is larger this causes a stretched distribution and shows higher probabilities of extreme events.

In order to create a transfer function $y = f(x)$, where x and y are the simulated and corrected values of precipitation respectively, and such that the distribution of y matches that of the observations, the cumulative distribution function is plotted (Piani et al., 2009). The Cumulative Distribution Function (CDF) is defined in equation 5.

$$CDF(x) = \int_0^x \frac{e^{\frac{-x'}{\beta}} \cdot x'^{(\alpha-1)}}{\beta^{\alpha} \cdot \Gamma(\alpha)} dx' + CDF(0) \qquad (5)$$

CDF (0) is the fraction of days with no precipitation. The transfer function of $y = f(x)$ will obey the equation: $CDF_{obs}(f(x)) = CDF_{sim}(x)$. Figure 8 shows a graphical representation of the process using a synthetic data set.

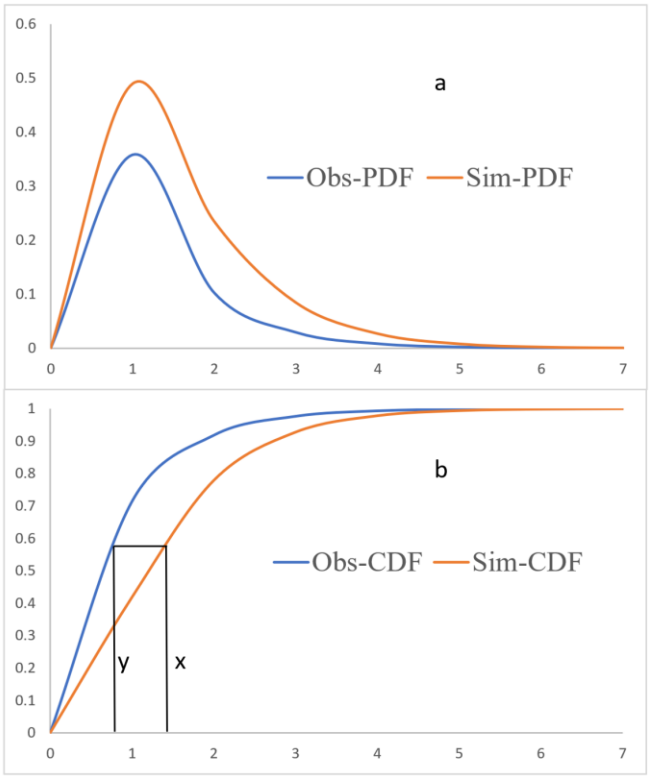

Figure 8: The Probability Density Function (PDF) (a) and Cumulative Distribution Function (CDF) (b) of a synthetic data set. Obs and sim are the observed and simulated data respectively. The CDF is obtained by integrating the PDF in **a.** The transfer function is obtained by solving: $CDF_{obs}(f(x)) = CDF_{sim}(x)$ in **b.**

Temperature is mapped similarly with a transfer function. Temperature is assumed to fit the Gaussian distribution in equation 6.

$$f_N(x|\mu,\delta^2) = x^{(\alpha-1)} \cdot \frac{1}{\delta\cdot\sqrt{2\pi}} \cdot e^{\frac{-(x-\mu)^2}{2\delta^2}}; x\epsilon\mathbb{R} \quad (6)$$

where μ is the location parameter and δ is the scaling parameter. The scale parameter, δ, determines the standard deviation which shows how much the Gaussian distribution is stretched or compressed. The location parameter, μ, is the mean and determines the location of the distribution. The transfer function is derived in a similar fashion to the precipitation, where the CDF is computed by integrating the Gaussian distribution and solving for $CDF_{obs}(f(x)) = CDF_{sim}(x)$.

The distribution mapping method was chosen because it gave the best correction results when compared against the linear scaling, local intensity scaling, power transformation and variance scaling methodologies (Teutschbein and Seibert, 2012).

The software used to bias correct the data was the tool called CMhyd. CMhyd is a tool that has many bias correction methodologies. Teutschbein and Seibert (2012) provide a review of the bias correction methodologies included in CMhyd.

3.2.6 Limitations of Data

It is important to note the limitations of the data used in this study. Lesotho is a small developing country, and as such publicly available data were limited in their capacity to produce accurate results. Any results elucidated from this study should be looked at with the knowledge of its limitations and should only be used to guide water policy or water resource allocation with much caution.

3.2.6.1 Limitations of SWAT Input Data

The sources of the main SWAT inputs were described in Sections 3.2.1-3.2.5. The limitations of those inputs are presented in Table 4. The soils map obtained from Food and Agricultural Organization is a global soil map since a soils map of Lesotho could not be found. The global soil map is very coarse, and does not show all of the soil types within Lesotho. There are five main soil types prevalent in Lesotho, and the FAO map only provides data on three. The land use map obtained from the RCMRD Geoportal is not up to date. The map presents land use in Lesotho in the year 2014. It also has land use classifications that are not within the SWAT land use classification database. While many of the RCMRD land use classifications could match with the appropriate SWAT classification, there was one RCMRD classification labeled 'Otherland' that could not be appropriately matched within the SWAT classification database. The author attempted to contact the map producer but was unable to obtain clarification on what 'Otherland' was and had to make a best estimation. The term 'Otherland' was approximately 3% of the total land use and was reclassified as 'South Western Range'. This choice was made based on the land use that was already classified, the land use that was missing, and the author's knowledge of Lesotho. The author lived in Lesotho for 2 years as a Peace Corps volunteer and traveled around the country.

CFSR weather data were used in lieu of observed weather data as stated previously. While observed weather data was available for some parts of Lesotho, it was missing several months, and sometimes years of data. The observed weather stations overlapped with the CFSR virtual stations in five locations within Lesotho. A Kruskal-Wallace test was performed to evaluate whether there was a significant difference between the precipitation data at these locations.

Of the five locations, two of them reported as having a significant difference between the data sets. This suggests the CFSR data set does not accurately capture precipitation events at all parts of Lesotho, but due to lack of available data the CFSR data was used.

Table 4: Limitations of Soil and Water Assessment Tool (SWAT) input data.

Type of Data	Source	Limitations
Soil Map	Food and Agricultural Organization	This is a global soil map and the resolution for the Senqu River basin is coarse. This map doesn't accurately capture all the soil variety within the study area.
Land Use Map	RCMRD Geoportal (http://geoportal.rcmrd.org)	This land use map is from 2014 and some of the land use types could not be found within the SWAT land use classification system. The term 'Otherland' within the land use map also was subject to the author's best estimation.
Weather	Climate Forecast System Reanalysis (CFSR)	CFSR weather data was used in lieu of observed weather data. CFSR data was significantly different in some locations than the observed weather data.

3.2.6.2 Limitations of Global Climate Model Data

As discussed previously, there have been limited SWAT studies evaluating the impact of climate change in Southern Africa. GCMs and RCMs such as the HadRM3P are prevalent for developed countries such as the United States (Mote et al., 2015). The CORDEX-Africa project provides 10 RCMs for the Africa region. The choice of GCM for the study region can have an impact on the future SWAT projections. The CORDEX-Africa GCMs were all able to simulate the seasonal mean and annual cycle accurately across Africa, but in some locations individual models can exhibit significant biases in some sub-regions and seasons (Nikulin et al., 2012). A common problem within a majority of the CORDEX-Africa GCMs is precipitation events occurring too early during the diurnal cycle.

It is recommended and has been shown that using a multi-model average helps offset climate variability errors within individual models and produces climate events similar to observation data (Pierce et al., 2009). However, using a multi-model ensemble does not correct the systematic bias in the precipitation during the diurnal cycle (Nikulin et al., 2012). This study used a multi-model ensemble as well as individual models, but because of the lack of studies within the region, the GCMs chosen for the study may not produce as accurate of results if other GCMs had been chosen.

3.2.7 Calibration and Validation

The Sequential Uncertainty Fitting (SUFI-2) algorithm (Abbaspour et al., 2004, Abbaspour et al., 2006) within SWAT-CUP (Abbaspour, 2011) was used for model calibration, validation, sensitivity, and uncertainty analysis. SUFI-2 utilizes an objective function to capture the majority of observed data within a 95% prediction uncertainty (95PPU) in an iterative process. The Nash-Sutcliffe (NS) objective function was chosen for this study. The 95PPU is calculated at the 2.5% and 97.5% level of the cumulative distribution of output variables obtained through Latin hypercube sampling. With each iteration the 95PPU gets smaller. The model was ran for 1000 simulations for 5 iterations. After each iteration of 1000 simulations, the program adjusted the input parameters.

Two statistics known as the P-factor and the R-factor are used to quantify the fit between the 95PPU and the observed variable. The P-factor is the percentage of observed data enveloped by the model and the R-factor is the thickness of the 95PPU envelope. The larger they are the better the 95PPU fit. It is recommended a P-factor > 70% and a R-factor close to 1 for streamflow (Abbaspour, 2011). Other common statistics used to measure the goodness of fit of the calibrated/validated model are the Pearson's correlation coefficient (r) and coefficient of

determination (R^2), Nash-Sutcliffe efficiency (NSE), Root Mean Square Error (RMSE), RMSE-observations standard deviation ratio (RSR), and Percent Bias (PBIAS). The statistics used to measure the goodness of fit in this study were the NSE, RSR, and PBIAS. Although the R^2 value is given by SWAT-CUP, it was not used as a determining statistic for this model evaluation. The R^2 statistic is oversensitive to outliers and insensitive to additive and proportional differences and has not been recommended to be used to determine the goodness of fit for hydraulic models (Legates and Mccabe, 1999).

The NSE is provided in equation 7 and is a normalized statistic that determines the relative magnitude of the residual variance compared to the measured data variance (Nash and Sutcliffe, 1970). Y_i^{obs} is the ith observation for the observed dataset being evaluated, Y_i^{sim} is the ith simulated value for the modeled dataset, Y^{mean} is the mean of the observed dataset, and n is the total number of observations.

$$NSE = \left[\frac{\sum_{i=1}^{n}\left(Y_i^{obs} - Y_i^{sim}\right)^2}{\sum_{i=1}^{n}\left(Y_i^{obs} - Y_i^{mean}\right)^2}\right] \qquad (7)$$

The NSE ranges from -∞ to 1, where 1 is the optimal value. If the NSE value is negative, it means the mean of the observed data set is a better predictor of the observed data than the simulated value, which is not acceptable. The NSE has been used in several hydrological studies, and Servat and Dezetter (1991) found the NSE to be the best objective function for reflecting the overall fit of a hydrograph. The generally accepted range of NSE values is provided by (Moriasi et al., 2007) and are in Table 5.

The PBIAS provided in equation 8, measures the average tendency of the simulated data to be larger or smaller than their observed counterparts (Gupta Hoshin et al., 1999). The variables in the given equation are the same as in the NSE equation.

$$PBIAS = \left[\frac{\sum_{i=1}^{n}(Y_i^{obs} - Y_i^{sim}) * (100)}{\sum_{i=1}^{n}(Y_i^{obs})}\right] \qquad (8)$$

The best value for the PBIAS is zero, where a low magnitude indicates accurate model simulation. The PBIAS is used in this study because 1) It was recommended by the American Society of Civil Engineers (Asce, 1993), and 2) it has the ability to clearly indicate poor model performance (Moriasi et al., 2007).

The RSR provided in equation 9 is calculated as the ratio of the RMSE and the standard deviation. The RSR standardizes the RSME using the observation's standard deviation.

$$RSR = \frac{RMSE}{STDEV_{obs}} = \left[\frac{\sqrt{\sum_{i=1}^{n}(Y_i^{obs} - Y_i^{sim})^2}}{\sqrt{\sum_{i=1}^{n}(Y_i^{obs} - Y_i^{mean})^2}}\right] \qquad (9)$$

The RSR has an optimal value of 0, which indicates a perfect model simulation. The RSR was chosen because it is a common statistic used in error index statistics and is a clear indicator of model performance (Moriasi et al., 2007).

Table 5: General performance ratings for recommended statistics for a monthly time step (Moriasi et al., 2007).

Performance Rating	RSR	NSE	PBIAS (%)
Very Good	0.00≤RSR≤0.50	0.75<NSE≤1.00	PBIAS < ±10
Good	0.50<RSR≤0.60	0.65<NSE≤0.75	±10 ≤ PBIAS < ±15
Satisfactory	0.60<RSR≤0.70	0.50<NSE≤0.65	±15 ≤ PBIAS < ±25
Unsatisfactory	RSR>.7	NSE≤0.50	PBIAS ≥ ±25

Three streamflow gauging stations were calibrated for the period given in Table 6. The two upstream streamflow gauges, SG5, and SG17, were calibrated from 1986 to 2002. The downstream streamflow gauge, SG3 was calibrated from 1985 to 2002 and validated from 2003 to 2013

Table 6: Calibration and validation periods for streamflow gauging stations.

Station	Calibration Period	Validation Period
SG3	1985-2002	2003-2013
SG5	1985-1990	-
SG17	1985-1990	-

3.3 Indicators of Hydrologic Alteration Analysis

An Indicators of Hydrologic Alteration analysis is a common tool used to evaluate whether dams impact the hydrologic characteristics of a river basin (Cochrane et al., 2014, Timpe and Kaplan, 2017). An Indicators of Hydrologic analysis was performed in this study to determine the impact of the Katse and Mohale dams on the flow of the river at the three gauging stations. Flow duration curves were created for each station for pre-dam and post-dam analysis. A Kruskal-Wallace test was performed on each flow duration curve to determine if there was a significant difference in change of streamflow between pre and post dam construction. The null hypothesis of the Kruskal-Wallace test assumes the two sets of data are not significantly different. If the calculated p-value is less than 0.05 ($p<0.05$) the null hypothesis can be rejected.

3.4 Water Scarcity

Blue water scarcity provided in equation 10 was defined as the ratio of the blue water footprint in the basin to the blue water available in that basin (Hoekstra et al., 2011).

$$BW_{scarcity\,(x,t)} = BW_{footprint\,(x,t)} / BW_{available\,(x,t)} \qquad (10)$$

The blue water footprint, $BW_{footprint(x,t)}$, of human activities is defined as "the volume of surface and groundwater consumed as a result of that activity, whereby consumption refers to the volume of freshwater used and then evaporated or incorporated into a product" (Hoekstra et al., 2012). $BW_{available}$ is the amount of water that is available for use for a specific location (x) at time of year (t). Not all of the water that resides within the river is available for use.

Hence, the definition of $BW_{available}$ is the amount of water that can be abstracted without affecting the ecology of the river. The amount of water needed by the river to maintain its ecology is known as the Environmental Flow Requirement (EFR). The EFR of the Senqu river is unknown, hence the presumptive standard method will be used (Richter et al., 2012). The presumptive standard method assumes that 20% of the natural monthly mean flow can be allocated for consumptive use. It has been used in similar previous studies in calculating water availability when the EFR of a river was unknown (Hoekstra et al., 2012, Rodrigues et al., 2014). Hoekstra et al. (2012) used the presumptive method when evaluating the water availability of the Senqu river within South Africa. EFR is represented in equation 11.

$$EFR_{x,t} = 0.8 * Q_{mean(x,t)} \qquad (11)$$

where $Q_{mean\ (x,\ t)}$ is the long term monthly mean, for a specific location (x) at time of year (t). In this study, $Q_{mean\ (x,\ t)}$ is defined as the streamflow at the SG3 location. The term $BW_{available}$ is then computed in equation 12.

$$BW_{available} = Q_{(x,t)} - EFR_{x,t} \qquad (12)$$

Hoekstra et al. (2012) measures the blue water footprint of water basins by converting the data from the National Water Footprint Report (Mekonnen and Hoekstra, 2011). The National Water Footprint Report gives the blue water footprints of individual countries. Hoekstra et al. (2012) converts this data into Blue Water Footprints by basins. This report will use the original data from the National Water Footprint Report and use the data to measure the Blue Water Scarcity of Lesotho.

This study calculated the Blue Water Scarcity on a yearly basis. The SWAT output provided the Blue Water Available from the SG3 river basin outlet. The Blue Water Footprint was assumed to be constant for the future scenarios. What this study answers, is given Lesotho's water footprint, how will future climate change scenarios impact Lesotho's blue water scarcity. The degree of blue water scarcity was divided into four categories as provided by Hoekstra and Mekonnen (2012):

- Low blue water scarcity (<100%): the blue water footprint is lower than 20% of natural runoff and does not exceed blue water availability; river runoff is unmodified or slightly modified; presumed environmental flow requirements are not violated.
- Moderate blue water scarcity (100–150%): the blue water footprint is between 20 and 30% of natural runoff; runoff is moderately modified; environmental flow requirements are not met.
- Significant blue water scarcity (150–200%): the blue water footprint is between 30 and 40% of natural runoff; runoff is significantly modified; environmental flow requirements are not met.
- Severe water scarcity (>200%). The monthly blue water footprint exceeds 40% of natural runoff; runoff is seriously modified; environmental flow requirements are not met.

The latest global water footprint analysis provides Lesotho's blue water footprint to be 2850 million m^3/year (Wang and Zimmerman, 2016). This is the blue water footprint for the entirety of Lesotho. Since the Senqu river basin is approximately two-thirds the size of Lesotho, it would not be accurate to judge Lesotho's level of water scarcity on its entire footprint. Three scenarios were used which evaluate the water footprint based on population.

The first scenario was a conservative outlook which evaluated the entire country assuming that the Senqu River basin is the sole source of water. Hence the entire water footprint of Lesotho was used. The second scenario took the national blue water footprint and divided by the total population of Lesotho to obtain a per capita water footprint. The modified water footprint was obtained by multiplying per capita water footprint by the population within the Senqu basin. The third scenario used the per capita blue water footprint and multiplied by the projected population growth per year. This provided a water footprint that increased yearly with expected population growth. The economic status of Lesotho was assumed to remain constant, and the increased blue water demand due to population growth was evaluated. Scenario 3 evaluated water scarcity over the entirety of Lesotho similar to Scenario 1. This was done because it is not known in which areas of Lesotho the population would increase. The projected population increase from 2020 to 2100 is presented in Figure 9.

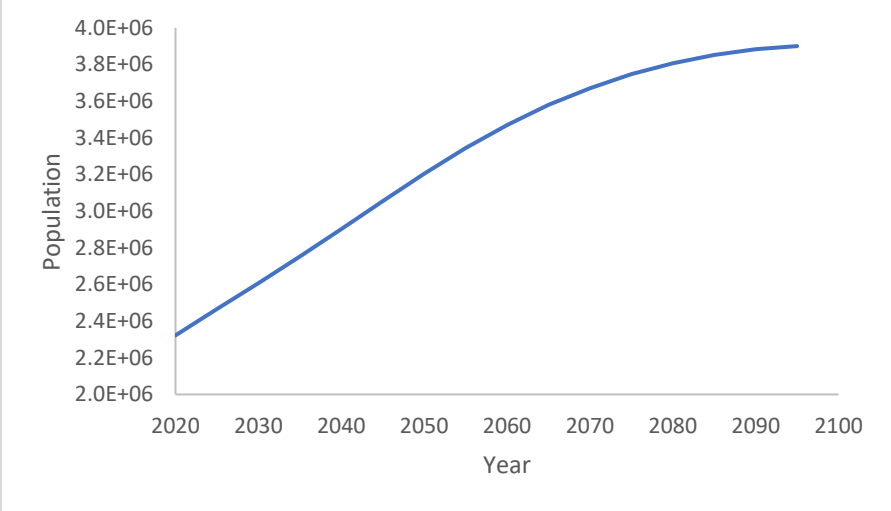

Figure 9: Projected population increase in Lesotho from 2020 to 2100. Data obtained from the World Population Review (Lesotho Population, 2018).

The projected population growth rate was obtained from the World Population Review online database (Lesotho Population, 2018). The population of Lesotho is expected to reach approximately 3.9 million people by 2100.

CHAPTER 4: RESULTS AND DISCUSSION

4.1 Results

4.1.1 Bias Correction

Each GCM station was downscaled using the same RCA4 method and had the same spatial location within Lesotho. Each downscaled GCM is henceforth referred to as RCM. Each RCM precipitation and min/max temperature were bias-corrected using the CDF mapping procedure. Figure 10 shows the results of the ICHEC CDF mapping procedure for precipitation while Figures 11 and 12 show CDF mapping for min and max temperatures respectively at RCM station 1. Only the ICHEC bias corrected data are shown below for the first station. The bias correction methodology corrects all of the RCM models at each station in the same way. It is not necessary to graphically represent each RCM result.

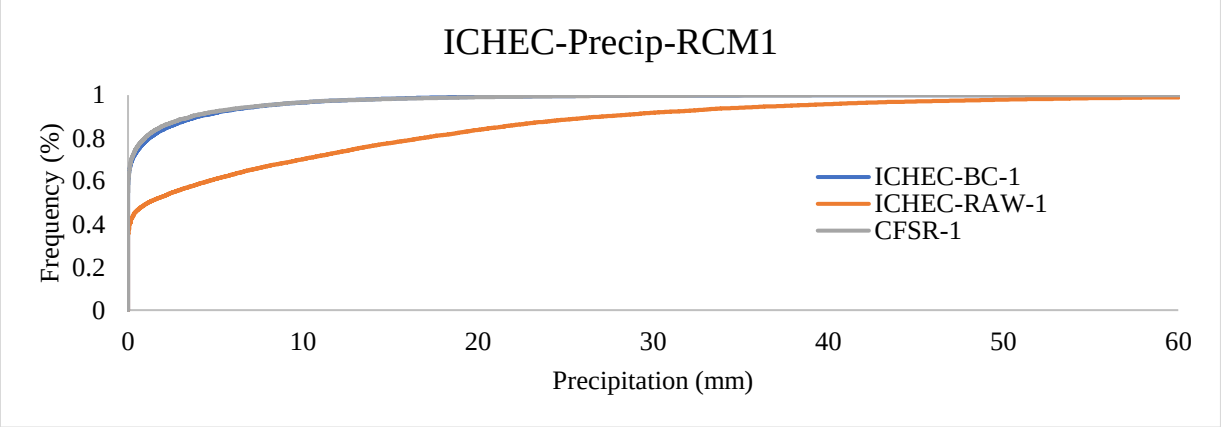

Figure 10: ICHEC precipitation Cumulative Distribution Function mapping results for station 1. ICHEC-BC-1 refers to the bias-corrected Regional Climate Model (RCM) data at location R1, ICHEC-RAW-1 refers to the unbias-corrected RCM weather data at location R1, and CFSR-1 refers to the Climate Forecast System Reanalysis weather data at location C1.

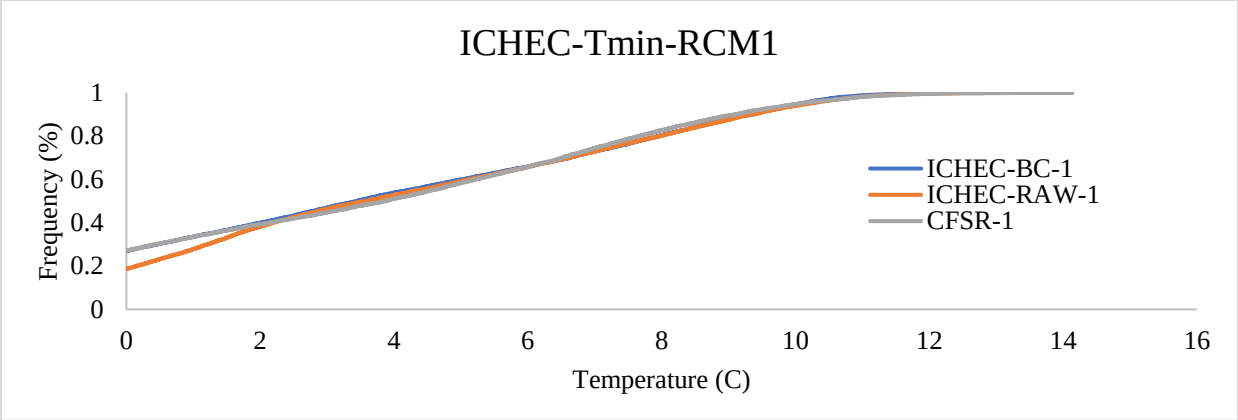

Figure 11: ICHEC minimum temperature Cumulative Distribution Function mapping results for station 1. ICHEC-BC-1 refers to the bias-corrected Regional Climate Model (RCM) data at location R1, ICHEC-RAW-1 refers to the unbias-corrected RCM weather data at location R1, and CFSR-1 refers to the Climate Forecast System Reanalysis weather data at location C1.

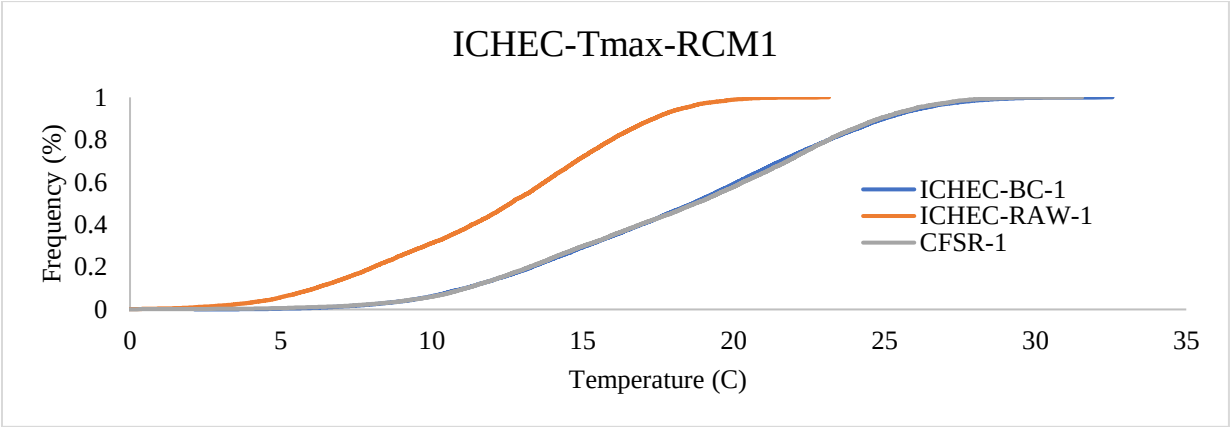

Figure 12: ICHEC maximum temperature Cumulative Distribution Function mapping results for station 1. ICHEC-BC-1 refers to the bias-corrected Regional Climate Model (RCM) data at location R1, ICHEC-RAW-1 refers to the unbias-corrected RCM weather data at location R1, and CFSR-1 refers to the Climate Forecast System Reanalysis weather data at location C1.

The term ICHEC-BC-1 refers to the bias-corrected RCM data at location R1, ICHEC-RAW-1 refers to the unbias-corrected RCM weather data at location R1, and CFSR-1 refers to the CFSR weather data at location C1. The bias correction was successful in correcting the raw RCM CDF to match the CFSR weather data. The bias-corrected precipitation and temperature results now reproduce the daily mean and the standard deviation on a monthly basis of the CFSR data set shown in Figures 13 through 16.

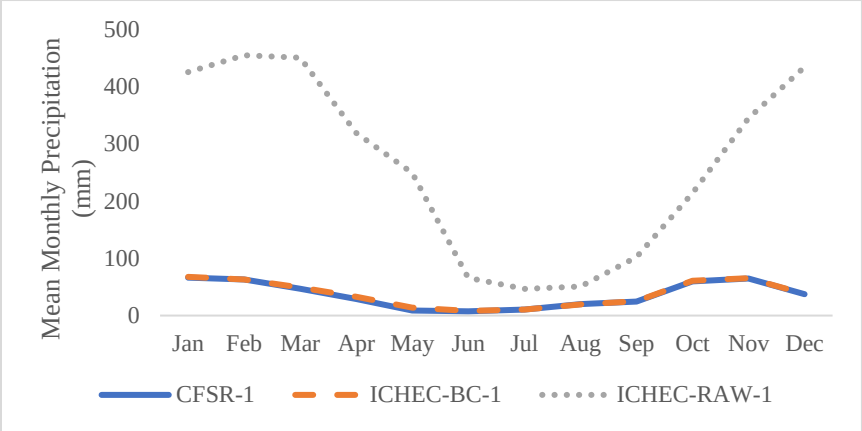

Figure 13: Monthly mean precipitation results for ICHEC bias correction. ICHEC-BC-1 refers to the bias-corrected Regional Climate Model (RCM) data at location R1, ICHEC-RAW-1 refers to the unbias-corrected RCM weather data at location R1, and CFSR-1 refers to the Climate Forecast System Reanalysis weather data at location C1.

The CDF mapping helped to correct the mean monthly precipitation as presented in Figure 13. The ICHEC-RAW-1 data was greatly over simulating the amount of precipitation for every month. After CDF mapping, the ICHEC-BC-1 matches the CFSR-1 precipitation.

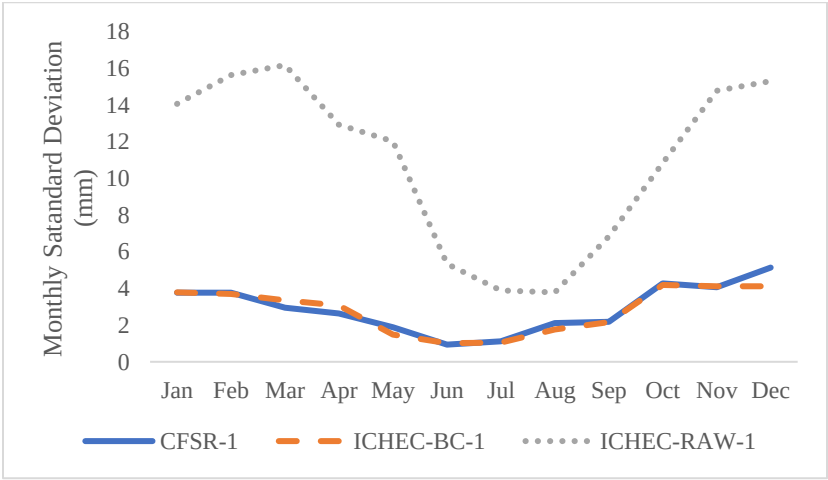

Figure 14: Monthly standard deviation precipitation results for ICHEC bias correction. ICHEC-BC-1 refers to the bias-corrected Regional Climate Model (RCM) data at location R1, ICHEC-RAW-1 refers to the unbias-corrected RCM weather data at location R1, and CFSR-1 refers to the Climate Forecast System Reanalysis weather data at location C1.

Figure 14 demonstrates that before CDF mapping, the raw RCM monthly standard deviation of precipitation, ICHEC-RAW-1, was much greater than the CFSR-1.

After CDF mapping, the bias corrected data, ICHEC-BC-1, much more closely matches CFSR-1. It is not an exact match in all instances, but it is much more representative of the precipitation in the region.

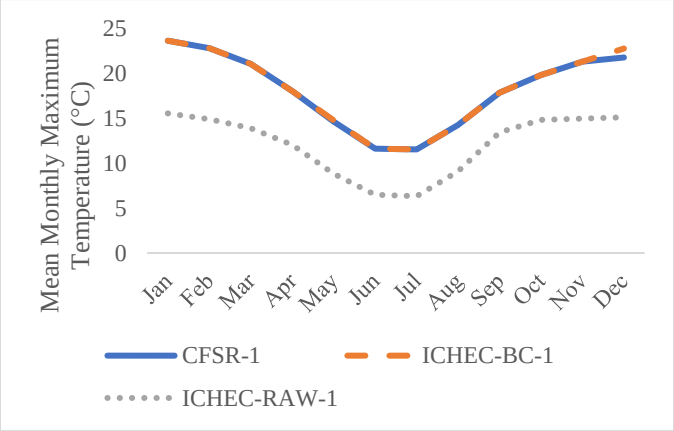

Figure 15: Monthly mean maximum temperature results for ICHEC bias correction. Regional Climate Model (RCM) data at location R1, ICHEC-RAW-1 refers to the unbias-corrected RCM weather data at location R1, and CFSR-1 refers to the Climate Forecast System Reanalysis weather data at location C1.

Figure 15 demonstrates that before CDF mapping, the raw RCM mean monthly maximum temperature, ICHEC-RAW-1, was significantly less than the CFSR-1. After CDF mapping, the bias corrected data, ICHEC-BC-1, much more closely matches CFSR-1.

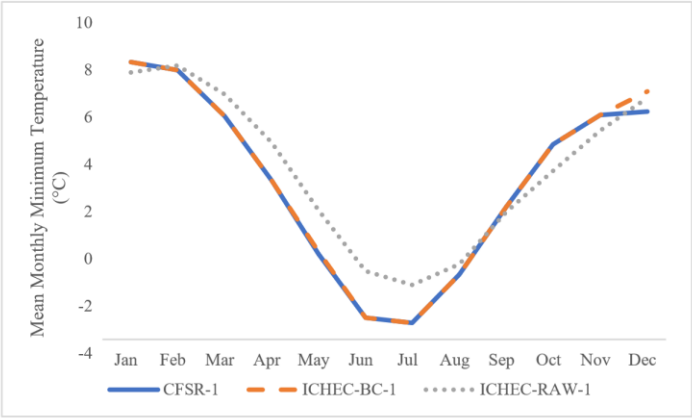

Figure 16: Monthly mean minimum temperature results for ICHEC bias correction. Regional Climate Model (RCM) data at location R1, ICHEC-RAW-1 refers to the unbias-corrected RCM weather data at location R1, and CFSR-1 refers to the Climate Forecast System Reanalysis weather data at location C1.

Figure 16 demonstrates that before CDF mapping, the raw RCM mean monthly minimum temperature, ICHEC-RAW-1, was similar to CFSR-1. Minimum temperature didn't have much variance and didn't differ from the CFSR. After CDF mapping, the bias corrected data, ICHEC-BC-1, matches CFSR-1.

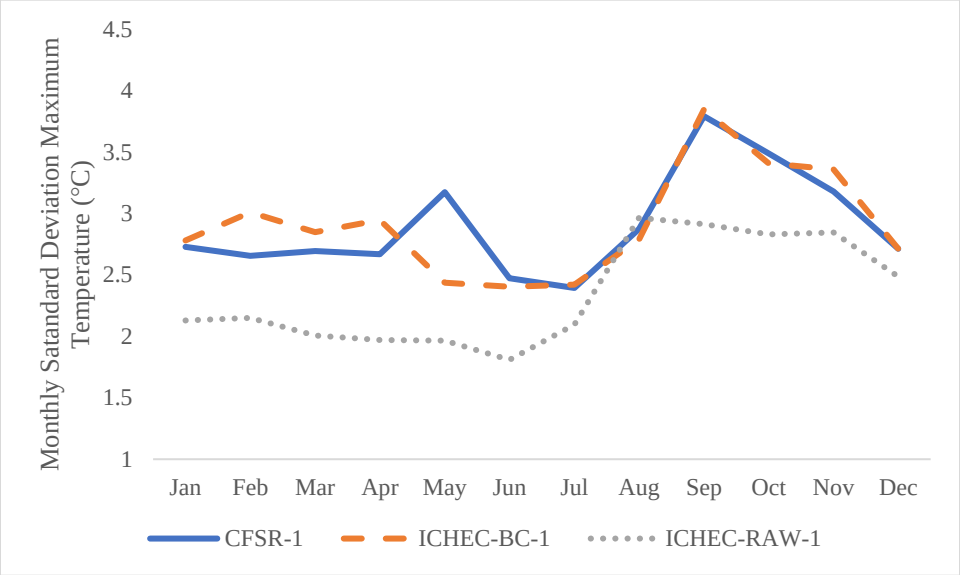

Figure 17: Monthly standard deviation of maximum temperature results for ICHEC bias correction. Regional Climate Model (RCM) data at location R1, ICHEC-RAW-1 refers to the unbias-corrected RCM weather data at location R1, and CFSR-1 refers to the Climate Forecast System Reanalysis weather data at location C1.

Figure 17 demonstrates that before CDF mapping, the raw RCM standard deviation of mean maximum temperature, ICHEC-RAW-1, was significantly less than CFSR-1. ICHEC-RAW-1 matched CFSR-1 between July and August. The overall shape of ICHEC-RAW-1 closely resembles CFSR-1. After CDF mapping, the bias corrected data, ICHEC-BC-1, much more closely matches CFSR-1.

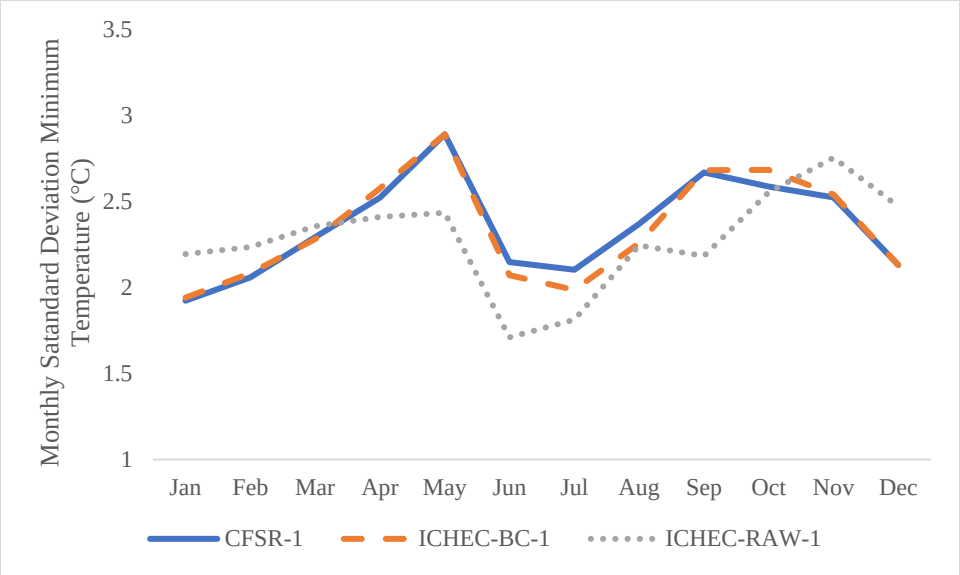

Figure 18: Monthly standard deviation of minimum temperature results for ICHEC bias correction. Regional Climate Model (RCM) data at location R1, ICHEC-RAW-1 refers to the unbias-corrected RCM weather data at location R1, and CFSR-1 refers to the Climate Forecast System Reanalysis weather data at location C1.

Figure 18 demonstrates that before CDF mapping, the raw RCM standard deviation of mean minimum temperature, ICHEC-RAW-1, did not resemble CFSR-1. ICHEC-RAW-1 was similar in value to CFSR-1 between January and May, then was significantly less than CFSR-1 between June and July. After CDF mapping, the bias corrected data, ICHEC-BC-1, much more closely matches CFSR-1.

4.1.2 Indicators of Hydrologic Alteration Results

The Indicators of Hydrologic Alteration analysis was performed for all three gauging stations, SG5, SG17 and SG3. The generated flow duration curves and subsequent Kruskal-Wallace test for pre and post dam periods demonstrated that for SG5 and SG17 a significant difference in streamflow occurred while SG3 was not significantly impacted by the construction of the dams. This is thought to be due to the SG3 station being significantly downstream of both of the dams. The flow duration curve along with the p-value statistic for SG5, SG17, and SG3 are shown in Figures 19, 20, and 21 respectively.

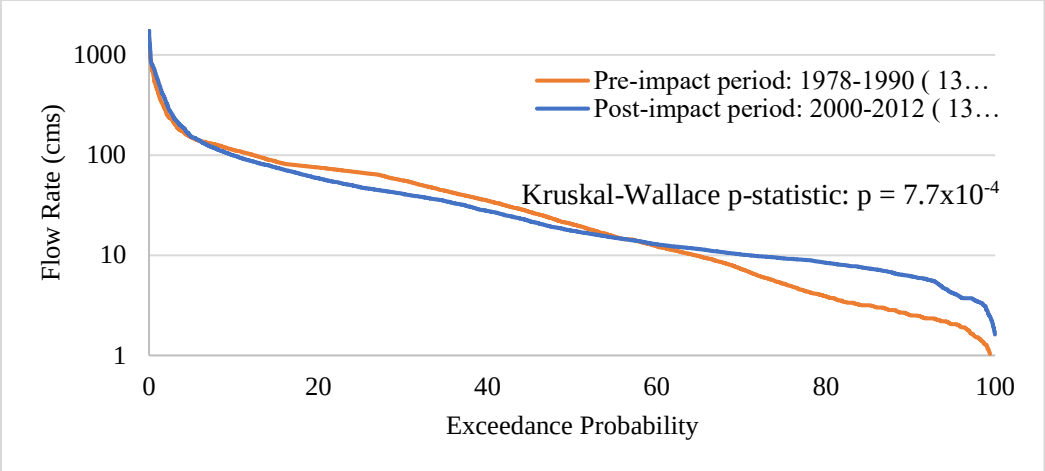

Figure 19: Flow Duration Curve displaying impact of the Katse dam on streamflow at the SG-5 gauging station as well as the Kruskal-Wallace p-statistic. The p-statistic is less than 0.05, thus the null hypothesis is rejected and the flows are determined to be significantly different.

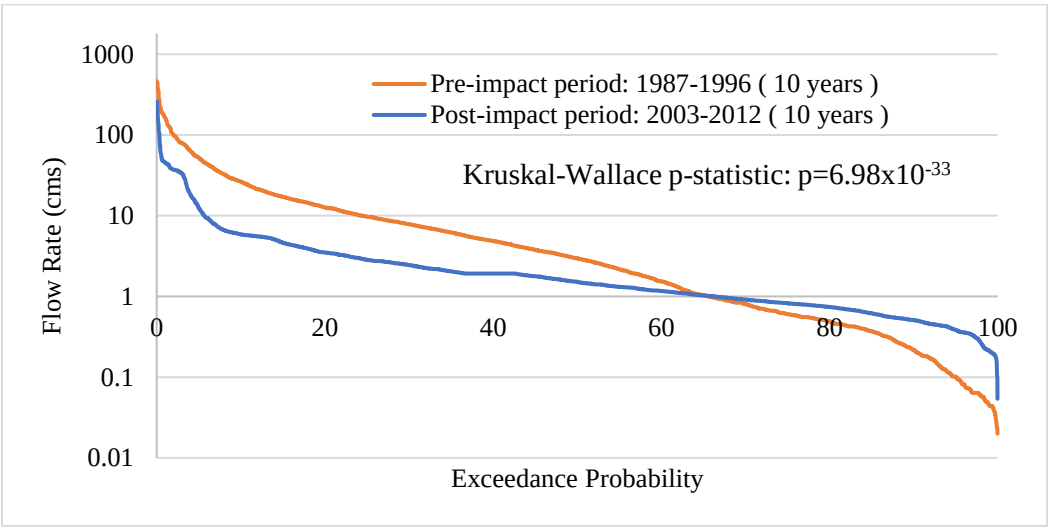

Figure 20: Flow Duration Curve displaying impact of the Mohale dam on streamflow at the SG-17 gauging station as well as the Kruskal-Wallace p-statistic. The p-statistic is less than 0.05, thus the null hypothesis is rejected and the flows are determined to be significantly different.

The flow duration curve displayed in Figure 19 shows the impact of the Katse dam on streamflow gauge SG-5 over a pre-impact and post-impact period of 13 years. High flows do not appear to be impacted by the dam, however, low flows that occur at least 60% of the time appear to be significantly different. The post-impact period has a higher flow rate on flows that occur at between 60% and 100% of the time. The Kruskal-Wallace test produced a p-statistic of $7.7x10^{-4}$ which signifies the null hypothesis may be rejected and the flows are significantly different.The

flow duration curve displayed in Figure 20 shows the displays of the Mohale dam on streamflow gauge SG-17 over a pre-impact and post-impact period of 10 years. Both the probability of high and low flows appears to be significantly different. The pre-impact period has a higher flow rate between 0% and 60% exceedance probability. The post-impact period has higher flow rate between 60% and 100% exceedance probability. The Kruskal-Wallace test produced a p-statistic of 6.98×10^{-33} which signifies the null hypothesis may be rejected and the flows are significantly different.

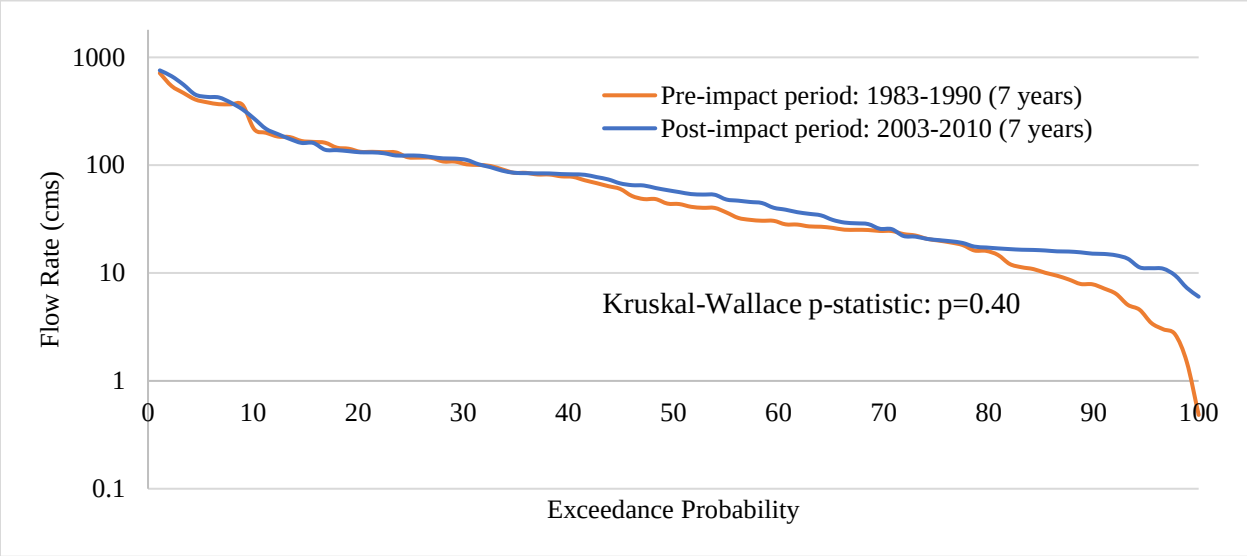

Figure 21: Flow Duration Curve displaying impact of the Katse and Mohale dam on streamflow at the SG-3 gauging station as well as the Kruskal-Wallace p-statistic. The p-statistic is greater than 0.05, thus the null hypothesis is not rejected and the flows are not determined to be significantly different.

The flow duration curve displayed in Figure 21 displays the impact of the Katse, and Mohale dam on streamflow gauge SG-3 over a pre-impact and post-impact period of 7 years. The pre-impact and post-impact period have a similar flow rate between 0% and 80% exceedance probability. The post-impact period has higher flow rate between 80% and 100% exceedance probability. The Kruskal-Wallace test produced a p-statistic of 0.04 which signifies the null hypothesis may not be rejected and the flows are not significantly different.

4.1.3 Calibration and Validation Results

A global sensitivity analysis was performed to identify the parameters stream flow was sensitive to. Overall, seven parameters were found to be most important: Snow fall temperature (SUB_SFTMP), precipitation lapse rate (PLAPS), temperature lapse rate (TLAPS), groundwater delay time (GW_DELAY), Soil evaporation compensation factor (ESCO), the SCS curve number (CN2), and the hydraulic conductivity (CH_K2). A complete description of all the SWAT parameters can be found in the SWAT user manual (Arnold et al., 2002).

Table 7 provides a list of these parameters and their descriptions, as well as the final minimum and maximum values used for calibration.

Table 7: Global sensitivity key parameters with the final minimum and maximum ranges for calibration.

Parameter Name	Description	Units	Min	Max
v_SUB_SFTMP().sno	Snow fall temperature	C	2.618	9.12
v_PLAPS.sub	Precipitation lapse rate	mm/km	71.68	994
v_TLAPS.sub	Temperature lapse rate	C/km	-11.6	-2.2
v_GW_DELAY.gw	Groundwater delay time	day	230.4	491.6
v_ESCO.hru	Soil evaporation compensation factor	-	0.487	0.853
r_CN2.mgt	SCS runoff curve number for moisture condition II	-	-0.19	0.118
v_CH_K2.rte	Effective hydraulic conductivity in the main channel	mm/h	109.5	369.2

SG5 and SG17 were calibrated first between the years of 1985 and 1990. These are the years before construction of the dams began. Because specific information regarding the design of the dams were unknown, they could not be simulated within ArcSWAT. The results of the Indicators of Hydrologic Alteration showed that the dams significantly altered the streamflow at the SG5 and SG17 gauge station, thus they were only calibrated for the years before dam construction and not validated. SG3 was not significantly impacted by dam construction and was used for calibration pre-dam construction and for validation post-dam construction.

The results of their calibration statistics are shown in Table 8 as well as Figures 22 and 23 respectively. SG5 and SG17 were only calibrated and not validated due to the lack of available data on the dam specifications. After SG5 and SG17 were calibrated their parameters were held steady and SG3 was calibrated. SG3 was calibrated from 1985-2002 and validated from 2003-2013. The results of the calibration and validation are shown in Figure 24.

Table 8: Calibration and validation statistics for the three streamflow gauges.

	Calibration			Validation
	SG5	SG17	SG3	SG3
NSE	0.47	0.57	0.55	0.59
PBIAS	4.3	10.1	-3.2	1.8
RSR	0.66	0.73	0.67	0.64

The calibration statistics for each of the stations varied in performance. The NSE value for SG5 was in the unsatisfactory range. This is due to the model's inability to simulate extreme events accurately. The NSE is also sensitive to outlying flows. Another reason for poor performance could be due to the lower number of observed data available for SG5 as compared to the other two stations. The NSE for SG17 and SG3 both fell into the satisfactory performance range. The PBIAS for SG5 and both SG3 calibration and validation were in the very good performance range while SG17 fell into the good range. This indicates an accurate model simulation when comparing the simulated values to the observed data. The RSR was in the unsatisfactory range for SG17, but in the satisfactory range for SG5 and SG3.

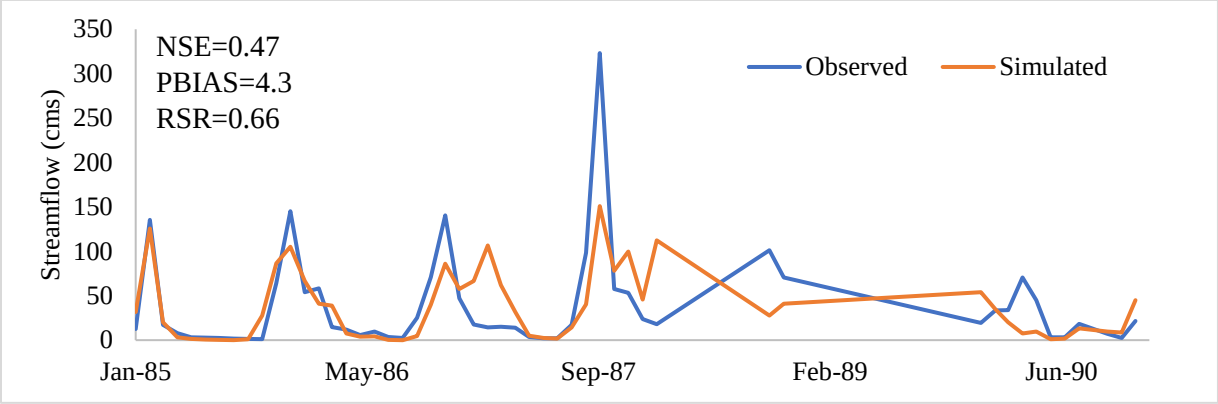

Figure 22: Calibration results for the SG5 streamflow gauge station.

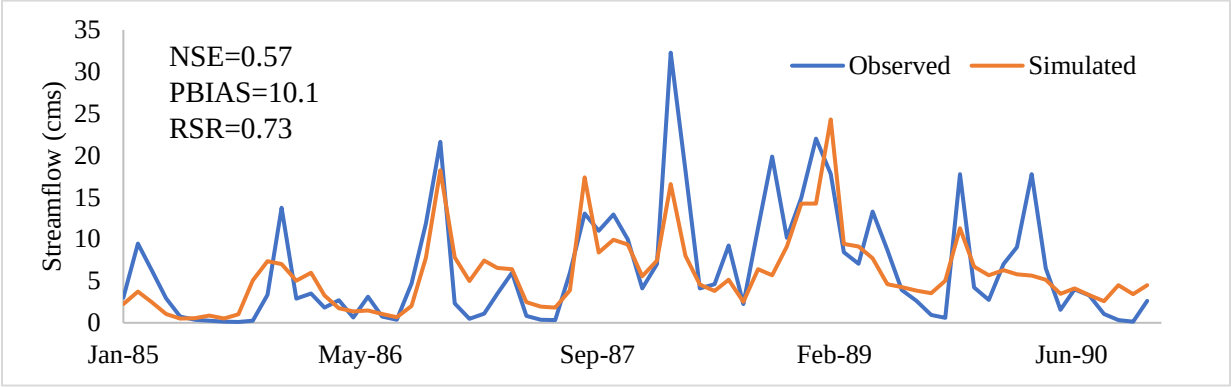

Figure 23: Calibration results for the SG17 streamflow gauge station.

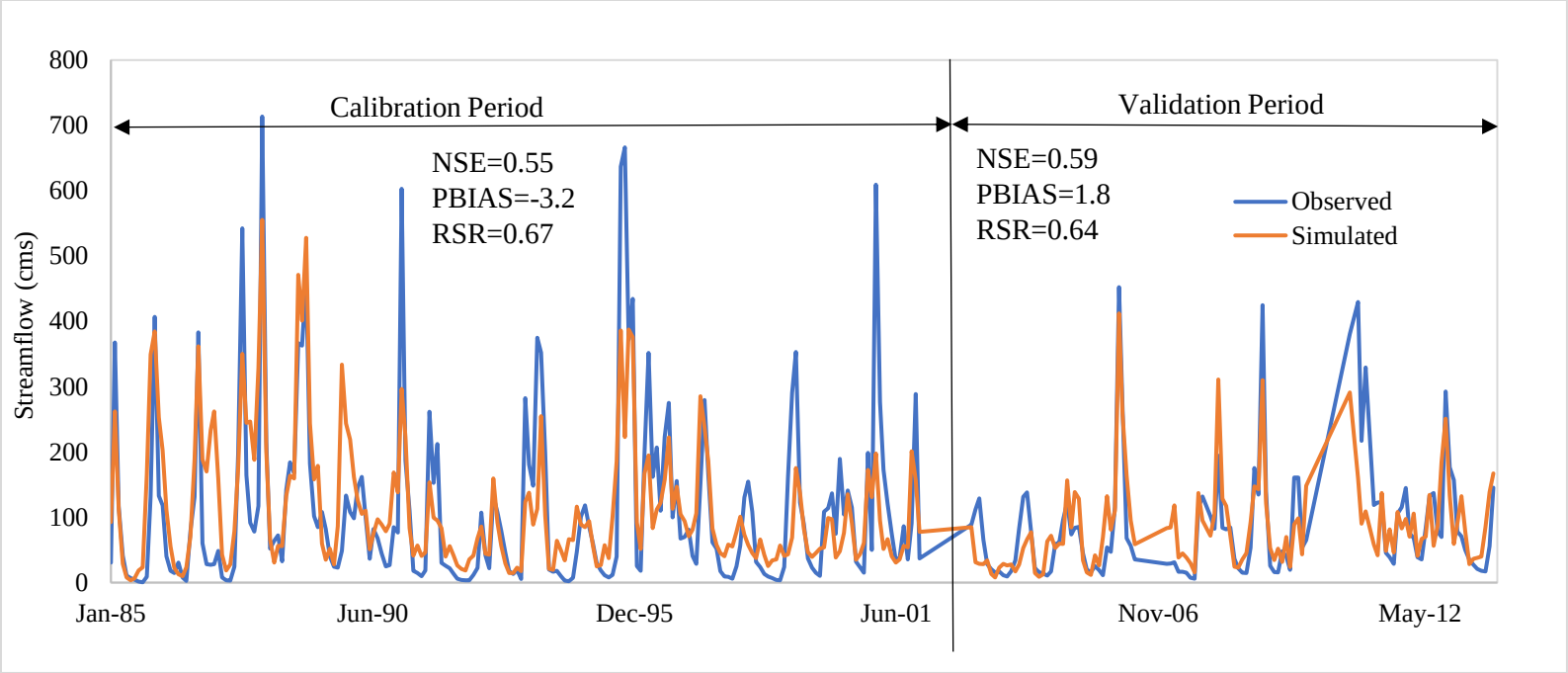

Figure 24: Calibration and validation results for the SG3 streamflow gauge station.

4.1.4 Climate Change Impact on Precipitation

After the SWAT model was calibrated and validated, the bias-corrected weather inputs for each RCM was inputted into the model. An average model ensemble was also inputted into the model by averaging the weather inputs of each RCM and it is denoted as Ensemble. The relative changes in precipitation and streamflow for each of the RCPs were analyzed based on the wet and dry seasons in Lesotho. The wet season is from October to April and the dry season is from May to September. The study period of 2020 to 2100 was broken into two periods denoted as mid-century and late-century. Mid-century is denoted from 2020-2060 and late-century is denoted from 2061-2100. Table 9 shows the relative precipitation change when compared to the respective model historic period (1979-2005).

Table 9: Relative changes in average precipitation for each Representative Concentration Pathway (RCP) during the wet season (Oct-Apr) and dry season (May-Sept). Mid-Century refers to the years 2020-2060 and late-century refers to 2061-2100. The highlighted figures in each column denote significant differences between the RCPs. The different colors for the MIROC model indicate which numbers should be compared.

	ICHEC	MIROC	CCCma	Ensemble
wet - RCP4.5 (Mid-Century)	0%	-7%	16%	3%
dry - RCP4.5 (Mid-Century)	-13%	-12%	-35%	-20%
wet - RCP4.5 (Late-Century)	5%	-7%	9%	2%
dry - RCP4.5 (Late-Century)	4%	17%	-15%	3%
wet - RCP8.5 (Mid-Century)	2%	-11%	11%	1%
dry - RCP8.5 (Mid-Century)	16%	2%	-21%	-1%
wet - RCP8.5 (Late-Century)	6%	-1%	10%	5%
dry - RCP8.5 (Late-Century)	-1%	-25%	-10%	-12%

The results of precipitation change varied between the wet and dry seasons. The results varied depending on the RCM used. Typically, 3 of the 4 RCM outputs agreed on an overall increase or decrease in precipitation. An increase in three of the model outputs for the wet season in both the mid and late century in RCP 4.5.

There was a decrease in the overall precipitation during the dry period in the RCP 4.5 during the mid-century and an increase in precipitation during the late century.

RCP 8.5 produced similar trends in precipitation change as RCP 4.5. The largest differences between RCP 4.5 and RCP 8.5 are highlighted in the table. For example, the ICHEC-RCP 4.5 model scenario resulted in a decrease of 13% in precipitation for the mid-century dry period, while the ICHEC-RCP 8.5 model resulted in an increase of 16% during the mid-century dry period. The different colors for the MIROC RCM indicate which numbers should be compared. Figures 25 and 26 show the average monthly relative precipitation change for RCP 4.5 and RCP 8.5 respectively.

The average monthly percent change in precipitation for RCP 4.5 is presented in Figure 25. The mid-century had a tendency to decrease in precipitation for all the RCMs. The late-century experienced an overall decrease to precipitation in the beginning of the year and an increase from September to December. The MIROC RCM showed the greatest increase in precipitation (104%) during September in the late-century.

The average monthly percent change in precipitation for RCP 8.5 is presented in Figure 26. The percent change fluctuated between increasing and decreasing for all the climate models during the mid-century. The ICEC RCM saw the greatest increase during August of the mid-century. The late century experienced an average decrease in precipitation until September where it increased through December.

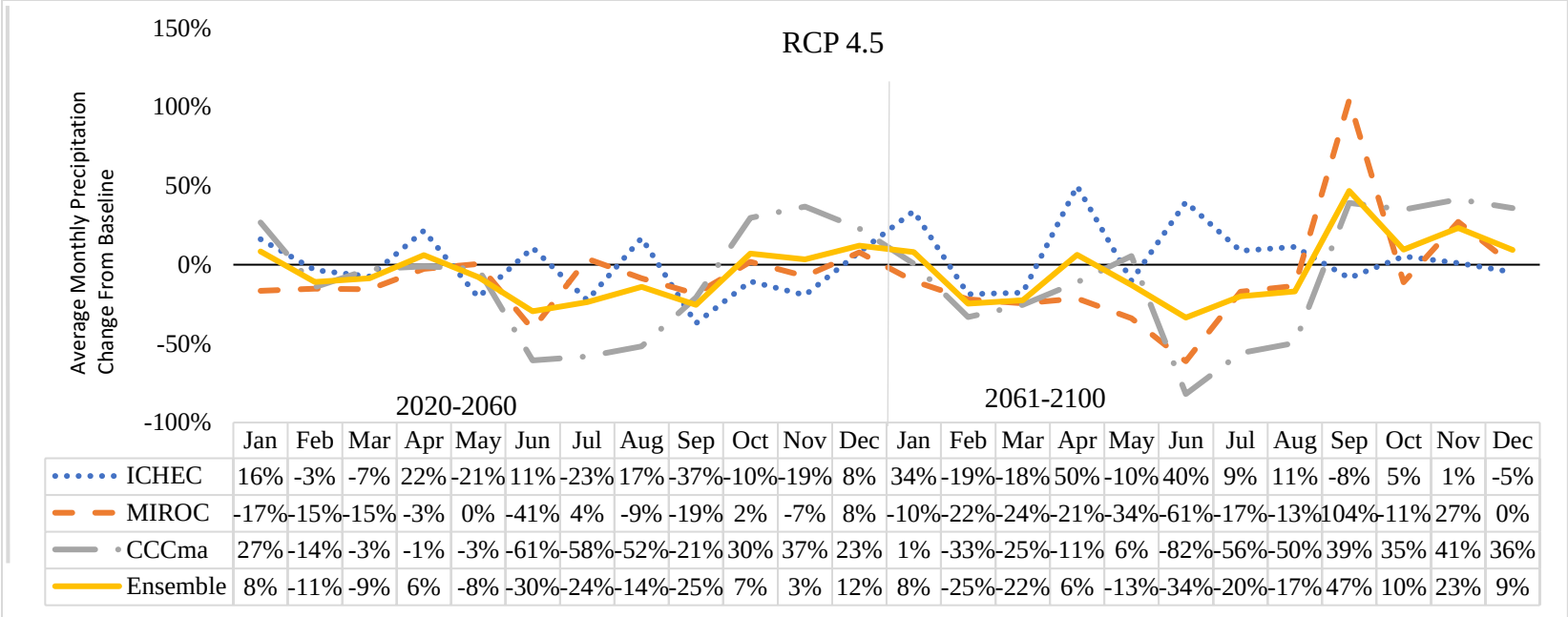

	Jan	Feb	Mar	Apr	May	Jun	Jul	Aug	Sep	Oct	Nov	Dec	Jan	Feb	Mar	Apr	May	Jun	Jul	Aug	Sep	Oct	Nov	Dec
ICHEC	16%	-3%	-7%	22%	-21%	11%	-23%	17%	-37%	-10%	-19%	8%	34%	-19%	-18%	50%	-10%	40%	9%	11%	-8%	5%	1%	-5%
MIROC	-17%	-15%	-15%	-3%	0%	-41%	4%	-9%	-19%	2%	-7%	8%	-10%	-22%	-24%	-21%	-34%	-61%	-17%	-13%	104%	-11%	27%	0%
CCCma	27%	-14%	-3%	-1%	-3%	-61%	-58%	-52%	-21%	30%	37%	23%	1%	-33%	-25%	-11%	6%	-82%	-56%	-50%	39%	35%	41%	36%
Ensemble	8%	-11%	-9%	6%	-8%	-30%	-24%	-14%	-25%	7%	3%	12%	8%	-25%	-22%	6%	-13%	-34%	-20%	-17%	47%	10%	23%	9%

Figure 25: Average Monthly Percent Change in Precipitation for Representative Concentration Pathway 4.5 for both mid-century (2020-2060) and late-century (2061-2100). Mid-century had a tendency to decrease in precipitation. The late-century experienced an overall decrease to precipitation in the beginning of the year and an increase from September to December.

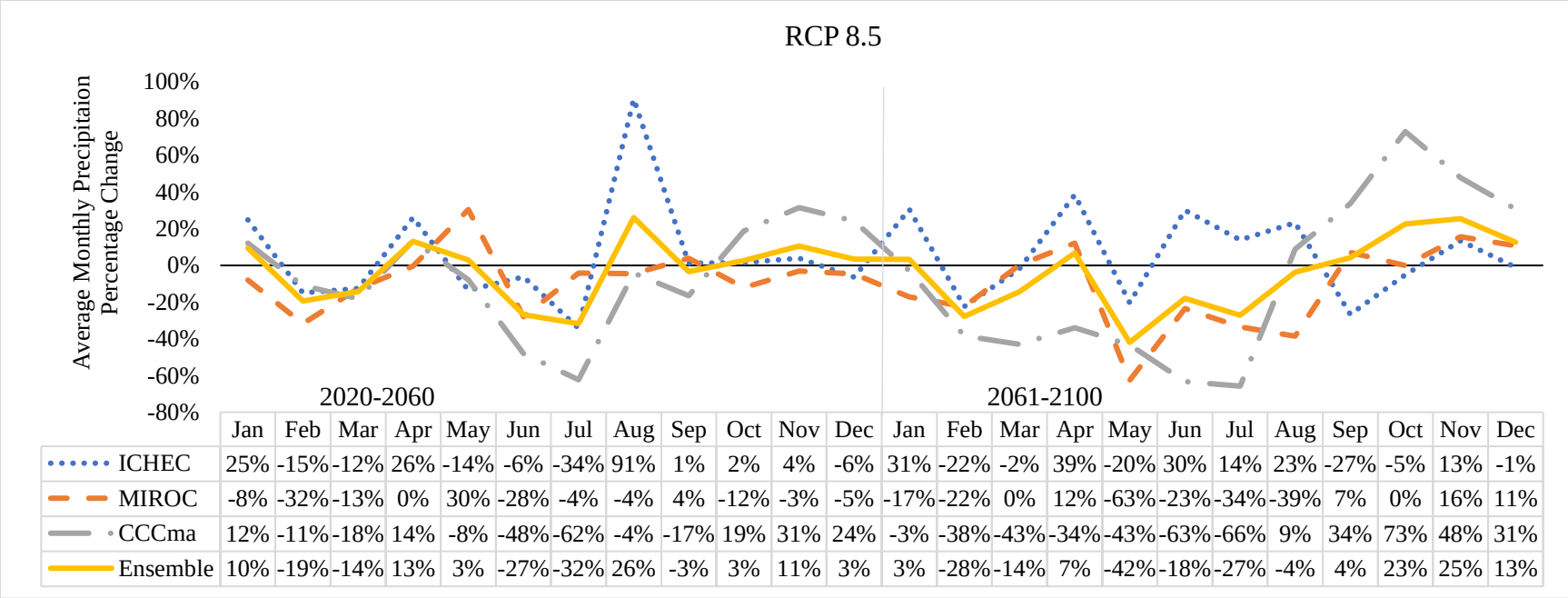

	Jan	Feb	Mar	Apr	May	Jun	Jul	Aug	Sep	Oct	Nov	Dec	Jan	Feb	Mar	Apr	May	Jun	Jul	Aug	Sep	Oct	Nov	Dec
ICHEC	25%	-15%	-12%	26%	-14%	-6%	-34%	91%	1%	2%	4%	-6%	31%	-22%	-2%	39%	-20%	30%	14%	23%	-27%	-5%	13%	-1%
MIROC	-8%	-32%	-13%	0%	30%	-28%	-4%	-4%	4%	-12%	-3%	-5%	-17%	-22%	0%	12%	-63%	-23%	-34%	-39%	7%	0%	16%	11%
CCCma	12%	-11%	-18%	14%	-8%	-48%	-62%	-4%	-17%	19%	31%	24%	-3%	-38%	-43%	-34%	-43%	-63%	-66%	9%	34%	73%	48%	31%
Ensemble	10%	-19%	-14%	13%	3%	-27%	-32%	26%	-3%	3%	11%	3%	3%	-28%	-14%	7%	-42%	-18%	-27%	-4%	4%	23%	25%	13%

Figure 26: Average Monthly Precipitation Percent Change for Representative Concentration Pathway 8.5 for both mid-century (2020-2060) and late-century (2061-2100). The percent change fluctuated between increasing and decreasing for all the climate models during the mid-century. The late century experienced a decrease in precipitation until September where it increased through December.

4.1.5 Projected Blue Water Yield (Streamflow)

The average relative change in streamflow for the wet and dry seasons of each RCP is presented in Table 10. Just as the relative change in precipitation was compared to the historic period, the relative change in streamflow was compared in the same way. Mid-century and late-century are defined the same way as in the previous section.

Table 10: Relative change in streamflow for wet season (Oct-Apr) and dry season (May-Sept) for each Representative Concentration Pathway. Mid-Century refers to the years 2020-2060 and late-century refers to 2061-2100.

	ICHEC	MIROC	CCCma	Ensemble
wet - RCP4.5 (Mid-Century)	-42%	-48%	-35%	-48%
dry - RCP4.5 (Mid-Century)	-48%	-54%	-50%	-52%
wet - RCP4.5 (Late-Century)	-36%	-42%	-33%	-41%
dry - RCP4.5 (Late-Century)	-39%	-54%	-47%	-48%
wet - RCP8.5 (Mid-Century)	-37%	-52%	-35%	-47%
dry - RCP8.5 (Mid-Century)	-39%	-56%	-47%	-51%
wet - RCP8.5 (Late-Century)	-37%	-48%	-34%	-43%
dry - RCP8.5 (Late-Century)	-41%	-60%	-57%	-52%

Each RCM was compared to its respective historic reference baseflow period. The historic reference baseflow period is from 1979-2005. Each RCM showed a significant decrease in streamflow for each RCP. The larger decreases in streamflow occurred during the dry season for both RCPs. There was not a large difference in percent change in streamflow between RCP4.5 and RCP8.5. Figures 27 and 28 show the average monthly percent changes in streamflow for RCP 4.5 and 8.5 respectively. There is not a large difference in the average monthly streamflow between the two periods (2020-2060 and 2061-2100). There is only one instance where there is a positive change in streamflow for both the RCP 4.5 and RCP 8.5 periods and that is produced by the CCCma RCM. The CCCma produced a positive change in average January streamflow in the late century.

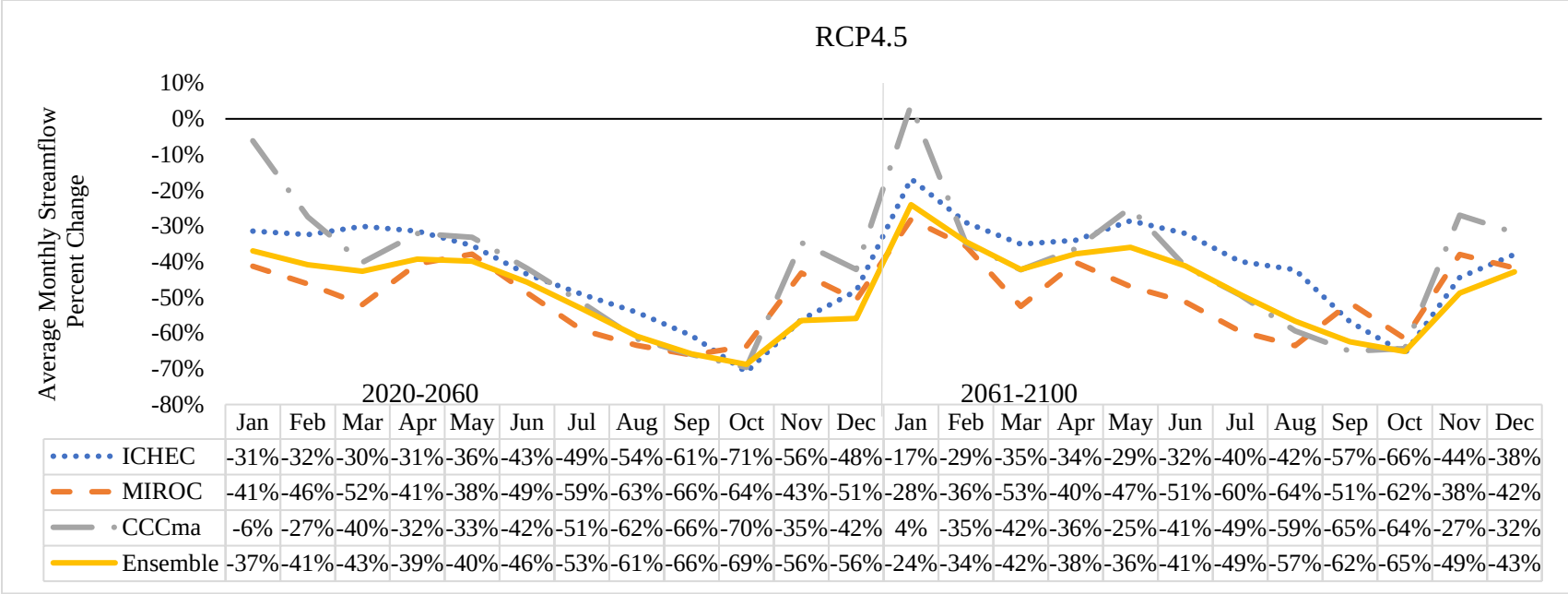

	Jan	Feb	Mar	Apr	May	Jun	Jul	Aug	Sep	Oct	Nov	Dec	Jan	Feb	Mar	Apr	May	Jun	Jul	Aug	Sep	Oct	Nov	Dec
ICHEC	-31%	-32%	-30%	-31%	-36%	-43%	-49%	-54%	-61%	-71%	-56%	-48%	-17%	-29%	-35%	-34%	-29%	-32%	-40%	-42%	-57%	-66%	-44%	-38%
MIROC	-41%	-46%	-52%	-41%	-38%	-49%	-59%	-63%	-66%	-64%	-43%	-51%	-28%	-36%	-53%	-40%	-47%	-51%	-60%	-64%	-51%	-62%	-38%	-42%
CCCma	-6%	-27%	-40%	-32%	-33%	-42%	-51%	-62%	-66%	-70%	-35%	-42%	4%	-35%	-42%	-36%	-25%	-41%	-49%	-59%	-65%	-64%	-27%	-32%
Ensemble	-37%	-41%	-43%	-39%	-40%	-46%	-53%	-61%	-66%	-69%	-56%	-56%	-24%	-34%	-42%	-38%	-36%	-41%	-49%	-57%	-62%	-65%	-49%	-43%

Figure 27: Average Monthly Percent Change in Streamflow Representative Concentration Pathway 4.5 for both mid-century (2020-2060) and late-century (2061-2100). Both periods experienced a negative decrease in streamflow. The CCCma model saw a brief increase in streamflow for January in the late century.

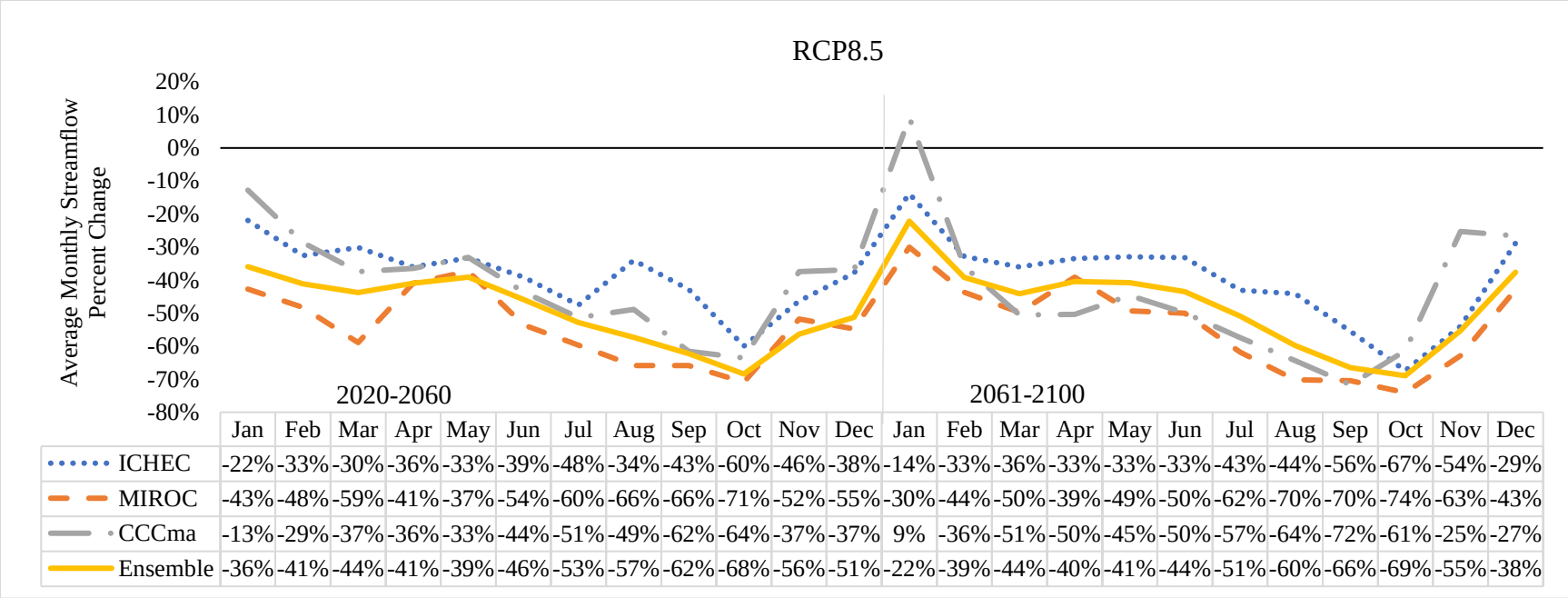

	Jan	Feb	Mar	Apr	May	Jun	Jul	Aug	Sep	Oct	Nov	Dec	Jan	Feb	Mar	Apr	May	Jun	Jul	Aug	Sep	Oct	Nov	Dec
ICHEC	-22%	-33%	-30%	-36%	-33%	-39%	-48%	-34%	-43%	-60%	-46%	-38%	-14%	-33%	-36%	-33%	-33%	-33%	-43%	-44%	-56%	-67%	-54%	-29%
MIROC	-43%	-48%	-59%	-41%	-37%	-54%	-60%	-66%	-66%	-71%	-52%	-55%	-30%	-44%	-50%	-39%	-49%	-50%	-62%	-70%	-70%	-74%	-63%	-43%
CCCma	-13%	-29%	-37%	-36%	-33%	-44%	-51%	-49%	-62%	-64%	-37%	-37%	9%	-36%	-51%	-50%	-45%	-50%	-57%	-64%	-72%	-61%	-25%	-27%
Ensemble	-36%	-41%	-44%	-41%	-39%	-46%	-53%	-57%	-62%	-68%	-56%	-51%	-22%	-39%	-44%	-40%	-41%	-44%	-51%	-60%	-66%	-69%	-55%	-38%

Figure 28: Average Monthly Streamflow Percent Change for Representative Concentration Pathway 8.5 for both mid-century (2020-2060) and late-century (2061-2100). Both periods experienced a negative decrease in streamflow. The CCCma model saw a brief increase in streamflow for January in the late century.

The average monthly percent change in streamflow for RCP 4.5 is presented in Figure 27. The percent change fluctuated between increasing and decreasing for all the climate models during the mid-century. Both periods experienced a negative decrease in streamflow for all the RCMs. The only increase in streamflow was simulated by the CCCma model for January (4%) during the late century. The average monthly percent change in streamflow for RCP 8.5 is presented in Figure 28. The percent change fluctuated between increasing and decreasing for all the climate models during the mid-century. Both periods experienced a negative decrease in streamflow for all the RCMs. The only increase in streamflow was simulated by the CCCma model for January (9%) during the late century.

4.1.6 Water Scarcity Analysis

4.1.6.1 Historic Water Scarcity

The historic water scarcity spanning the years 1979-2005 is displayed in Figure 29.

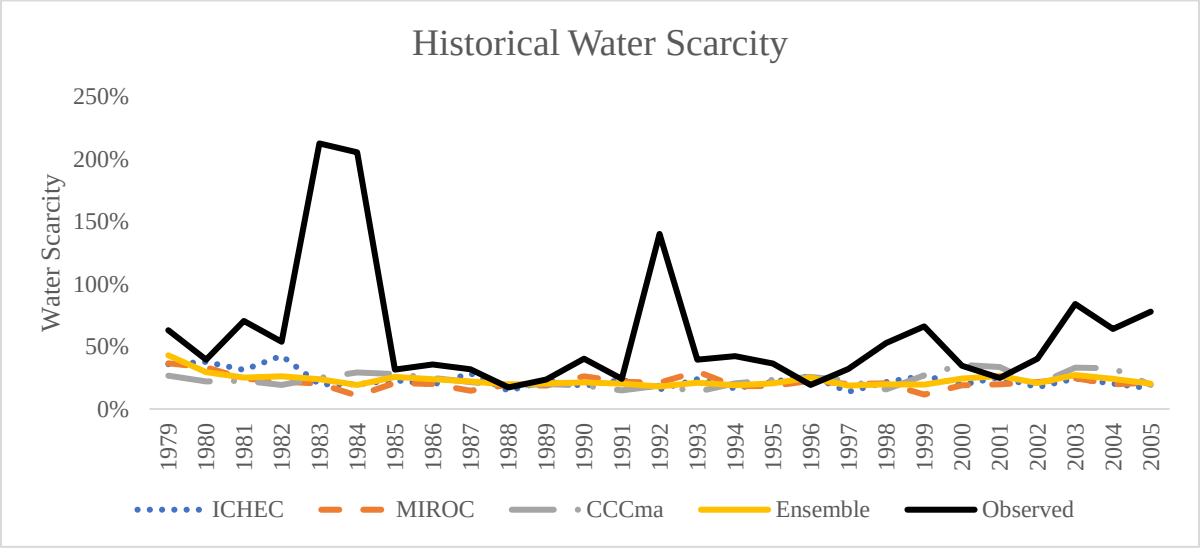

Figure 29: Historic water scarcity from 1979-2005. The observed water scarcity was calculated using observed streamflow.

The historic water scarcity was calculated by adjusting the national blue water footprint to represent the population during the respective year. The historic national blue water footprint was estimated by multiplying the national water footprint per capita (1519 m^3yr^{-1} per person) by the population of the nation during the appropriate year. All of the RCMs in Figure 29 have very low water scarcity as compared with the estimated water scarcity based on the observed streamflow data. The historic water scarcity showed two instances of significant water scarcity in 1983 and 1984, and one instance of moderate water scarcity in 1992. The years of water scarcity in the historical water scarcity match the years Lesotho faced drought, documented for the years 1983, 1990, and 2002 (Masih et al., 2014). The RCMs failed to capture the extreme climate events that resulted in drought occurrence. This is not uncommon as RCMs have difficulty capturing and replicating historical extreme weather events (Panaou et al., 2018). This increases uncertainty in their ability to capture future extreme weather events.

4.1.6.2 Future Water Scarcity

Water scarcity was calculated using the water footprint in three scenarios. Scenario 1 assumes the Senqu river basin is the sole source of blue water available, and the entire national blue water footprint of 2850 million m^3yr^{-1} is used in the calculation of water scarcity. The water footprint for scenario 2 was calculated as 1425 million m^3yr^{-1}, which is estimated as the product of the water footprint per capita (1519 m^3yr^{-1} per person) and the population living in the water basin. The water footprint for scenario 3 was calculated by using the water footprint per capita (1519 m^3yr^{-1} per person) and multiplying by the projected population of Lesotho through 2100. Figures 30 – 33 display the results of the water scarcity analysis for scenario 1 on an annual basis.

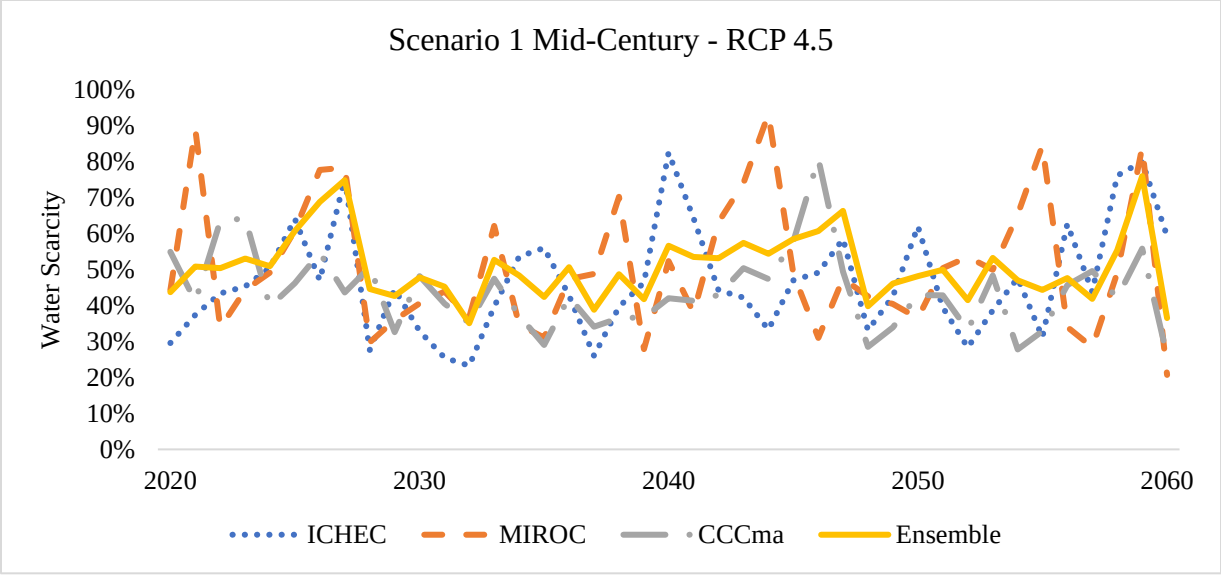

Figure 30: Water Scarcity Scenario 1 mid-century (2020-2060) for Representative Concentration Pathway 4.5. Scenario 1 assumes the Senqu river basin is the sole source of blue water available, and the entire national blue water footprint is used in the calculation of water scarcity.

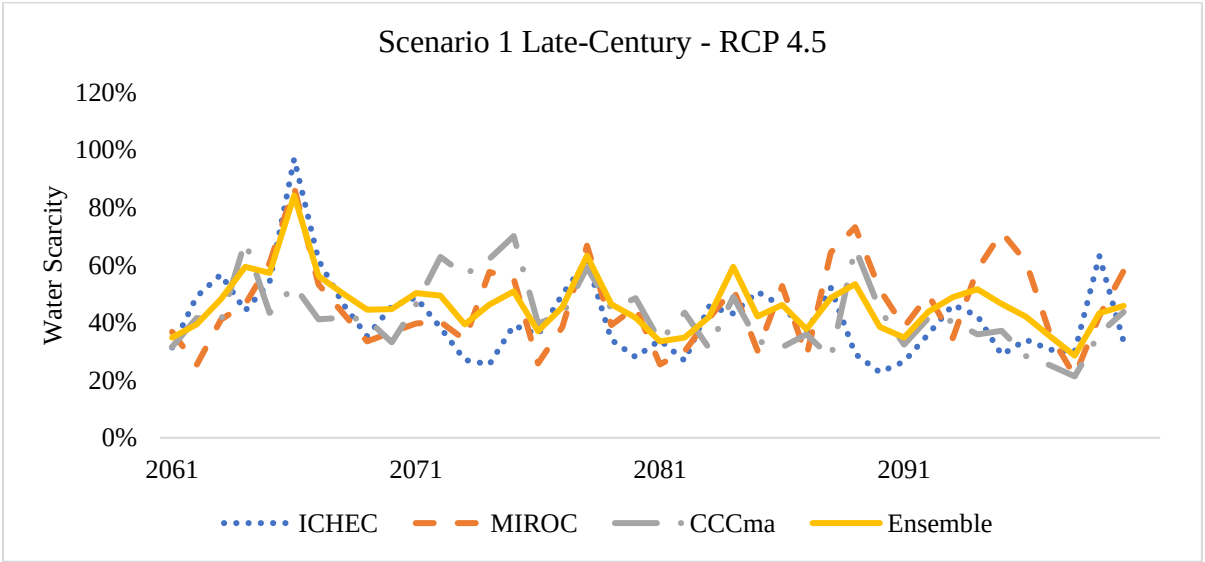

Figure 31: Water Scarcity Scenario 1 late century (2061-2100) for Representative Concentration Pathway 4.5. Scenario 1 assumes the Senqu river basin is the sole source of blue water available, and the entire national blue water footprint is used in the calculation of water scarcity.

There were no water scarcity measurements above 100% for RCP 4.5 for both the mid and late century time periods. This indicates low blue water scarcity for the period. The MIROC RCM produced the water scarcity measurement of 93% during the year 2044. The ICHEC, MIROC, and Ensemble each produced a similar peak in water scarcity in the years 2060, 2066, and 2078.

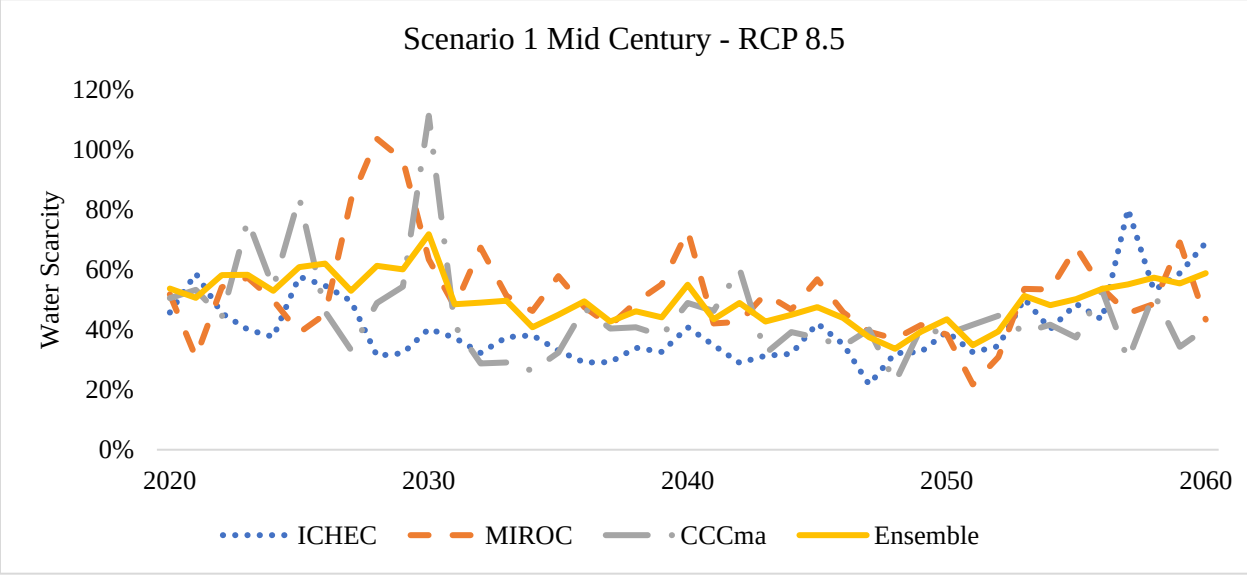

Figure 32: Water Scarcity Scenario 1 mid-century (2020-2060) for Representative Concentration Pathway 8.5. Scenario 1 assumes the Senqu river basin is the sole source of blue water available, and the entire national blue water footprint is used in the calculation of water scarcity.

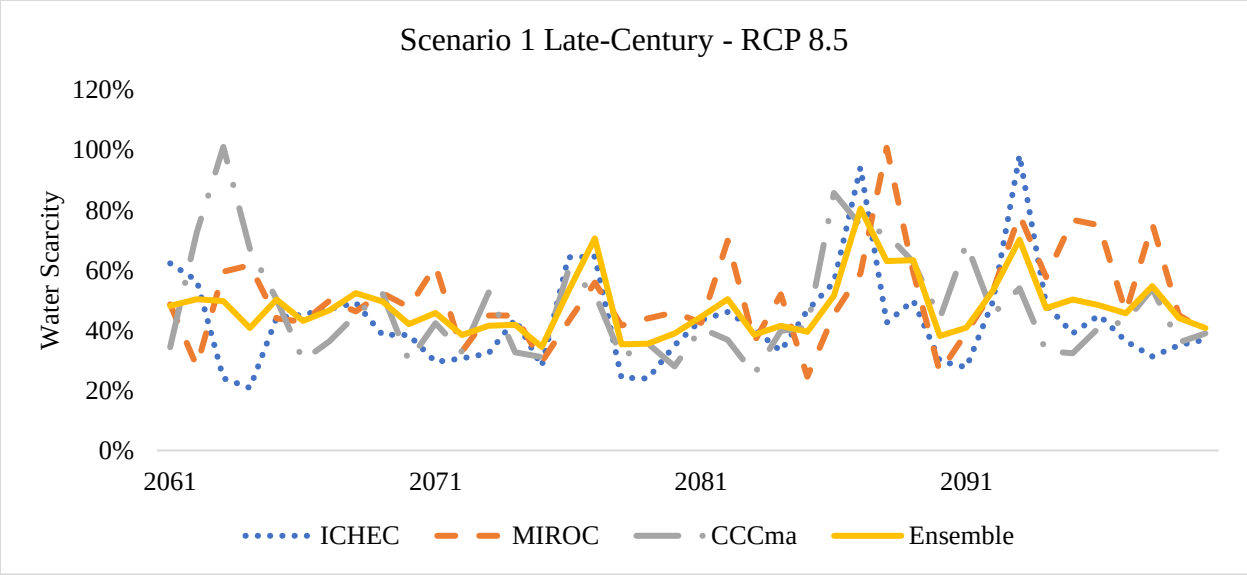

Figure 33: Water Scarcity Scenario 1 late-century (2061-2100) for Representative Concentration Pathway 8.5. Scenario 1 assumes the Senqu river basin is the sole source of blue water available, and the entire national blue water footprint is used in the calculation of water scarcity.

RCP 8.5 produced four years in total that the water scarcity was above 100%. The MIROC model produced a value of 104% in 2028 and 101% in 2088. The CCCma model produced a value of 111% in 2030 and 101% in 2063. Values between 100% and 150% represent the blue water availability is exceeded and the environmental flow requirements of the stream are not met.

The results for scenario 2 have significantly lower water scarcity measurements than scenario 1. The time series graphs for scenario 2 are presented in Figures 34-37. There were only 2 years in mid-century RCP 8.5 where the water scarcity measurement was above 50% but no measurement exceeded 60%.

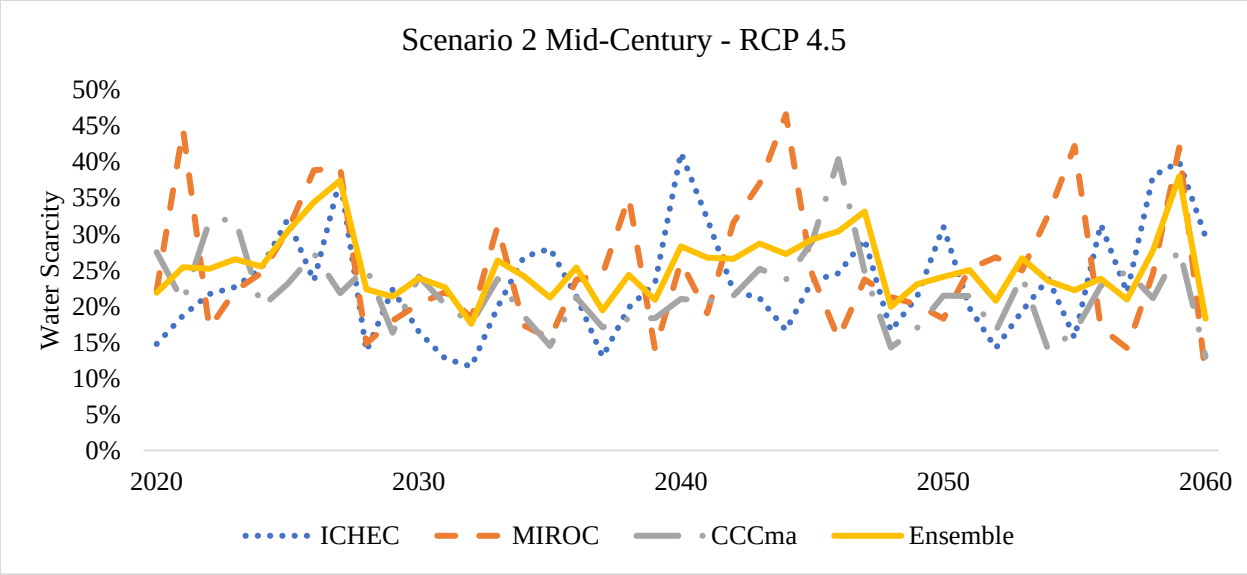

Figure 34: Water Scarcity Scenario 2 mid-century (2020-2060) for Representative Concentration Pathway 4.5. Scenario 2 is a modified national water footprint using only the population within the Senqu basin.

The MIROC RCM within Figure 34 produced the highest incidence of water scarcity of 47% in 2044. All the values fell within low water scarcity.

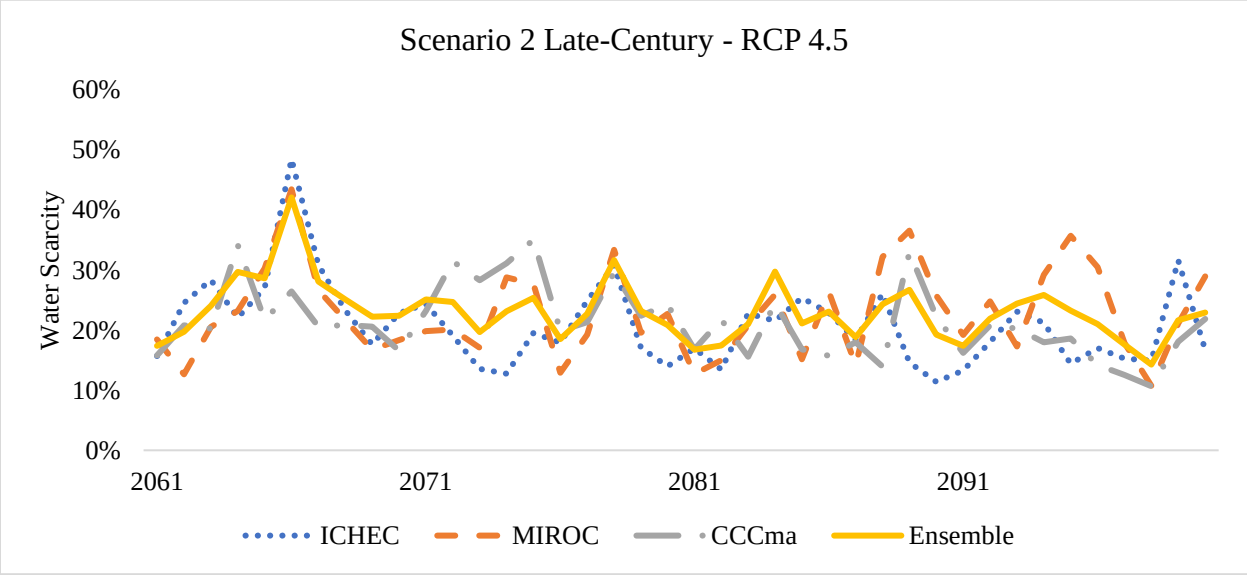

Figure 35: Water Scarcity Scenario 2 late-century (2061-2100) Representative Concentration Pathway 4.5. Scenario 2 is a modified national water footprint using only the population within the Senqu basin.

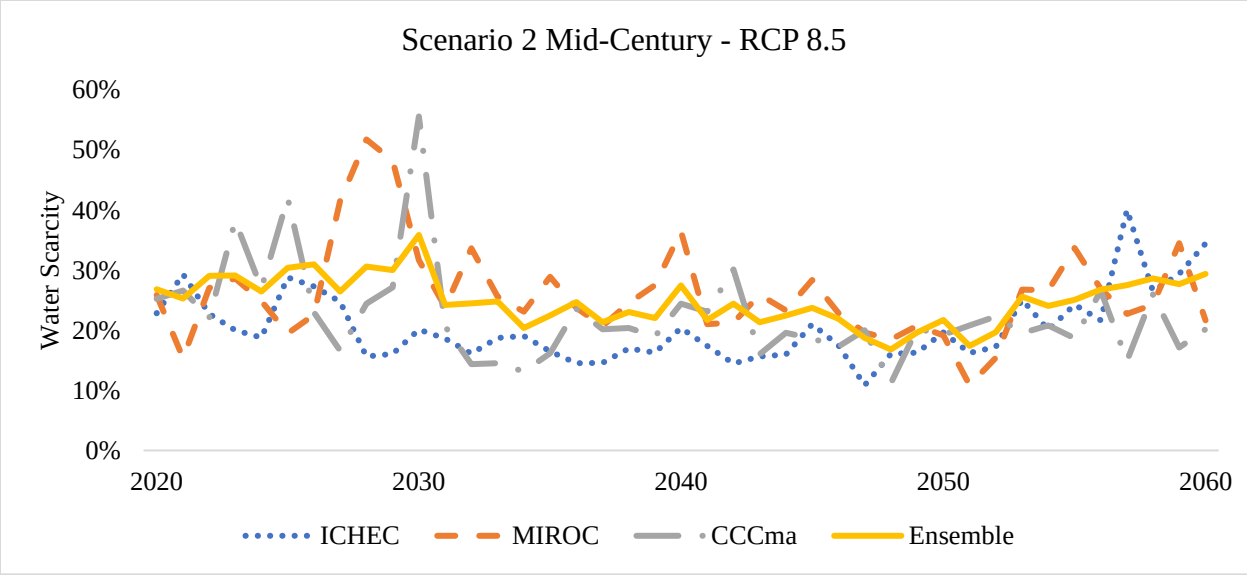

Figure 36: Water Scarcity Scenario 2 mid-century (2020-2060) Representative Concentration Pathway 8.5. Scenario 2 is a modified national water footprint using only the population within the Senqu basin.

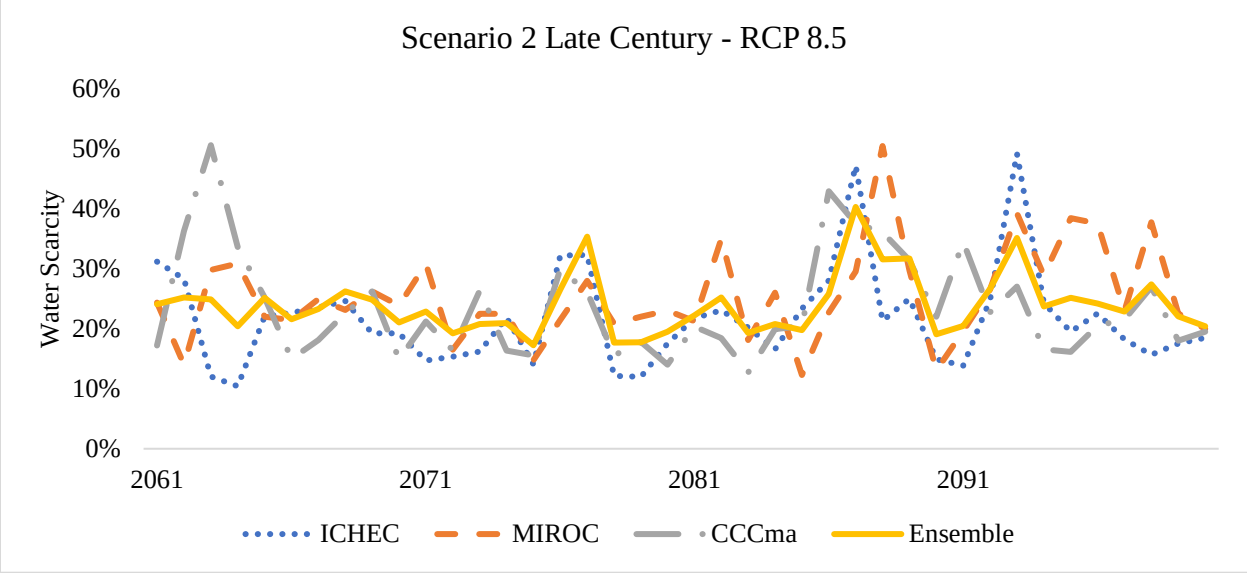

Figure 37: Water Scarcity Scenario 2 late-century (2061-2100) Representative Concentration Pathway 8.5. Scenario 2 is a modified national water footprint using only the population within the Senqu basin.

The RCP 4.5 Scenario 3 (including population growth) mid-century results give multiple years of moderate water scarcity and a few years of significant water scarcity. The MIROC RCM produced the largest values of water scarcity of 151% in 2044 and 2055 and a value of 154% in 2059. The time series graphs for Scenario 3 are presented in Figures 38-41.

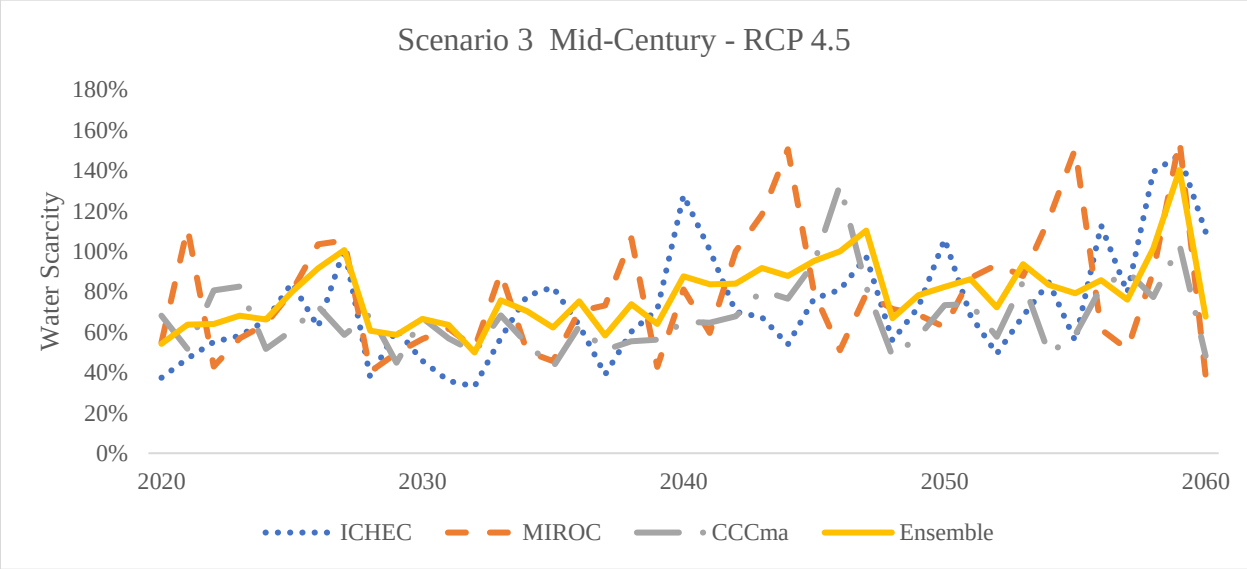

Figure 38: Water Scarcity Scenario 3 mid-century (2020-2060) Representative Concentration Pathway 4.5. Scenario 3 is a modified national water footprint that increases with projected population within Lesotho.

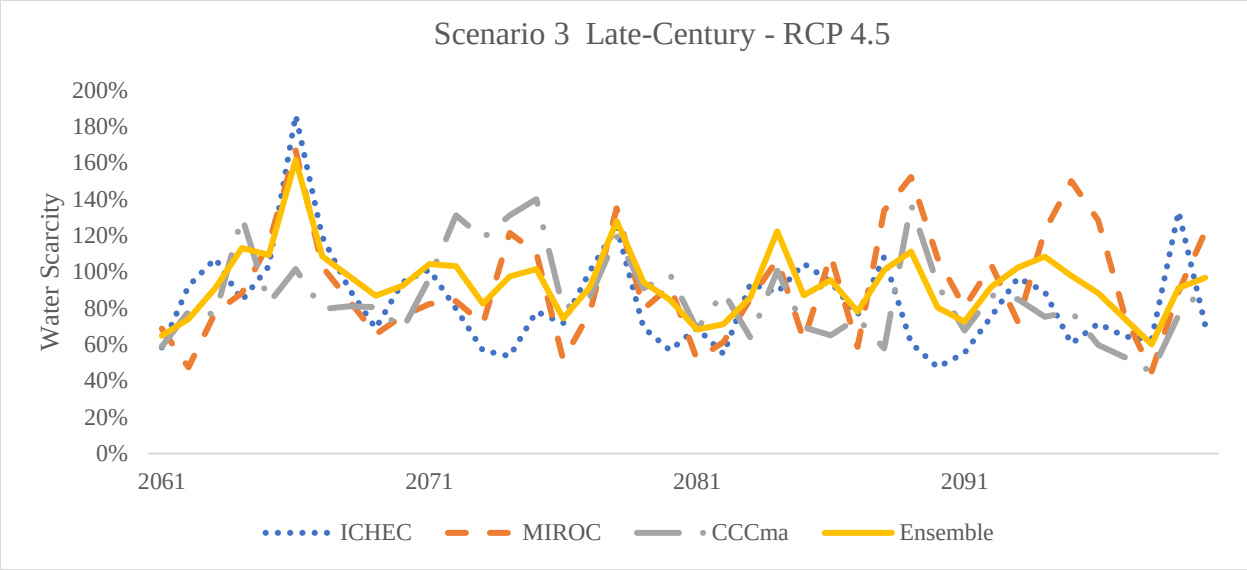

Figure 39: Water Scarcity Scenario 3 late-century (2061-2100) Representative Concentration Pathway 4.5. Scenario 3 is a modified national water footprint that increases with projected population within Lesotho.

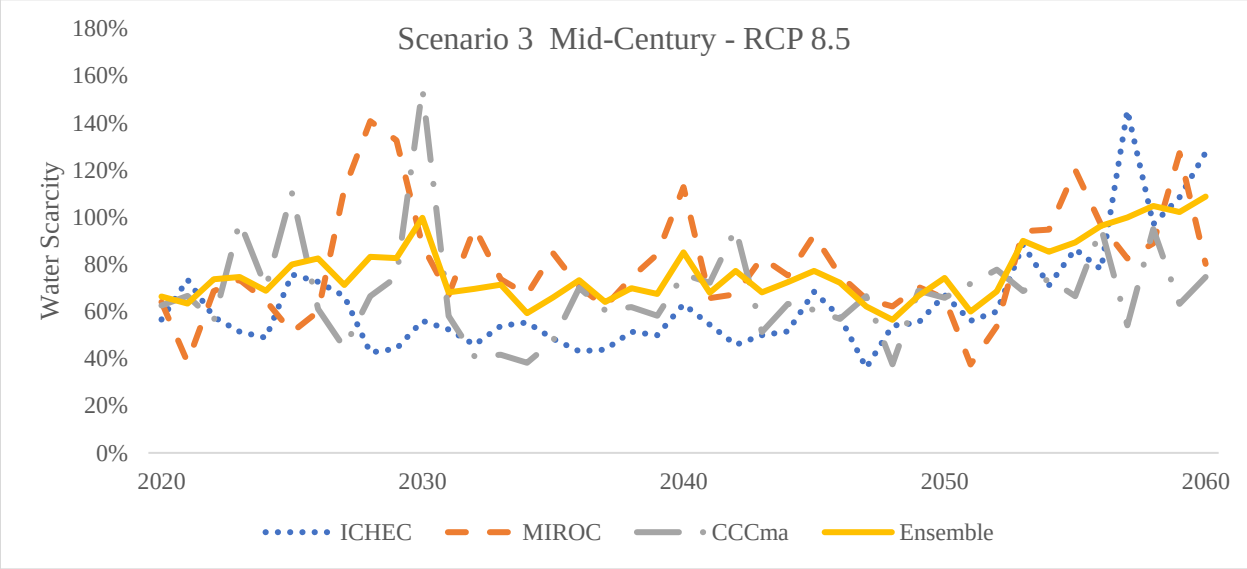

Figure 40: Water Scarcity Scenario 3 mid-century (2020-2060) Representative Concentration Pathway 8.5. Scenario 3 is a modified national water footprint that increases with projected population within Lesotho.

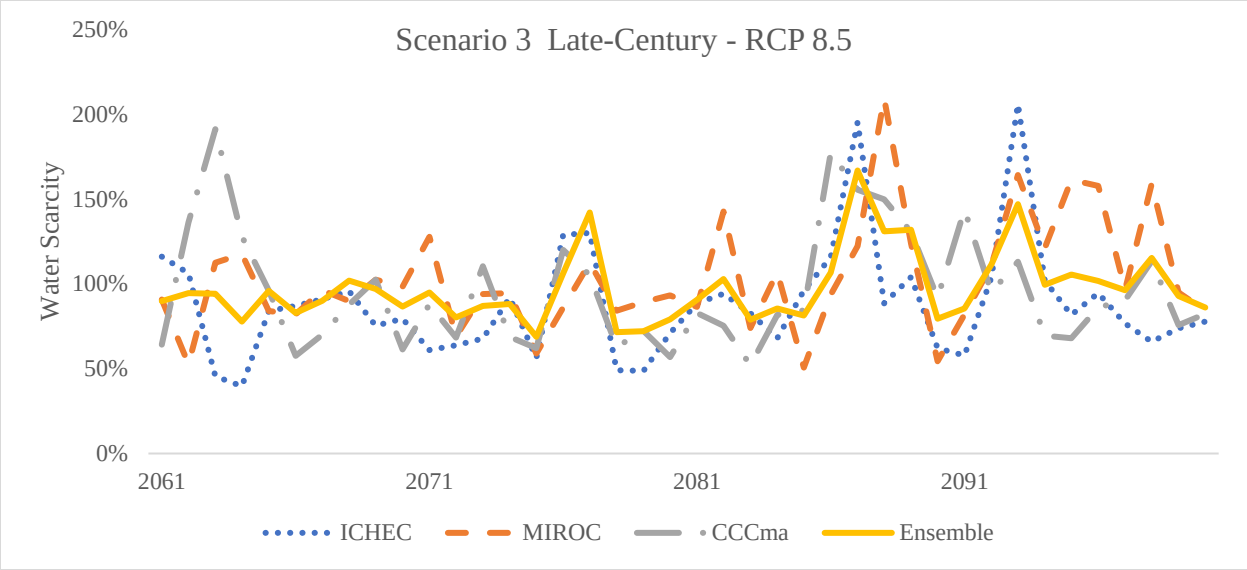

Figure 41: Water Scarcity Scenario 3 mid-century (2020-2060) Representative Concentration Pathway 8.5. Scenario 3 is a modified national water footprint that increases with projected population within Lesotho.

The RCP 4.5 Scenario 3 late-century results have multiple years of moderate and significant water scarcity. The Ensemble RCM produced 12 years of moderate water scarcity and 1 year of significant water scarcity. The ICHEC, MIROC, and Ensemble each produced a year of significant water scarcity in the year 2066 with values of 186%, 167%, and 162% respectively. The MIROC RCM produced the other reported year of significant water scarcity of 152% in 2089.

The RCP 8.5 Scenario 3 mid-century results have multiple years of moderate water scarcity and significant water scarcity. The Ensemble RCM produced 5 years of moderate water scarcity in the years 2030, and 2057-2060. The CCCma RCM produced the year of significant water scarcity in the year 2030 with a percentage of 155%. The MIRCO RCM produced 6 years of moderate water scarcity which was the most of any of the RCMs. The RCP 8.5 Scenario 3 mid-century results have multiple years of moderate water scarcity and significant water scarcity and two years of severe water scarcity. The MIROC and ICHEC RCMs produce the severe water scarcity results of 209% in 2088 and 206% in 2093.

The MIROC RCM produced the most years of water scarcity with 11 years of moderate water scarcity, 4 years of significant water scarcity, and 1 year of severe water scarcity.

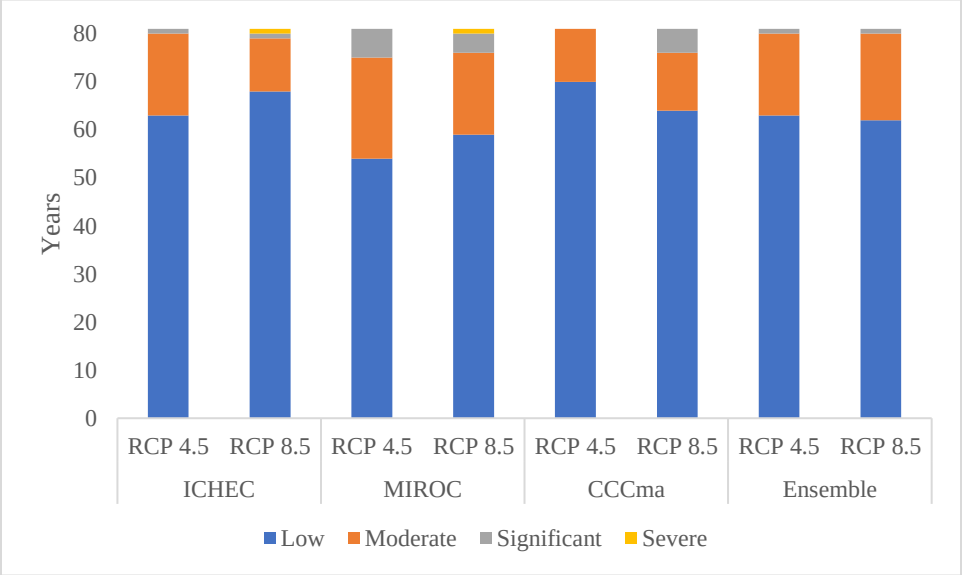

Figure 42: A comparison of the frequency of water scarcity events between each Regional Climate Model for scenario 3 from 2020-2100. Scenario 3 is a modified national water footprint that increases with projected population within Lesotho. Representation Concentration Pathway 4.5 and 8.5 are both given for comparison.

Figure 42 is a comparison of the frequency of water scarcity events within scenario 3 between each RCM. The ICHEC and MIROC RCMs had a greater number of years with moderate water scarcity in RCP 4.5 than RCP 8.5. The ICHEC and MIROC RCMs each produced a year of severe water scarcity in RCP 8.5. The MIRCO RCM produced more water scarcity events greater than 100% (low water scarcity), than any other RCM.

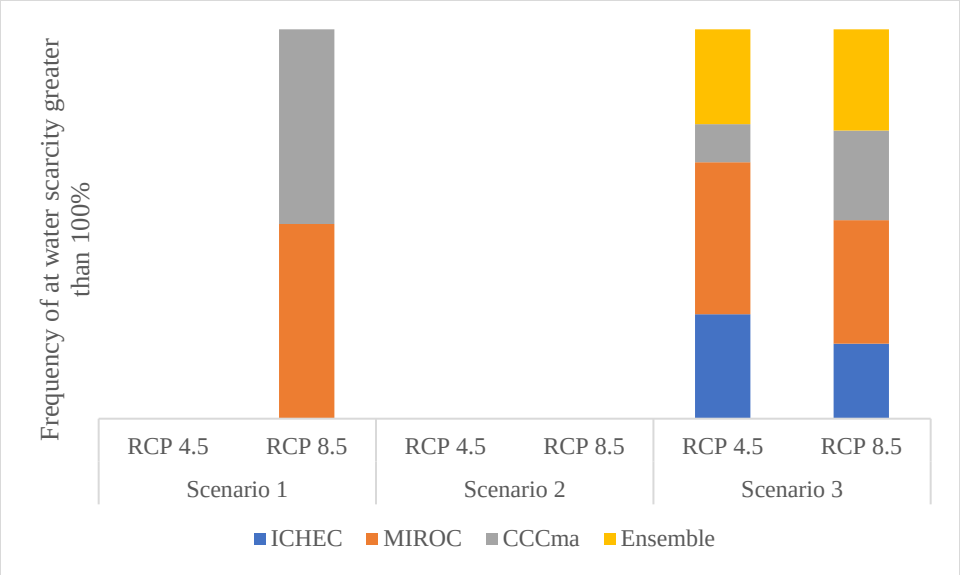

Figure 43: Comparison between each scenario of the frequency a Regional Climate Model (RCM) produced a water scarcity value greater than 100% with respect to the other RCMs. Scenario 1 assumes the Senqu river basin is the sole source of blue water available, and the entire national blue water footprint is used in the calculation of water scarcity. Scenario 2 is a modified national water footprint using only the population within the Senqu basin. Scenario 3 is a modified national water footprint that increases with projected population within Lesotho. Representation Concentration Pathway 4.5 and 8.5 are both given for comparison.

Figure 43 represents a comparison between each scenario of the number of times an RCM produced a water scarcity value greater than 100% with respect to the other RCMs. In scenario 1 RCP 4.5, no RCM produced a water scarcity value greater than 100%. In scenario 1 RCP 8.5 the MICROC and CCCma RCMs both produced the same amount of water scarcity values greater than 100%. Scenario 2 had no water scarcity events for both RCPs. Within scenario 3 RCP 4.5 the MIROC RCM had the greatest number of water scarcity events, followed by the ICHEC, Ensemble, then CCCma RCMs. Within scenario 3 RCP 8.5 the MIROC RCM also produced more water scarcity events than the other RCMs, followed by the Ensemble, CCCma, then ICHEC RCMs.

4.2 Discussion

The major findings of this research show that Lesotho is not likely to suffer from Blue Water Scarcity in the future within the Senqu river basin in scenario 1 and scenario 2. However, Lesotho is likely to suffer from moderate, significant and even severe cases of water scarcity under Scenario 3, which incorporates expected rates of population growth. As expected, the most severe cases of waters scarcity occurred in RCP 8.5 for all the scenarios. It makes sense that RCP 8.5 showed higher percentages of water scarcity than RCP 4.5, as it is representative of a more extreme climate induced radiative forcing. The MIROC RCM produced the most water scarcity events across all the scenarios. Adjusting the national water footprint to estimate future demand in response to population growth in scenario 3 resulted in many more cases of future water scarcity. Since the MIROC RCM produced the most water scarcity events and scenario 3 produced the most severe cases of water scarcity, the MIROC RCM within scenario 3 can be considered as a worst-case scenario for this study. In RCP 4.5 MIROC produced 56 years of low water scarcity, 21 years of moderate water scarcity, and 6 years of significant water scarcity from 2020-2100. In RCP 8.5 MIROC produced 59 years of low water scarcity, 17 years of moderate water scarcity, 4 years of significant water scarcity and 1 year of severe water scarcity from 2020-2100. Any year of water scarcity worse than 'low water scarcity' will not only have adverse effects on the Basotho, but also on the ecological system within the Senqu river. In order to meet water needs, Basotho will have to withdraw more water than is necessary to maintain the ecology of the Senqu river. This can have cascading effects on the economy and nutrition of Basotho who use the river as a source of food and livelihood. Droughts have stricken Lesotho in the past, 1968, 1983, 1990, 2002, 2007, 2011 leaving many Basotho without reliable access to blue water (Masih et al., 2014).

One reason droughts are hard on Basotho, and why future water scarcity is dangerous is the lack of integrated water resource infrastructure within Lesotho. Currently there are not interconnections between the water sources used to support the LHWP and the domestic and industrial demands of the Basotho in the lowlands (The World Bank, 2016). While one part of the country may have water, it is unable to effectively supply it to needed areas.

An important note to consider when evaluating the results of this study is the uncertainty attributed to future projections of the GCMs. Each of the RCMs in this study produced varying results and depending on the RCM one chooses to look at, they may find different levels of water scarcity. For example, in scenario 3 in RCP 8.5 the ICHEC RCM yields a water scarcity rating of 45% while the CCCma RCM yields 191% in the year 2063. That is the difference between low water scarcity and significant water scarcity respectively. When the RCMs evaluated past water scarcity in Lesotho, they failed to capture historical extreme weather events which resulted in droughts. RCMs have difficulty capturing and replicating historical extreme weather events (Panaou et al., 2018). A study by Shrestha et al. (2016) demonstrates the uncertainty of the choice of GCM on predicted future streamflow projections produced by SWAT (Shrestha et al., 2016). This increases uncertainty in their ability to capture future extreme weather events.

This study found an overall decrease of streamflow in Lesotho for each RCP, which disagrees with the results of a study performed by Farmarzi et al. in which the impacts of climate change on freshwater availability for the entirety of Africa were evaluated with SWAT (Faramarzi et al., 2013). The study by Farmarzi et al. found that the blue water available in Lesotho will increase in the future.

The two studies differ in that 1) Farmarzi et al. evaluates the blue water available for the entirety of Lesotho, 2) blue water available is calculated using the water yield plus the deep aquifer recharge for each SWAT sub-basin as opposed to the available streamflow, 3) CMIP3 scenarios were used as opposed to CMIP5 RCP scenarios.

The results of decreasing streamflow in the Senqu river basin agrees with previous SWAT studies that evaluate the effect of climate change on mountainous streamflow. The mountainous regions which show an overall decrease to mean streamflow include India (Reshmidevi et al., 2017), the western United States (Burke William and Ficklin Darren, 2017), Portugal (Carvalho-Santos et al., 2017), and the south western Balkans (Papadaki et al., 2016). Study sites which saw an increase in streamflow are Canada (Shrestha et al., 2017), and Nepal (Omani et al., 2016). Other studies reported both increases and decreases throughout the year as between spring and winter months (Bharati et al., 2016, Ficklin et al., 2016, Xu et al., 2016). It is evident that an increase or decrease in overall streamflow will vary depending on location of the study area and the climate of the region. For example, mountainous watersheds that are heavily influenced by glacier melt in studies were shown as having an increase in streamflow as temperatures rose (Ficklin et al., 2016, Omani et al., 2016, Schwank et al., 2014, Shrestha et al., 2017). In regions not influenced by glacier runoff, temperature rise can have the opposite effect. In areas such as Lesotho not influenced by glacier runoff, an increase in mean temperature is a major factor in increasing evapotranspiration and as a result decreases streamflow (Salmoral et al., 2015).

This study is important as while SWAT output has been used with the blue water footprint to measure existing blue water scarcity, it has not been used to measure future blue water scarcity using CMIP5 RCPs and the water footprint. It is also important because it uses

the methodology to evaluate the potential blue water scarcity of Lesotho, which is a region that has not been largely studied in this regard. The Senqu river is a major source of water for the people of Lesotho and knowing how climate change will impact the blue water availability can help with water resource management decisions.

This study has limitations which should be considered when evaluating the results. Scenario 3 adjusted the water footprint for projected population growth but did not adjust for Lesotho's potential industrialization. Scenario 3 also evaluated the water scarcity across the entirety of Lesotho with respect to population growth, without considering water sources outside of the Senqu river basin. The land use within Lesotho will also change in the future which was not considered. While there are currently two dams, Katse and Mohale, along the Senqu River, three more are scheduled to be built and one of those three, the Polihali dam is currently being designed in Mokhotlong (Burger, 2018). The goal of these dams is to transfer water to South Africa. Once completed a total of 70 cms (2208 million m^3y^{-1}) will be transferred. Currently the Katse and Mohale transfer a total of 30 cms (950 million m^3y^{-1}) (LHWP, 2008). This water transfer was not captured in this model. This model only evaluated the water available at the SG3 outlet streamflow gauge station which had an average flow of 30000 million $m^3\,y^{-1}$. The current water transfer of 30 cms does not have a noticeable impact at SG3. This is shown by the results of the Indicators of Hydrologic Alteration. However, these future dams are likely to have a significant impact on the water available in the Senqu river. The Indicators of Hydrologic Alteration results showed the Senqu river was significantly impacted at the SG5 and SG17 gauge stations directly downstream of the Katse and Mohale dam respectively. Basotho who live near these streamflow gauging stations are more likely to have less water available to them as opposed to living further downstream.

With proper SWAT input data of the Katse and Mohale dams, the water available at these upstream locations can be modeled in the future along with the water transferred out of Lesotho, and a better picture of the water available throughout the river basin can be elucidated as opposed to just the basin outlet.

CHAPTER 5: CONCLUSION AND RECOMMENDATIONS

This research expanded the framework developed by Rodrigues et al. (2014) by incorporating climate change impacts to measure future potential blue water scarcity of a river basin. Climate change affects hydrological cycles and streamflow of rivers and has the potential to affect the amount of water available for use within a country. Thus, the ability to evaluate the potential blue water scarcity caused by climate change is important to help adequately plan for future water resource management. The addition of measuring blue water scarcity with respect to climate change is an important step in this direction. The framework developed in this thesis was applied to the Senqu river basin within Lesotho under three different scenarios. The results showed an overall decrease in available streamflow of the Senqu river. Scenario 1 and Scenario 2 used the national water footprint to measure water scarcity of Lesotho and within the basin respectively and did not indicate future water scarcity. Scenario 3 adjusted the future national water footprint to account for projected population demand, indicating several years between 2020 and 2100 that would experience some form of water scarcity. The MIROC RCM produced the most cases of water scarcity within scenario 3. Within RCP 4.5 it produced 56 years of low water scarcity, 21 years of moderate water scarcity, and 6 years of significant water scarcity from 2020-2100. In RCP 8.5 MIROC produced 59 years of low water scarcity, 17 years of moderate water scarcity, 4 years of significant water scarcity and 1 year of severe water scarcity from 2020-2100. The most extreme water scarcity event produced by the MIROC RCM occurred in 2088 with a severe water scarcity score of 209%.

It is important to remember the limitations within this study and therefore its results should only be used carefully to inform future policy and water resource decisions. Future work could improve on the methodology developed in this research to better understand water scarcity within Lesotho. The overall model prediction could be improved by incorporating SWAT input data on the dams to investigate the impacts of the dams on water scarcity. This would allow the change in streamflow and water scarcity throughout the basin to be measured providing more insight into potential areas that would experience greater water scarcity than others. The LHWP plans on constructing a total of five dams on the Senqu River. Incorporating the water transfer of the dams to South Africa will elucidate the loss of available water within the Senqu River basin. The current water transfer of 30 cms does not significantly impact the water available at SG3, however it does impact the water available at SG5 and SG17 as shown by the results of the Indicators of Hydrologic Alteration analysis. The ability to model the impact of climate change on water availability throughout the river basin will be important for water resource allocation of those who depend on the Senqu River for livelihood. Currently Lesotho lacks infrastructure to transfer water sources throughout villages in the river basin (The World Bank, 2016). Evaluating blue water scarcity on a monthly scale as was done by Hoekstra et al. (2012) rather than an annual scale will also elucidate on the potential for greater water scarcity concern during the dry and wet seasons.

REFERENCES

Abbaspour, K. C. 2011. SWAT-CUP2: SWAT Calibration and Uncertainty Programs Manual Version 2. Duebendorf, Switzerland: Department of Systems Analysis, Integrated Assessment and Modelling (SIAM), Eawag. Federal Institute of Aquatic Science and Technology.

Abbaspour, K. C., Johnson, C. A. & Van Genuchten, M. T. 2004. Estimating uncertain flow and transport parameters using a sequential uncertainty fitting procedure. *Vadose Zone,* 3**,** 1340-1352.

Abbaspour, K. C., Yang, J., Maximov, I., Siber, R., Bogner, K., Mieleitner, J., Zobrist, J. & Srinivasan, R. 2006. Modelling hydrology and water quality in the pre alpine Thur watershed using SWAT. *Journal of Hydrology,* 333**,** 413-430.

Abu-Allaban, M., El-Naqa, A., Jaber, M. & Hammouri, N. 2015. Water scarcity impact of climate change in semi-arid regions: a case study in Mujib basin, Jordan. *Arabian Journal of Geosciences,* 8**,** 951-959.

Alcamo, J., Henrichs, T. & Rosch, T. 2000. World water in 2025 global modeling scenario analysis for the world commission on water for the 21st century. *Kassel World Water Series Report No. 2.* Center for Environmental Systems Research: Germany: University of Kassel.

Arias, M. E., Cochrane, T. A., Kummu, M., Lauri, H., Holtgrieve, G. W., Koponen, J. & Piman, T. 2014. Impacts of hydropower and climate change on drivers of ecological productivity of Southeast Asia's most important wetland. *Ecological Modeling,* 272**,** 252-263.

Arias, M. E., Cochrane, T. A., Piman, T., Kummu, M., Caruso, B. S. & Killeen, T. J. 2012. Quantifying changes in flooding and habitats in the Tonle Sap Lake (Cambodia) caused by water infrastructure development and climate change in the Mekong Basin. *Journal Environmental Management,* 112**,** 53-66.

Arnell, N. W. 2003. Effects of IPCC SRES emissions scenarios on river runoff: a global perspective. *Hydrology and Earth System Sciences,* 7**,** 619-641.

Arnell, N. W. 2004. Climate change and global water resources: SRES emissions and socio-economic scenarios. *Global Environmental Change,* 14**,** 31-52.

Arnold, J. G., Moriasi, D. N., Gassman, P. W., Abbaspour, K. C., White, M. J., Srinivasan, R., Santhi, C., Harmel, R. D., Griensven, A. V., Liew, M. W. V., Kannan, N. & Jha, M. K. 2012. SWAT: Model Use, Calibration, and Validation. *American Society of Agricultural and Biological Engineers,* 55**,** 1499-1508.

Arnold, J. G., Neitsch, S. L., Kiniry, J. R., Srinivasan, R. & Williams, J. R. 2002. *Soil and Water Assessment Tool User's Manual Version 2000*.

Arnold, J. G., Srinivasan, R., Muttiah, R. S. & Williams, J. R. 1998. Large area hyrologic modeling and assessment part 1: Model Development. *American Water Rescources Association,* 34**,** 73-89.

Asce 1993. Criteria for evaluation of watershed models. *Journal of Irrigation and Drainage Engineering,* 119**,** 429-442.

Asheesh, M. 2003. Allocating the gaps of shared water resources (the scarcity index) case study Palesine Israel. *IGME,* 797-805.

Basheer, A. K., Lu, H., Omer, A., Ali, A. B. & Abdelgader, A. M. S. 2016. Impacts of climate change under CMIP5 RCP scenarios on the streamflow in the Dinder River and ecosystem habitats in Dinder National Park, Sudan. *Hydrology and Earth System Sciences,* 20**,** 1331-1353.

Bello, H. M., Malefane, M. R. & Babatope-Obasa, S. 2010. Household water supply and use in some peri-urban settlements of Lesotho. *Asian-African Journal of Economics and Econometrics,* 10**,** 15-28.

Bharati, L., Gurung, P., Maharjan, L. & Bhattarai, U. 2016. Past and future variability in the hydrological regime of the Koshi Basin, Nepal. *Hydrological Sciences Journal,* 61**,** 79-93.

Block Paul, J., Souza Filho Francisco, A., Sun, L. & Kwon, H. H. 2009. A streamflow forecasting framework using multiple climate and hydrological models. *Journal of the American Water Resources Association,* 45**,** 828-843.

Boé, J., Terray, L., Habets, F. & Martin, E. 2007. Statistical and dynamical downscaling of the Seine basin climate for hydro-meteorological studies. *International Journal of Climatology,* 27**,** 1643-1655.

Brown, M. 2011. A Review of water scarcity indices and methodologies. *The Sustainability Consortium.*

Burger, S. 2018. *LHDA awards Polihli transfer tunnel design contract* [Online]. Available: http://m.engineeringnews.co.za/article/lhda-awards-polihali-transfer-tunnel-design-contract-2018-01-10/rep_id:4433 [Accessed May 10 2018].

Burke William, D. & Ficklin Darren, L. 2017. Future projections of streamflow magnitude and timing differ across coastal watersheds of the western United States. *International Journal of Climatology,* 37**,** 4493-4508.

Carvalho-Santos, C., Monteiro, A. T., Azevedo, J. C., Honrado, J. P. & Nunes, J. P. 2017. Climate change impacts on water resources and reservoir management: uncertainty and adaptation for a mountain catchment in northeast portugal. *Water Resources Management,* 31**,** 3355-3370.

Chaves, M. L. & Alipaz, S. 2007. An integrated indicator for basin hydrology, environment, life, and policy: the watershed sustainability index. *Water Resources Management,* 21**,** 883-895.

Chen, J., Brissette, F. P. & Leconte, R. 2011. Uncertainty of downscaling method in quantifying the impact of climate change on hydrology. *Journal of Hydrology,* 401**,** 190-202.

Cochrane, T. A., Arias, M. E. & Piman, T. 2014. Historical impact of water infrastructure on water levels of the Mekong River and the Tonle Sap system. *Hydrology and Earth System Sciences,* 18**,** 4529-4541.

Cousino, L. K., Becker, R. H. & Zmijewski, K. A. 2015. Modeling the effects of climate change on water, sediment, and nutrient yields from the Maumee River watershed. *Journal of Hydrology: Regional Studies,* 4**,** 762-775.

Cridf. 2017. *Climate Resilient Infrastructure Development Facility - Lesotho* [Online]. Available: http://cridf.net/wp-content/uploads/2017/12/5_CRIDF_VirtualWater_Infographic_Lesotho_LR.pdf [Accessed].

Diaz, H., Grosjean, M. & Graumlich, L. 2003. Climate variability and change in high elevation regions past present and future. *Climatic Change,* 59**,** 1-4.

Elhassan, A., Xie, H., Al-Othman, A. A., Mcclelland, J. & Sharif, H. O. 2015. Water quality modelling in the San Antonio River Basin driven by radar rainfall data. *Geomatics, Natural Hazards and Risk,* 7**,** 953-970.

Enes. 2017. *CMIP5 models and grid resolution* [Online]. Available: https://verc.enes.org/data/enes-model-data/cmip5/resolution [Accessed January 20 2017].

Fader, M., Gerten, D., Thammer, M., Heinke, J., Lotze-Campen, Lucht, W. & Cramer, W. 2011. Internal and external green-blue agricultural water footprints of nations, and related water and land savings through trade. *Hydrology and Earth System Sciences,* 15.

Falkenmark, M., Lundqvist, J. & Widstrand, C. 1989. Macro-scale water scarcity requires micro-scale approaches: Aspects of vulberability in semi-arid development. *Natural Resources Forum,* 13**,** 258-263.

Falkenmark, M. & Widstrand, C. 1992. *Population and water resources: A Delicate Balance,* Washington, DC, USA, Population Reference Bureau.

Faramarzi, M., Abbaspour, K. C., Ashraf Vaghefi, S., Farzaneh, M. R., Zehnder, A. J. B., Srinivasan, R. & Yang, H. 2013. Modeling impacts of climate change on freshwater availability in Africa. *Journal of Hydrology,* 480**,** 85-101.

Ficklin, D. L., Letsinger, S. L., Stewart, I. T. & Maurer, E. P. 2015. Assessing differences in snowmelt-dependent hydrologic projections using CMIP3 and CMIP5 climate forcing data for the western United States. *Hydrology Research***,** nh2015101.

Ficklin, D. L., Letsinger, S. L., Stewart, I. T. & Maurer, E. P. 2016. Assessing differences in snowmelt-dependent hydrologic projections using CMIP3 and CMIP5 climate forcing data for the western United States. *Hydrology Research,* 47**,** 483.

Fry, L. M., Mihelcic, J. R. & Watkins, D. W. 2008. Water and non-water-related challenges of achieving global sanitation coverage. *Environmental Science & Technology,* 42**,** 4298-4304.

Fry, L. M., Watkins, D. W., Reents, N., Rowe, M. D. & Mihelcic, J. R. 2012. Climate change and development impacts on the sustainability of spring-fed water supply systems in the Alto Beni region of Bolivia. *Journal of Hydrology***,** 120-129.

Fuka, D. R., Walter, M. T., Macalister, C., Degaetano, A. T., Steenhuis, T. S. & Easton, Z. M. 2014. Using the climate forecast system reanalysis as weather input data for watershed models. *Hydrological Processes,* 28**,** 5613-5623.

Geza, M. & Mccray, J. E. 2008. Effects of soil data resolution on SWAT model stream flow and water quality predictions. *Journal Environmental Management,* 88**,** 393-406.

Gleick, P. 1996. Basic water requirements for human activities: meeting basic needs. *Water International,* 21**,** 83-92.

Graham, L. P., Hagemann, S., Jaun, S. & Beniston, M. 2007. On interpreting hydrological change from regional climate models. *Climatic Change,* 81**,** 97-122.

Gupta Hoshin, V., Sorooshian, S. & Yapo Patrice, O. 1999. Status of automatic calibration for hydrologic models: comparison with multilevel expert calibration. *Journal of Hydrologic Engineering,* 4**,** 135-143.

Hansen, J. W., Challinor, A., Ines, A., Wheeler, T. & Moron, V. 2006. Translating climate forecasts into agricultural terms: advances and challenges. *Climate Research,* 33**,** 27-41.

Hayhoe, K. July 2007. Regional climate change projections for the Northeast U.S. *Mitigation and Adaption Strategies for Global Change*.

Heath, R. & Brown, C. 2007. Environmental considerations pertaining to the Orange River.

Hoekstra, A. Y. 2003. Virtual water trade: proceedings of the international expert meeting on virtual water trade. *Value of Water Research Report Series.* The Netherlands: UNESCO-IHE.

Hoekstra, A. Y. & Chapagain, A. K. 2007. Water footprints of nations: Water use by people as a function of their consumption pattern. *In:* CRASWELL, E., BONNELL, M., BOSSIO, D., DEMUTH, S. & VAN DE GIESEN, N. (eds.) *Integrated Assessment of Water Resources and Global Change: A North-South Analysis.* Dordrecht: Springer Netherlands.

Hoekstra, A. Y., Chapagain, A. K., Aldaya, M. M. & Mekonnen, M. M. 2011. The Water Footprint Assessment Manual: setting the global standard. London, UK: Earthscan.

Hoekstra, A. Y. & Hung, P. Q. 2005. Globalisation of water resources: international virtual water flows in relation to crop trade. *Global Environmental Change,* 15**,** 45-56.

Hoekstra, A. Y. & Mekonnen, M. M. 2012. The water footprint of humanity. *Proceedings of the National Academy of Sciences,* 109**,** 3232.

Hoekstra, A. Y., Mekonnen, M. M., Chapagain, A. K., Mathews, R. E. & Richter, B. D. 2012. Global monthly water scarcity: blue water footprints versus blue water availability. *PLOS One,* 7**,** e32688.

Ines, A. V. M. & Hansen, J. W. 2006. Bias correction of daily GCM rainfall for crop simulation studies. *Agricultural and Forest Meteorology,* 138**,** 44-53.

Ipcc 2013. *Climate Change 2013: the physical science basis. Contribution of working group I to the fifth assessment report of the Intergovernmental Panel on Climate Change,* Cambridge, United Kingdom and New York, NY, USA, Cambridge University Press.

Johnson, F. & Sharma, A. 2011. Accounting for interannual variability: A comparison of options for water resources climate change impact assessments. *Water Resources Research,* 47.

Kang, B., Kim, Y. D., Lee, J. M. & Kim, S. J. 2015. Hydro-environmental runoff projection under GCM scenario downscaled by Artificial Neural Network in the Namgang Dam watershed, Korea. *KSCE Journal of Civil Engineering,* 19**,** 434-445.

Kjellstrom, E., Barring, L., Nikulin, G., Nilsson, C., Persson, G. & Strandberg, G. 2016. Production and use of regional climate model projections – A Swedish perspective on building climate services. *Climate Services,* 2**,** 15-29.

Knutti, R., Masson, D. & Gettelman, A. 2013. Climate model genealogy: Generation CMIP5 and how we got there. *Geophysical Research Letters,* 40**,** 1194-1199.

Lam, Q. D., Schmalz, B. & Fohrer, N. 2010. Modelling point and diffuse source pollution of nitrate in a rural lowland catchment using the SWAT model. *Agricultural Water Management,* 97**,** 317-325.

Le, T. & Sharif, H. 2015. Modeling the projected changes of river flow in central vietnam under different climate change scenarios. *Water,* 7**,** 3579-3598.

Leander, R. & Buishand, T. A. 2007. Resampling of regional climate model output for the simulation of extreme river flows. *Journal of Hydrology,* 332**,** 487-496.

Legates, D. & Mccabe, G. 1999. Evaluating the use of "goodness-of-fit" measures in hydrologic and hydroclimatic model validation. *Water Resources Research,* 35**,** 233-241.

Lenderink, G., Buishand, A. & Van Deursen, W. 2007. Estimates of future discharges of the river Rhine using two scenario methodologies: direct versus delta approach. *Hydrology and Earth System Sciences,* 11**,** 1145-1159.

Lennard, C., Nikulin, G. & Centre, R. 2015. CORDEX Africa Analysis Campaign Phase 2.

Lesotho Population. 2018. *Lesotho Population* [Online]. Available: http://worldpopulationreview.com/countries/lesotho-population/ [Accessed May 9 2018].

Lhwp 2008. Creating benefits from cooperation in shared water resources: Lesotho's highlands water project phases IA and IB. World Bank.

Li, F., Zhang, G. & Xu, Y. 2016. Assessing climate change impacts on water resources in the Songhua river basin. *Water,* 8**,** 420.

Lms. 2013. *Climate of Lesotho | Lesotho Meteorological Services* [Online]. Lesotho Meteorological Services. Available: http://www.lesmet.org.ls/cimatology/climate-lesotho [Accessed January 22 2017].

London, L. H. C. I. 2017. *Lesotho Fact Sheet | Lesotho* [Online]. Lesotho High Commission. Available: http://www.lesotholondon.org.uk/quick [Accessed January 15 2017].

Maliehe, M. & Mulungu, D. M. M. 2017. Assessment of water availability for competing uses using SWAT and WEAP in South Phuthiatsana catchment, Lesotho. *Physics and Chemistry of the Earth, Parts A/B/C,* 100**,** 305-316.

Maraun, D., Wetterhall, F., Ireson, A. M., Chandler, R. E., Kendon, E. J., Widmann, M., Brienen, S., Rust, H. W., Sauter, T., Themeßl, M., Venema, V. K. C., Chun, K. P., Goodess, C. M., Jones, R. G., Onof, C., Vrac, M. & Thiele-Eich, I. 2010. Precipitation downscaling under climate change: Recent developments to bridge the gap between dynamical models and the end user. *Reviews of Geophysics,* 48.

Masih, I., Maskey, S., Mussá, F. E. F. & Trambauer, P. 2014. A review of droughts on the African continent: a geospatial and long-term perspective. *Hydrology and Earth System Sciences,* 18**,** 3635-3649.

Mcnulty, S., Sun, G., Myers, J. M., Cohen, E. & Caldwell, P. 2010. Robbing Peter to pay Paul: tradeoffs between ecosystem carbon sequestration and water yield. *Watershed Management*.

Mdg 2013. Kingdom of Lesotho Millenium Development Goals Status Report 2013. *In:* MILLER, H. (ed.) *Millenium Development Goals Report.*

Mekonnen, M. M. & Hoekstra, A. Y. 2011. National Water Footprint Accounts: The Green, Gray, and Blue water footprint of production and consumption. UNESCO-IHE.

Ministry of Health [Lesotho] 2014. Lesotho Demographic and Health Survey 2014. Maseru, Lesotho: Ministry of Health and ICF International.

Mittal, N., Bhave, A. G., Mishra, A. & Singh, R. 2015. Impact of human intervention and climate change on natural flow regime. *Water Resources Management,* 30**,** 685-699.

Moriasi, D. N., Arnold, J. G., Liew, M. W. V., Bingner, R. L., Harmel, R. D. & Veith, T. L. 2007. Model evaluation guidelines for systematic quantification of Accuracy in Watershed Simulations. *American Society of Agricultural and Biological Engineers,* 50**,** 885-900.

Moss, R. H., Edmonds, J. A., Hibbard, K. A., Manning, M. R., Rose, S. K., Van Vuuren, D. P., Carter, T. R., Emori, S., Kainuma, M., Kram, T., Meehl, G. A., Mitchell, J. F., Nakicenovic, N., Riahi, K., Smith, S. J., Stouffer, R. J., Thomson, A. M., Weyant, J. P. & Wilbanks, T. J. 2010. The next generation of scenarios for climate change research and assessment. *Nature,* 463**,** 747-56.

Mote, P. W., Allen, M. R., Jones, R. G., Li, S., Mera, R., Rupp, D. E., Salahuddin, A. & Vickers, D. 2015. Superensemble regional climate modeling for the western United States. *Bulletin of the American Meteorological Society,* 97**,** 203-215.

Nash, J. E. & Sutcliffe, J. V. 1970. River flow forecasting through conceptual models part I — A discussion of principles. *Journal of Hydrology,* 10**,** 282-290.

Ncar. 2017. *The Climate Data Guide: Climate Forecast System Reanalysis (CFSR)* [Online]. Available: https://climatedataguide.ucar.edu/climate-data/climate-forecast-system-reanalysis-cfsr [Accessed].

Neitsch, S. L., Arnold, J. G., Kiniry, J. R. & Williams, J. R. 2011. Soil and Water Assessment Tool Theoretical Documentation Version 2009. Texas Water Resources Institute.

Nikulin, G., Jones, C., Giorgi, F., Asrar, G., Büchner, M., Cerezo-Mota, R., Christensen, O. B., Déqué, M., Fernandez, J., Hänsler, A., Van Meijgaard, E., Samuelsson, P., Sylla, M. B. & Sushama, L. 2012. Precipitation climatology in an ensemble of CORDEX-Africa Regional Climate Simulations. *Journal of Climate,* 25**,** 6057-6078.

Oecd 2012. OECD environmental outlook to 2050: The consequences of inaction key facts and figures. OECD Publishing.

Ohlsson, L. 2000. Water conflicts and social resource scarcity. *Physics and Chemistry of the Earth, Part B: Hydrology, Oceans and Atmosphere,* 25**,** 213-220.

Omani, N., Srinivasan, R., Karthikeyan, R., Reddy K, V. & K. Smith, P. 2016. Impacts of climate change on the glacier melt runoff from five river basins. *Transactions of the ASABE,* 59**,** 829.

Onishi, N. & Sengupta, S. 2018. Dangerously low on water, Cape Town now faces 'Day Zero'. *The New York Times*.

Pachauri, R. K., Allen, M. R., Barros, V. R., Broome, J., Cramer, W., Christ, R., Church, J. A., Dahe, Q., Dasgupta, P. & Dubash, N. K. 2014. *Synthesis Report. Fifth Assessment Report of the Intergovernmental Panel on Climate Change***,** 151-165.

Panaou, T., Asefa, T. & Nachabe, M. H. 2018. Keeping us honest: examining climate states and transition probabilities of precipitation projections in general circulation models. *Journal of Water Resources Planning and Management,* 144.

Papadaki, C., Soulis, K., Muñoz-Mas, R., Martinez-Capel, F., Zogaris, S., Ntoanidis, L. & Dimitriou, E. 2016. Potential impacts of climate change on flow regime and fish habitat in mountain rivers of the south-western Balkans. *Science of The Total Environment,* 540**,** 418-428.

Parajuli, P. B., Jayakody, P., Sassenrath, G. F. & Ouyang, Y. 2016. Assessing the impacts of climate change and tillage practices on stream flow, crop and sediment yields from the Mississippi River Basin. *Agricultural Water Management,* 168**,** 112-124.

Parish, R. & Funnell, D. C. 1999. Climate change in mountain regions: some possible consequences in the Moroccan High Atlas. *Global Environmental Change,* 9**,** 45-58.

Park, J. Y., Park, M. J., Ahn, S. R., Park, G. A., Yi, J. E., Kim, G. S., Srinivasan, R. & Kim, S. J. 2011. Assessment of future climate change impacts on water quantity and quality for a mountainous dam watershed using SWAT. *American Society of Agricultural and Biological Engineers,* 54**,** 1725-1737.

Pcmdi. 2017. *CMIP - Overview* [Online]. Available: http://cmip-pcmdi.llnl.gov/ [Accessed January 16 2017].

Pfister, S., Koehler, A. & Hellweg, S. 2009. Assessing the environmental impacts of freshwater consumption in LCA. *Evnironmentsl Science & Technology,* 43**,** 4098-4104.

Piani, C., Haerter, J. O. & Coppola, E. 2009. Statistical bias correction for daily precipitation in regional climate models over Europe. *Theoretical and Applied Climatology,* 99**,** 187-192.

Piani, C., Weedon, G. P., Best, M., Gomes, S. M., Viterbo, P., Hagemann, S. & Haerter, J. O. 2010. Statistical bias correction of global simulated daily precipitation and temperature for the application of hydrological models. *Journal of Hydrology,* 395**,** 199-215.

Pierce, D., Barnett, T., Santer, B. & Glecker, P. 2009. Selecting global climate models for regional climate change studies. *PNAS,* 106.

Pisinaras, V. 2016. Assessment of future climate change impacts in a Mediterranean aquifer. *Global NEST,* 18**,** 119-130.

Postal, S. 2000. Entering an era of water scarcity: the challenges ahead. *Ecological Applications,* 10**,** 941-948.

Prasad, G., Boulle, M., Boyd, A., Rahlao, S., Wlokas, H. & Yaholnitsky, I. Energy water and climate change in Southern Africa. University of Cape Town.

Prüss-Ustün, A., Bartram, J., Clasen, T., Colford John, M., Cumming, O., Curtis, V., Bonjour, S., Dangour Alan, D., De France, J., Fewtrell, L., Freeman Matthew, C., Gordon, B., Hunter Paul, R., Johnston Richard, B., Mathers, C., Mäusezahl, D., Medlicott, K., Neira, M., Stocks, M., Wolf, J. & Cairncross, S. 2014. Burden of disease from inadequate water, sanitation and hygiene in low- and middle-income settings: a retrospective analysis of data from 145 countries. *Tropical Medicine & International Health,* 19**,** 894-905.

Raskin, P., Gleick, P., Kirshen, P., Pontius, G. & Strzepek, K. 1997. Water futures: assessment of long range patterns and problems. Stockholm, Sweden: Stockhold Environment Institute.

Reshmidevi, T. V., Kumar, N., Mehrotra, R. & Sharma, A. 2017. Estimation of the climate change impact on a catchment water balance using an ensemble of GCMs. *Journal of Hydrology,* 556**,** 1192-1204.

Richter, B. D., Davis, M. M., Apse, C. & Konrad, C. 2012. A presumptive standard for environmental flow protection. *River Research and Applications,* 28**,** 1312-1321.

Rijsberman, F. R. 2006. Water scarcity: Fact or fiction? *Agricultural Water Management,* 80**,** 5-22.

Rodrigues, D. B. B., Gupta, H. V. & Mendiondo, E. M. 2014. A blue/green water-based accounting framework for assessment of water security. *Water Resources Research,* 50**,** 7187-7205.

Rojas, R., Feyen, L., Dosio, A. & Bavera, D. 2011. Improving pan-European hydrological simulation of extreme events through statistical bias correction of RCM-driven climate simulations. *Hydrology and Earth System Sciences,* 15**,** 2599-2620.

Salmoral, G., Willaarts, B. A., Troch, P. A. & Garrido, A. 2015. Drivers influencing streamflow changes in the Upper Turia basin, Spain. *Science of The Total Environment,* 503-504**,** 258-68.

Schewe, J., Heinke, J., Gerten, D., Haddeland, I., Arnell, N. W., Clark, D. B., Dankers, R., Eisner, S., Fekete, B. M., Colon-Gonzalez, F. J., Gosling, S. N., Kim, H., Liu, X., Masaki, Y., Portmann, F. T., Satoh, Y., Stacke, T., Tang, Q., Wada, Y., Wisser, D., Albrecht, T., Frieler, K., Piontek, F., Warszawski, L. & Kabat, P. 2014. Multimodel assessment of water scarcity under climate change. *Proceedings of the National Academy of Sciences of the United States of America,* 111**,** 3245-50.

Schmidli, J., Frei, C. & Vidale Pier, L. 2006. Downscaling from GCM precipitation: a benchmark for dynamical and statistical downscaling methods. *International Journal of Climatology,* 26**,** 679-689.

Schuol, J. R., Abbaspour, K. C., Yang, H., Srinivasan, R. & Zehnder, A. J. B. 2008. Modeling blue and green water availability in Africa. *Water Resources Research,* 44.

Schwank, J., Escobar, R., Girón, G. H. & Morán-Tejeda, E. 2014. Modeling of the Mendoza river watershed as a tool to study climate change impacts on water availability. *Environmental Science & Policy,* 43**,** 91-97.

Seckler, D., Barker, R. & Amarasinghe, U. 1999. Water Scarcity in the Twenty-first Century. *International Journal of Water Resources Development,* 15**,** 29-42.

Sennikovs, J. & Bethers, U. 2009. *Statistical downscaling method of regional climate model results for hydological modeling*.

Servat, E. & Dezetter, A. 1991. Selection of calibration objective fonctions in the context of rainfall-ronoff modelling in a Sudanese savannah area. *Hydrological Sciences Journal,* 36**,** 307-330.

Sharma, D., Gupta, A. D. & Babel, M. S. 2007. Spatial disaggregation of bias-corrected GCM precipitation for improved hydrologic simulation: Ping River Basin, Thailand. *Hydrology andEarth System Sciences Discussions, European Geosciences Union,* 11**,** 1373-1390.

Shrestha, B., Cochrane, T. A., Caruso, B. S., Arias, M. E. & Piman, T. 2016. Uncertainty in flow and sediment projections due to future climate scenarios for the 3S Rivers in the Mekong Basin. *Journal of Hydrology,* 540**,** 1088-1104.

Shrestha, N. K., Du, X. & Wang, J. 2017. Assessing climate change impacts on fresh water resources of the Athabasca River Basin, Canada. *Science of The Total Environment,* 601-602**,** 425-440.

Smakhtin, V., Revenga, C. & Doll, P. 2005. Taking into Account Environmental Water Requirements in Global-scale Water Resources Assessments. International Water Management Institute.

Sullivan, C. 2002. Calculating a water poverty index. *World Development,* 30**,** 1195-1210.

Taylor, K. E., Stouffer, R. J. & Meehl, G. A. 2011. A summary of the CMIP5 experiment design.

Team, G. 2007. *GeoNetwork opensource portal to spatial data and information* [Online]. Available: http://www.fao.org/geonetwork/srv/en/metadata.show?id=14116 [Accessed].

Teutschbein, C. & Seibert, J. 2012. Bias correction of regional climate model simulations for hydrological climate-change impact studies: Review and evaluation of different methods. *Journal of Hydrology,* 456-457**,** 12-29.

The World Bank 2016. Lesotho water security and climate change assessment. Washington D.C.: The World Bank.

Thom, H. C. S. 1958. A note of the Gamma distribution *Monthly Weather Review,* 86**,** 117-122.

Thompson, J., Porras, I. T., Tumwine, J. K., Mujwahuzi, M. R., Katui-Katua, M., Johnstone, N. & Wood, L. 2001. *Drawers of water II: 30 years of change in domestic water use & environmental health in East Africa - summary,* London, International Institute for Environment and Development (IIED).

Timpe, K. & Kaplan, D. 2017. The changing hydrology of a dammed Amazon. *Science Advances,* 3.

Ullrich, A. & Volk, M. 2009. Application of the Soil and Water Assessment Tool (SWAT) to predict the impact of alternative management practices on water quality and quantity. *Agricultural Water Management,* 96**,** 1207-1217.

Vorosmarty, C. J. 2000. Global water resources: vulnerability from climate change and population growth. *Science,* 289**,** 284-288.

Vorosmarty, C. J., Douglas, E., Green, P. & Revenga, C. 2005. Geospatial indicators of emerging water stress: an application to Africa. *Ambio,* 34**,** 230-236.

Vorosmarty, C. J., Mcintyre, P. B., Gessner, M. O., Dudgeon, D., Prusevich, A., Green, P., Glidden, S., Bunn, S. E., Sullivan, C. A., Liermann, C. R. & Davies, P. M. 2010. Global threats to human water security and river biodiversity. *Nature,* 467**,** 555-61.

Wang, R. & Zimmerman, J. 2016. Hybrid analysis of blue water consumption and water scarcity implications at the global, national, and basin Levels in an increasingly globalized world. *Environmental Science & Technology,* 50**,** 5143-53.

Wwdr 2016. The United Nations world water development report 2016. United Nations Educational, Scientific and Cultural Organization, 7, place de Fontenoy, 75352 Paris 07 SP, France.

Xu, C., Zhao, J., Deng, H., Fang, G., Tan, J., He, D., Chen, Y., Chen, Y. & Fu, A. 2016. Scenario-based runoff prediction for the Kaidu River basin of the Tianshan Mountains, Northwest China. *Environmental Earth Sciences,* 75**,** 1126.

Yan, D., Werners, S. E., Ludwig, F. & Huang, H. Q. 2015. Hydrological response to climate change: The Pearl River, China under different RCP scenarios. *Journal of Hydrology: Regional Studies,* 4**,** 228-245.